AD-A159 215 LASER GUIDANCE WITH TRIAD DETECTOR ARRAY STRAPDOWN SEEKER(U) AIR FORCE INST OF TECH WRIGHT-PATTERSON AFB OH SCHOOL OF ENGINEERING N KASIKCIOGLU JUN 85 1/2

UNCLASSIFIED AFIT/GE/ENG/85J-3 F/G 17/7 NL

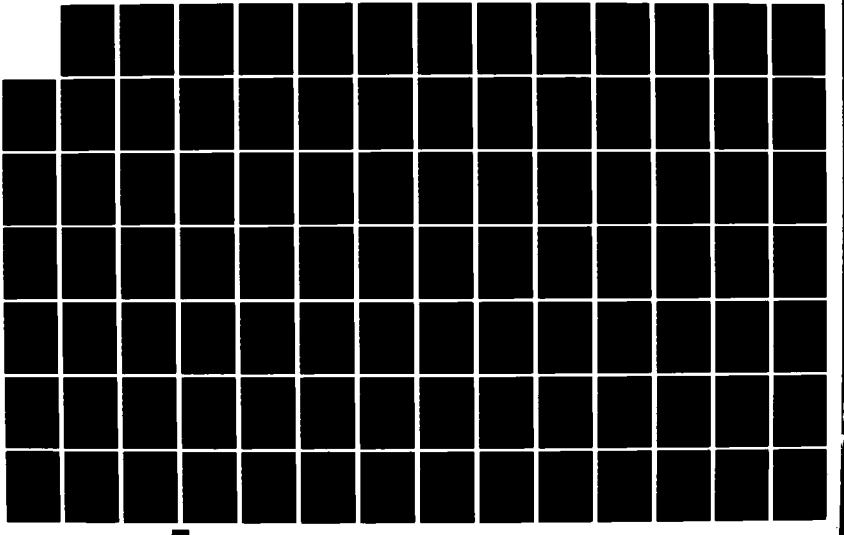

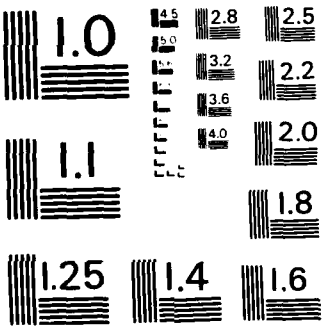

LASER GUIDANCE WITH TRIAD DETECTOR ARRAY STRAPDOWN SEEKER

THESIS

AFIT/GE/ENG/85J-3 Nafi Kasikcioglu
1st Lt TUAF

DEPARTMENT OF THE AIR FORCE
AIR UNIVERSITY
AIR FORCE INSTITUTE OF TECHNOLOGY

Wright-Patterson Air Force Base, Ohio

AFIT/GE/ENG/85J-3

LASER GUIDANCE WITH TRIAD DETECTOR ARRAY STRAPDOWN SEEKER

THESIS

AFIT/GE/ENG/85J-3 Nafi Kasikcioglu
1st Lt TUAF

Approved for public release; distribution unlimited

AFIT/GE/ENG/85J-3

LASER GUIDANCE WITH TRIAD DETECTOR ARRAY STRAPDOWN SEEKER

THESIS

Presented to the Faculty of the School of Engineering
of the Air Force Institute of Technology
Air University
in Partial Fulfillement of the
Requirements for the Degree of
Master of Science in
Electrical Engineering

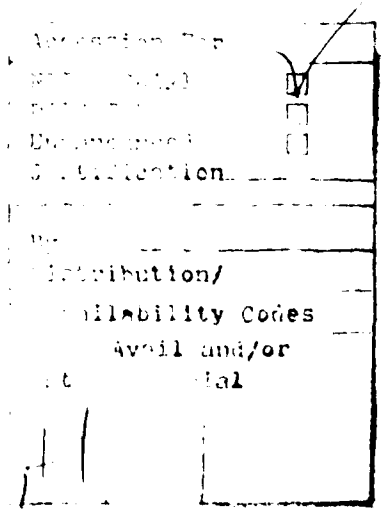

By

Nafi Kasikcioglu, BSEE
1st Lt TUAF

June 1985

Approved for public release; Distribution unlimited

Contents

Contents

List of Figures

List of Figures

List of Figures

List of Tables

List of symbols

θ : Bomb pitch angle
ψ : Bomb yaw angle

u : Bomb true velocity

α : Bomb angle of attack

β : Bomb side slip angle

v : Bomb lateral velocity

γ : Bomb flight path angle

$\delta\theta$: Bomb pitch angle perturbation

$\delta\theta$: Bomb yaw angle perturbation

δu : Bomb true velocity perturbation

$\delta\alpha$: Bomb angle of attack perturbation

$\delta\beta$: Bomb side slip angle perturbation

δv : Bomb lateral velocity perturbation

δe : Elevator deflection

δr : Rudder deflection

XB : Bomb position along x-axis

YB : Bomb position along y-axis

ZB : Bomb position along z-axis

XT : Target position along x-axis

YT : Target position along y-axis

Xb : Body fixed x-axis of the bomb

Yb : Body fixed y-axis of the bomb

Zb : Body fixed z-axis of the bomb

Xt : Target frame x-axis

Yt : Target frame y-axis

List of symbols

Xd : Laser spot x-axis location on detector

Yd : Laser spot y-axis location on detector

Eel : Elevation error angle

Eaz : Azimuth error angle

Xi : Inertial frame x-axis

Yi : Inertial frame y-axis

Zi : Inertial frame z-axis

INT : Intermediate longitudinal angle

INT : Intermediate lateral angle

Xu : Bomb true velocity x-axis component wrt the IF

Yu : Bomb true velocity y-axis component wrt the IF

Zu : Bomb true velocity z-axis component wrt the IF

Vx : Bomb lateral velocity x-axis component wrt the IF

Vy : Bomb lateral velocity y-axis component wrt the IF

Vt : Target velocity

Vtx : Target velocity x-axis component wrt the IF

Vty : Target velocity y-axis component wrt the IF

Δt : Calculation step size

λ : Wavelenght

σ : Attenuation coefficient

IF : Inertial Frame

ABSTRACT

The triad detector array strapdown seeker is designed to guide a bomb toward the target designated by a laser. The signal processor determines the error signals related to the error angles of the bomb fixed x-axis from target LOS. Error signals are employed as correction commands to the bomb control surfaces in order to keep the bomb in the target LOS. The complete system is simulated as a computer algorithm to evaluate the performance of the triad detector array strapdown seeker. The trajectory of the bomb is determined by the computer algorithm from the release point to the impact point.

The results revealed that the triad detector array strapdown seeker provided pursuit guidance for nonmoving targets and achieved destuction.

LASER GUIDANCE WITH TRIAD DETECTOR ARRAY STRAPDOWN SEEKER

I. INTRODUCTION

Background.

One of the most important missions of the Air Force is to destroy the enemy targets that maintain the enemy resistance. Before the use of guided munitions, conventional weapons, high-explosive bombs dropped from high or medium altitude and bombs or rockets delivered in a diving attack, were employed. The use of these conventional weapons require the aircraft to be flown steadily for some seconds at an altitude and range which make the attacker airplane extremely vulnerable to modern ground-to-air weapon defenses. To avoid destruction, the attacker must release his bombs from outside the range of the anti-aircraft defenses or, alternatively, must attack at an altitude of a few hundred feet so that the enemy has inadequate warning of the impending attack and can not bring effective fire to bear.

The guided bomb is one attempt to apply guided weapons to reduce the exposure while maintaining the desired probability of destruction on the enemy targets. The bomb, which either glides or carries its own motor to give it additional range, is released by the bomber in the direction of the target. One of two guidance methods are then

employed. Either the bomb guides itself toward the target, having had the target designated before release, or a controller in the aircraft observes the bomb and the position of the target, and sends the necessary steering signals so that the bomb hits the target. In both cases it is possible for the bomber to turn away to safety, after it has released its weapon. The advantages are then :

1) the attacking aircraft stays out of danger and

2) greater accuracy of delivery.

For a low level attack, the price that the attacking aircraft pays for the concealment is that the pilot may not acquire the target until shortly before release of the weapon. In fact, he may not see the target accurately until he is passing it. This makes it difficult to employ conventional high explosive weapons accurately. However, it is possible with guided-weapon technics for the attacking aircraft to release a weapon when it is near the target area then, subsequently, to guide the weapon accurately to the target when launching aircraft is speeding away from the area. Against some small but vital targets, there is a need for a precisely steered missile to be fired in a diving attack from the aircraft. The guidance system greatly improves the accuracy of the missile attack above that of the unguided case; in addition, the attack is concluded at a longer range from the target, reducing the exposure of the attacking aircraft. (Ref.2)

The evolution of guidance technics :

One of the earliest short-range guided missiles was the German X-4 of World War II. Control signals were transmitted over a pair of wires from the aircraft to this air-to-air missile. About three miles of 0.2 milimeter (mm) insulated steel wire was reeled from the wing tips of the missile as it sped toward an enemy aircraft. The position of the missile relative to the target was observed optically from the launching aircraft, and it was directed onto the desired trajectory without using any form of radio or radar signals.

Another World War II development was Radar Fire Control. In this operation, a tracker radar followed the oncoming enemy bomber, and a computer directed the antiaircraft gun into the proper position to fire into a zone calculated to intercept the bomber. Actually, The tracking movement of the radar antenna was fed across to the gun mount with corrections made by the computer for the proper lead angle. The arrangement used for transferring this motion to the gun known as a synchro system. Radar fire control technics in particular contribute to a typical ground-launched system utilizing radar command guidance.

Using two radars and a computer, both the target and the missile can be followed and the correct course for the missile determined. One radar tracks the target; the other the missile. Commands are sent to the missile over its radar guidance channel or by seperate communication channel. This technique was used by the Germans during World War II.

Another well known radar-guidance method is the beam-rider technique in which the target is illuminated by the ground radar. The missile is launched into this beam and follows it to the target. Deviations from the beam pattern are detected by a receiver in the missile. Corrections are made to insure that the correct path is followed.

Guided missiles launched from an aircraft may employ a self-contained radar receiver to receive the radar reflections from a target illuminated by the launching aircraft. The missile may operate as a beam-rider and follow the illuminated beam to the target, or it may simply home on the reflected radar signal. This technique is known as semi-active homing guidance, since there is a radar signal from the launcher or a seperate site, and the missile does not radiate a signal. Another form of target seeking known as passive homing, is also utilized in some designs. In this type of guidance, a receiver in this missile may pick up radar signals from the target aircraft or an infrared receiver may utilize the heat radiations from the engines of the enemy aircraft. (Ref. 5)

Semi Active Laser-Guidance Concept.

After the invention of the laser in 1960, the first military application of the lasers was a laser rangefinder. It measures the time difference between transmitted and reflected radiation from aimed object, and this time difference is converted into distance data. The laser

rangefinder depends on the reflection of the laser radiation from objects. The same phenomena has enabled the lasers to be used in the guidance concept as laser beam-riding guidance. In the laser guidance concept, a laser is used to illuminate the target, and the laser seeker mounted on the bomb or missile provides error signals which are used to guide the bomb or missile toward the target. Laser radiation has such properties which enable its use to illuminate the targets to be destroyed by guided munitions. These properties are stated as follows : (Refs. 7,10,12)

1) Laser radiation is nearly monochromatic, and it has spatial and temporal coherence. This simply means that such a beam is composed of almost one frequency of radiation, or the band width is very narrow and centered around the operating frequency. A laser can operate in the infrared (IR), visible or ultraviolet region of electromagnetic radiation. So its operating frequency is between $25X10^{12}$ Hertz (Hz) and $75X10^{13}$ Hz. But its operation bandwidth is not more than $2X10^{9}$ Hz. Also this beam has continuing (in phase) properties and polarizations as it travels away from its generating source.

2) The shape of the resonator and the shortness of the wavelenght of the radiation make the laser emission look like a pencil beam. A narrow beam is produced because many of the excited atoms are stimulated to emit in a specific direction, other than in all random directions. This accounts for the extreme brightness and directionality of a laser. The energy contained in a laser beam can be concentrated on a spot less

than 0.001 inch in diameter. Also a very small beam divergence enables the laser radiation to be sent long distances without attenuating its energy. Further it is possible to illuminate an area that was less than the size of a target, eliminating reflections from the surrounding area.

These properties led to the development of air-to-surface and surface-to-surface semiactive laser terminal homing systems for use against tactical targets. In the laser semiactive guidance, rather than calling these laser devices "illuminators", as in the radar case, they became known as "designators", because their angle resolution is high enough to designate a specific target. They serve the same function as the radar illuminator, but in a slightly different manner. Their very small beamwidth makes them difficult to employ against a maneuvering target, such as an airplane. Moreover laser designators are commonly aimed at the target by a human operator using some type of optical sight or imaging system. Therefore, laser designators are usually used against stationary or slowly moving targets. (Ref.4)

Weapons employing semiactive laser seekers may be launched from a position near the laser designator or from a remote location. The seeker may be locked on before launch or it may go through a search and acquisition phase and lock-on after launch. The laser designator signals may be coded so that a given missile will only track its intended target, allowing multiple designators to be used in an area

containing many targets.

Figure 1.1 illustrates the semiactive laser guidance employing a ground based laser designator and a remotely launched missile containing a laser seeker. The designator beam is very narrow shown by the small arc extending from designator to the target. The designator is pointed at the target by an operator using an optical sighting device. The laser energy is scattered in all direction by the target, due to its surface roughness. This reflected signal is received by the laser seeker in the nose of the incoming missile and is processed to provide guidance commands to guide the missile to impact the target as the source of the reflection.(Ref.4)

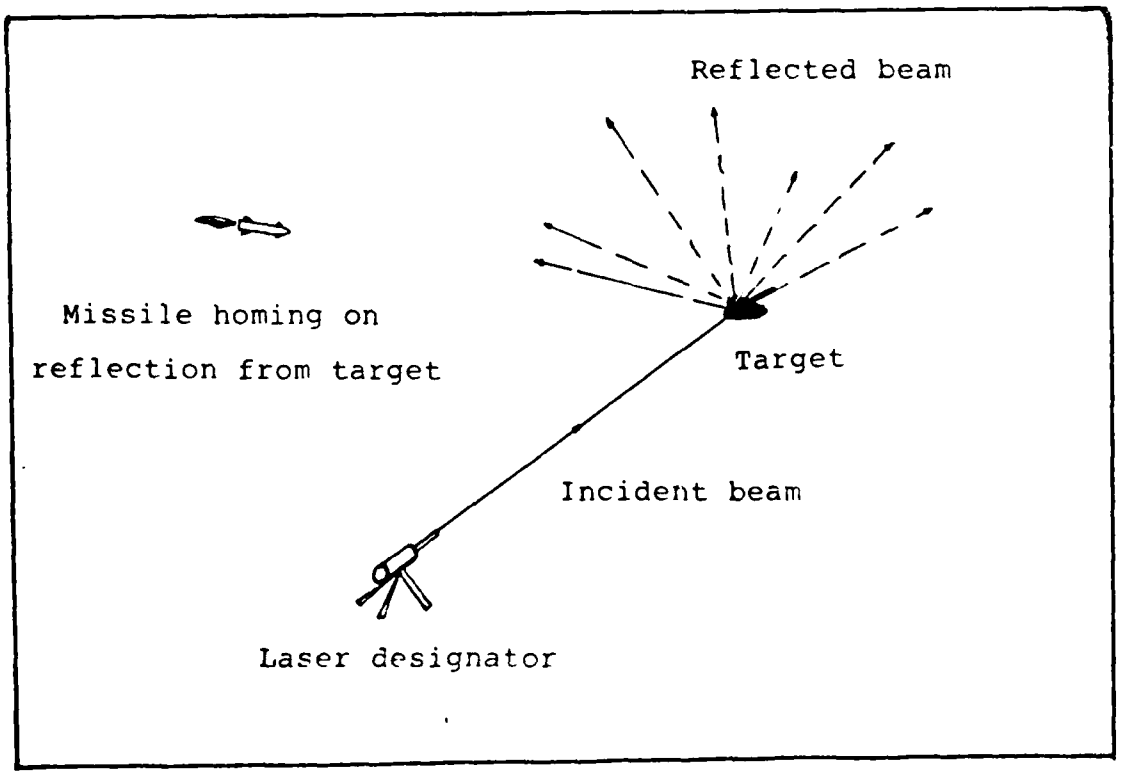

Figure 1.1 Semi-Active Laser Guidance.

Semiactive laser guided weapons are not qualified as fire and forget or launch and leave weapons. The designator must be pointed at the target to provide the homing signal throughout the bomb's or missile's flight; however an aircraft may leave the area immediately after launching missiles or bombs that are intended to home on the reflection from a laser designator aimed by a forward observer on the ground (Ref.4). Since laser-guided weapons depend on laser radiation reflected from the target for guidance during terminal flight, the laser beam must be maintained exactly on the target to prevent laser energy "overspill" which would create a false target (Ref.9)

Laser-Guidance Requirements.

1-Transmitter.

The main reasons for the use of guided weapons are to increase the probability of hitting the target and decrease our equipment, ammunition, and personnel losses. The designator transmitter, actually a laser, has to provide enough energy to designate the target at a safe distance. For power applications, three particular lasers are most often used: The Neodymium:Yttrium Aluminum Garnet (Nd:YAG), Neodymium:Glass (Nd:Glass) and the carbon dioxide (CO2) lasers.(Ref.10)

Both the Nd:YAG and the Nd:Glass lasers emit at the infrared wavelenght of 1.06 micrometer (μm). In Nd:YAG lasers, the neodymium ion (Nd+3) is doped into a host crystal

(YAG). The Nd:YAG laser can be operated in a continuous wave (CW) mode, but it is usually operated in a pulsed mode at rates up to 4000 pulses per second (pps). Although the output energy of the Nd:YAG laser is limited mainly by the small size of the synthetic YAG crystal rarely larger than a pencil, at a reduced pulse rate with sufficient time for the laser material to cool, as much as 10 joules per pulse can be delivered with 100 microsecond (μsec.) pulse widths.

In the Nd:Glass laser, the Nd+3 ion is doped into a noncrystalline medium, glass. The storage volume of the glass laser is considerably larger than that of the crystalline laser, because there are no size limitations on the medium beyond those imposed by uniformity of the material and the ability to cool it. The glass medium broadens the neodymium ion lasing transition more than the garnet crystal does; therefore for Nd:Glass lasers, more modes are available for mode locking which is a technique for producing high-power, short duration laser pulses.

The other laser frequently used for power applications, the CO2 laser can furnish up to ten kilowatts of power when used in CW mode. If this laser is used in pulsed mode, then it can provide several hundred joules in a 100 nanoseconds (nsec) pulse, corresponding to peak power of approximately one gigawatt (10 Watts). The output of CO2 lasers is in the infrared region of 10.6 μm. (Ref.10)

2-Atmospheric Transmission.

For laser guidance, the atmosphere is the medium for transmission of the laser radiation from the laser transmitter to the target, then from the target to the receiver mounted on the bomb. So, the atmospheric effect on the laser radiation is one of the limitation factor for the laser guidance.

Optical transmission of radiation energy is most usually expressed by:

$$T=\exp(-\sigma R),$$

where σ is the attenuation coefficient and R is the lenght of the transmission path (Ref.11). The attenuation coefficient is the result of two processes: scattering and absorption. The scattering portion of the attenuation coefficient may be further broken down into scattering from air molecules and from aerosols. Since the pressure and the aerosol density in the atmosphere differ from location to location on the Earth, scattering from aerosols is a function of atmospheric pressure and geographic location. In addition, the absorption portion of the attenuation coefficient is actually a function of the radiation wavelenght. Since the molecules in the atmosphere absorb different wavelenghts, the transmission of the different wavelenghts (and the absorption of the different wavelenghts) are different. Water and carbon dioxide in the atmosphere have a weak absorption on the 10.6 m. radiation wavelenght. But, for 1.06 μm. radiation, there is no specific absorber. So that the attenuation of the

atmosphere for the 1.06 μm. radiation wavelenght is considerably low. For that reason, Nd:YAG and Nd:Glass lasers can be used more effectively than the CO2 lasers. Slant path transmittence at 1.06 μm. radiation wavelenght for a model standard clear atmosphere is shown on Figure 1.2. (Ref.14)

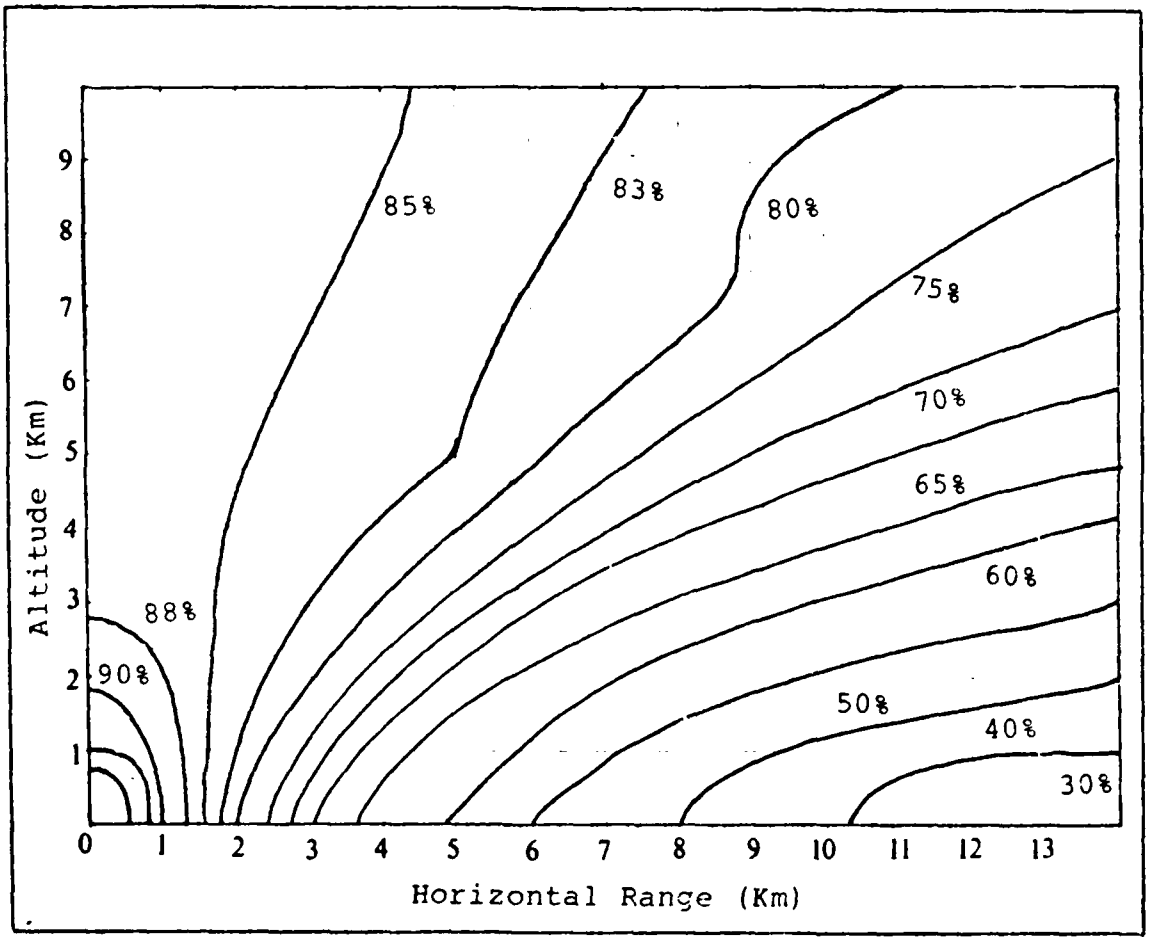

Figure 1.2 Contours of Percent of Atmospheric Transmission for Radiation at 1.06 m.

3-Laser Seeker and Receiver.

Two types of laser seekers have been used for semiactive laser guidance : gimballed and strapdown seekers. The major difference between gimballed and strapdown seekers is the information provided mechanically by a gimballed seeker is derived electronically in a strapdown seeker. Such information may be the azimuth and elevation angles of the line-of-sight (LOS) to the target, the rates of change of these angles , target range and target range rate. The other important difference is the coordinate frame in which the information is measured. To implement most guidance techniques, inertially referenced angle information is necessary. (Ref.13)

A gimballed seeker is characterized by the ability to rotate its sensitive axis with respect to the vehicle (missile or bomb). This rotation is accomplished using two gimbals and torquer motors to keep the seeker antenna centerline aligned with the LOS to the target. The LOS can be quantitized by potentiometer measurements of the two gimbal angles. Inertially referenced azimuth and elevation angles, and the angle rates can be measured directly from rate gyroscopes on the inner gimbal. The basic gimballed seeker is shown in Figure 1.3. The instantaneous field of view (FOV) is an angular region about the seeker boresight from which it receives usable energy. The total FOV is the region swept out by the instantaneous FOV as the gimbals are rotated to their limits.

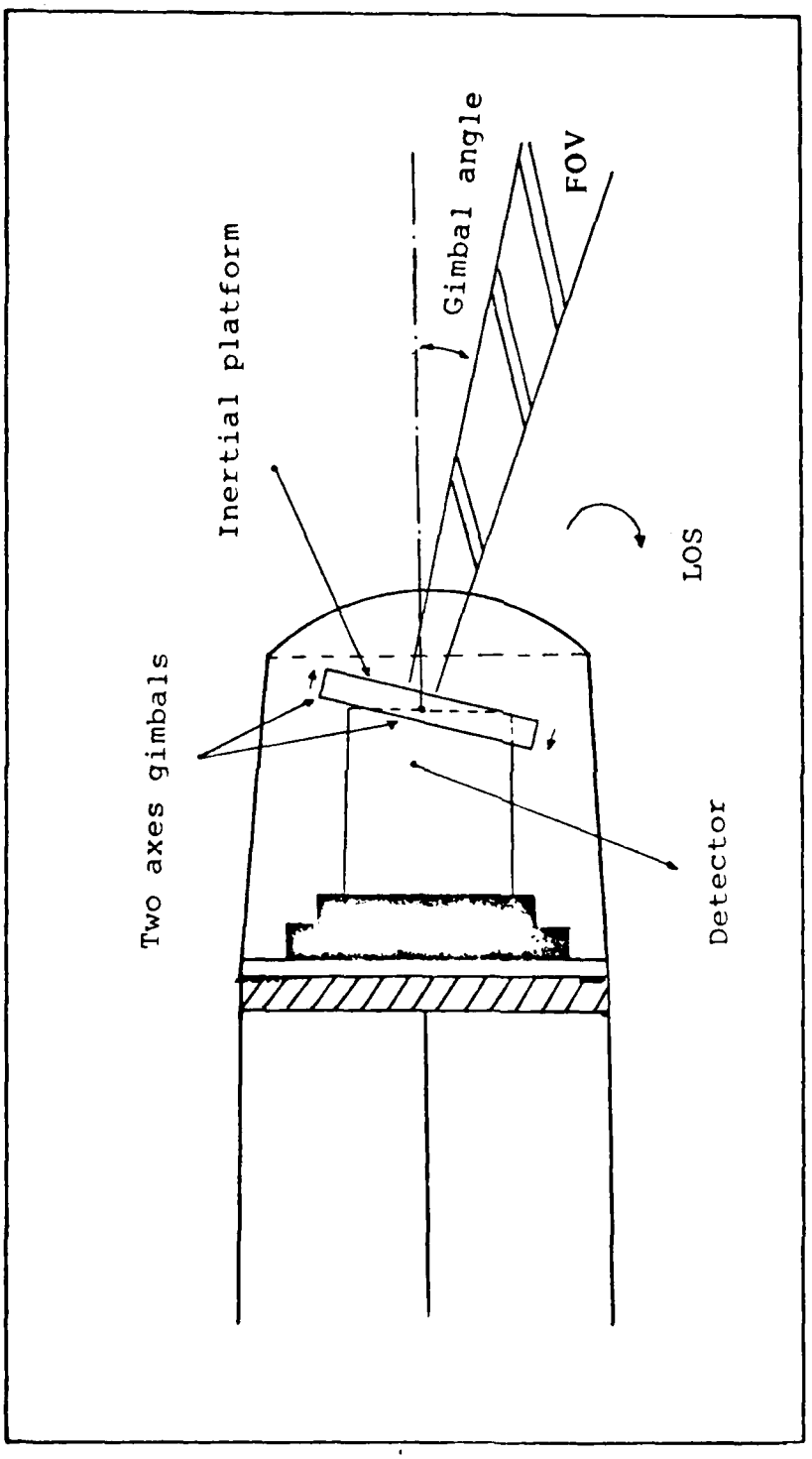

Figure 1.3 Basic Gimballed Seeker

A strapdown seeker, on the other hand, is fixed to the body of the missile or the bomb. Such a seeker operates by electronically measuring the LOS angles with respect to the vehicle body and, possibly, the range and/or range rate to the target. Inertial LOS rates cannot be measured directly from a strapdown seeker.

There are two basic types of strapdown seekers : beam-steered and staring (Figure 1.4). The beam-steered seeker is similar to a gimballed seeker in that it has a small instantaneos FOV which can be moved relative to the vehicle body. An active radar seeker with phased array antenna is an example of beam-steering. The staring type has an instantaneous FOV equal to tha total FOV. An example of a staring type strapdown seeker is the semi-active laser seeker with a wide FOV (Ref.3)

Strapdown or body-fixed seekers with sufficient FOV for the terminal guidance of many tactical weapons have now being used. Such seekers have a number of advantages over gimballed seekers, including increased reliability and unlimited LOS rate capability. The maior disadvantage is that inertial LOS rates are not directly available for the implementation of proportional navigation (Ref.14)

Both, the strapdown and the gimballed seekers have sensing systems to track the radar or the laser energy. For the strapdown seeker, a mozaic detector array that consists of several detectors can be used to track the laser energy.

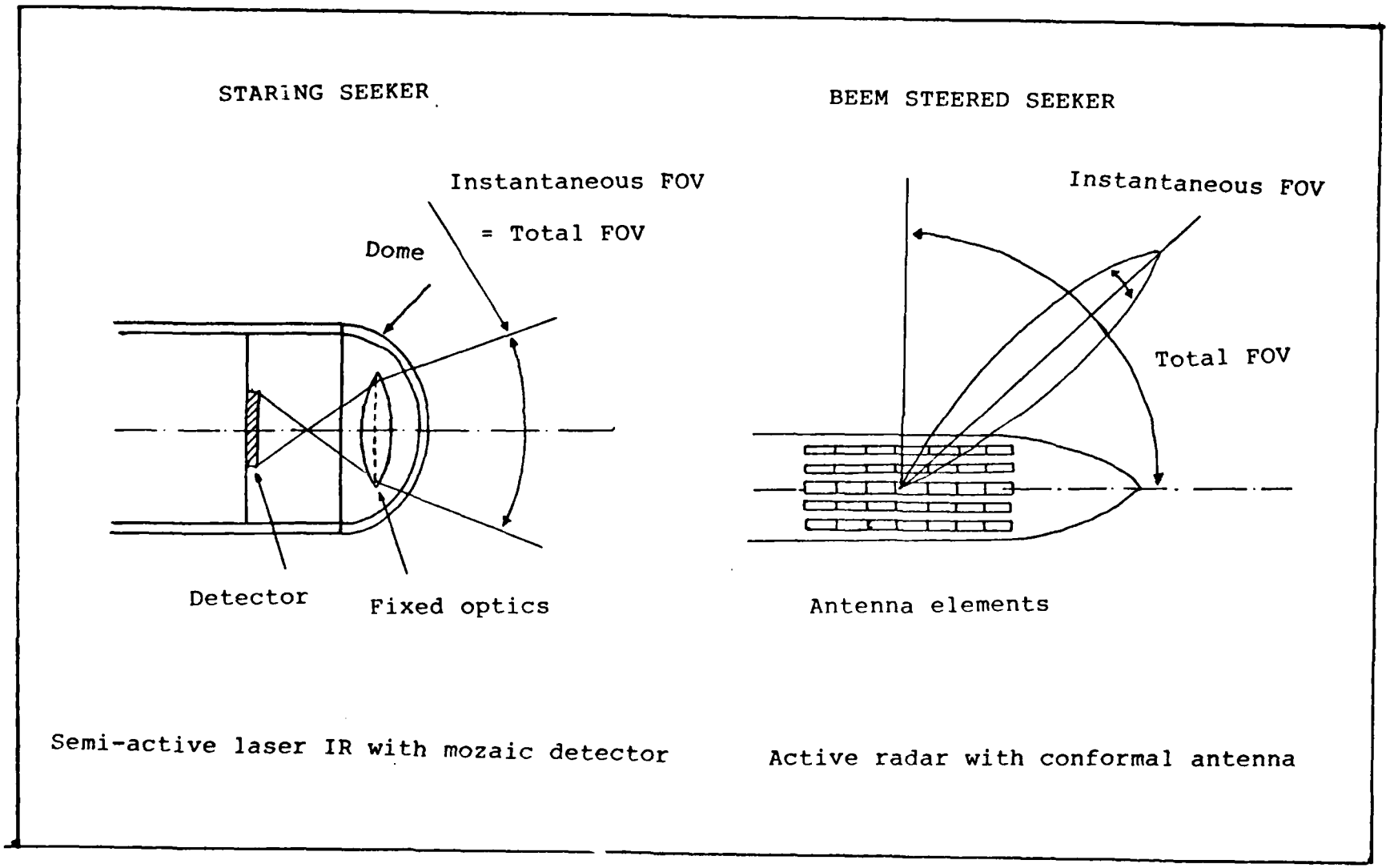

Figure 1.4 Basic Types of Strapdown Seekers.

An array with four detectors is called a quadrant detector array and provides enough information to track the reflected laser energy from the target. As the seeker is tracking the reflected laser energy, it enables the vehicle to guide itself toward the target.

Quadrant Detector Array Sensor for Strapdown Seeker.

This sensor can be used to track pulses of radiant energy which may come directly from a laser beacon, or may be reflected from an illuminated target. In reflected beam trackers, the laser source may be included as part of the tracker system (active tracking) or positioned at some remote site. Figure 1.5 shows a diagram of the optics and the detection system (Ref.14). The angular subtense of the laser beam radiated from the target must be consistent with the target-to-laser distance and the target size to provide clear designation for the tracker.

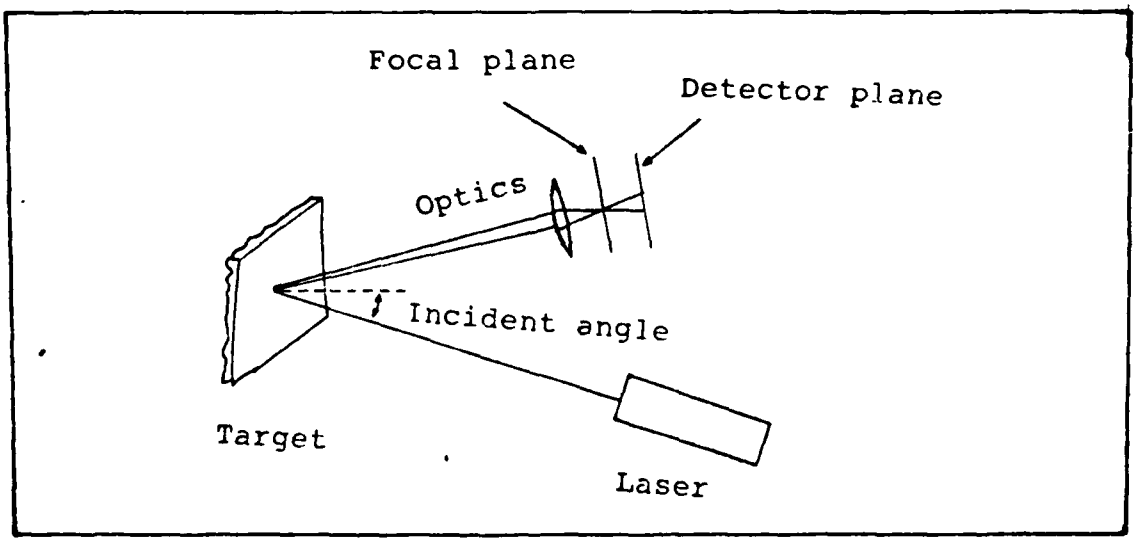

Figure 1.5 Optics and the Detection System.

The tracker computes the estimates of position error from each detected pulse to recenter the receiver (Figure 1.6). The four element array is connected in a quadrant detector configuration, and this scheme provides a nearly linear error signal versus position offset.

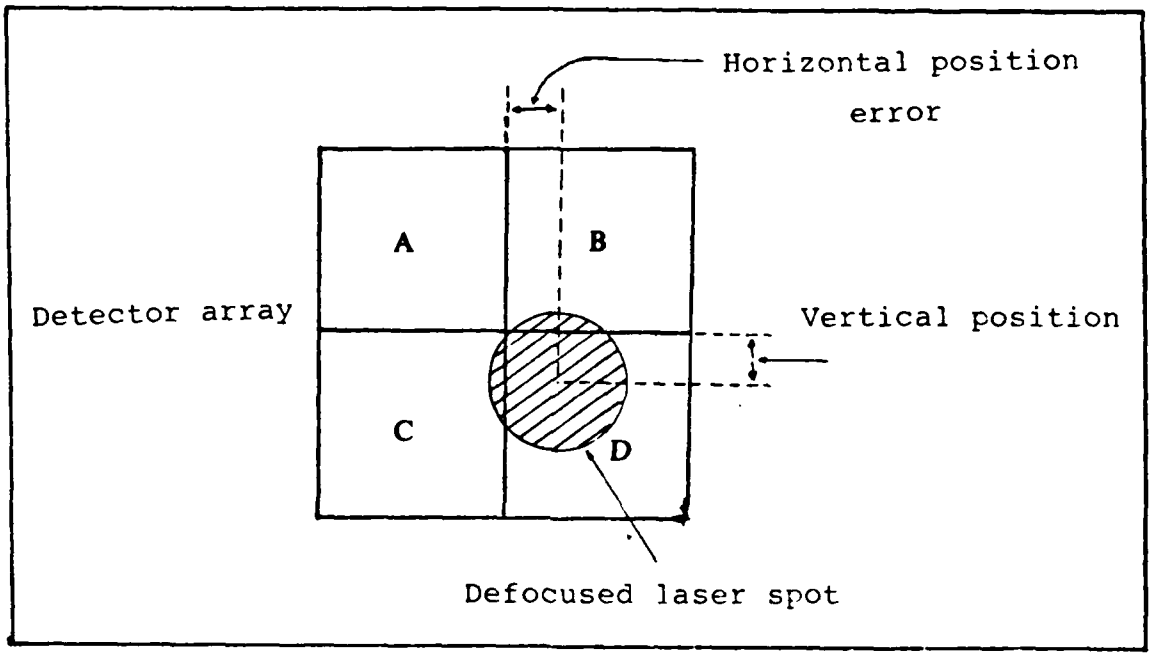

Figure 1.6 Defocused Laser Spot on the Quadrant.

The output of each detector is proportional to the image power incident upon its sensitive area. The tracker electronics determine the position offset as the elevation and the azimuth error signals according to the location of the incident laser beam on these four detectors. A block diagram in Figure 1.7 shows the signal processing functions of pulsed laser quadrant detector array sensor system .

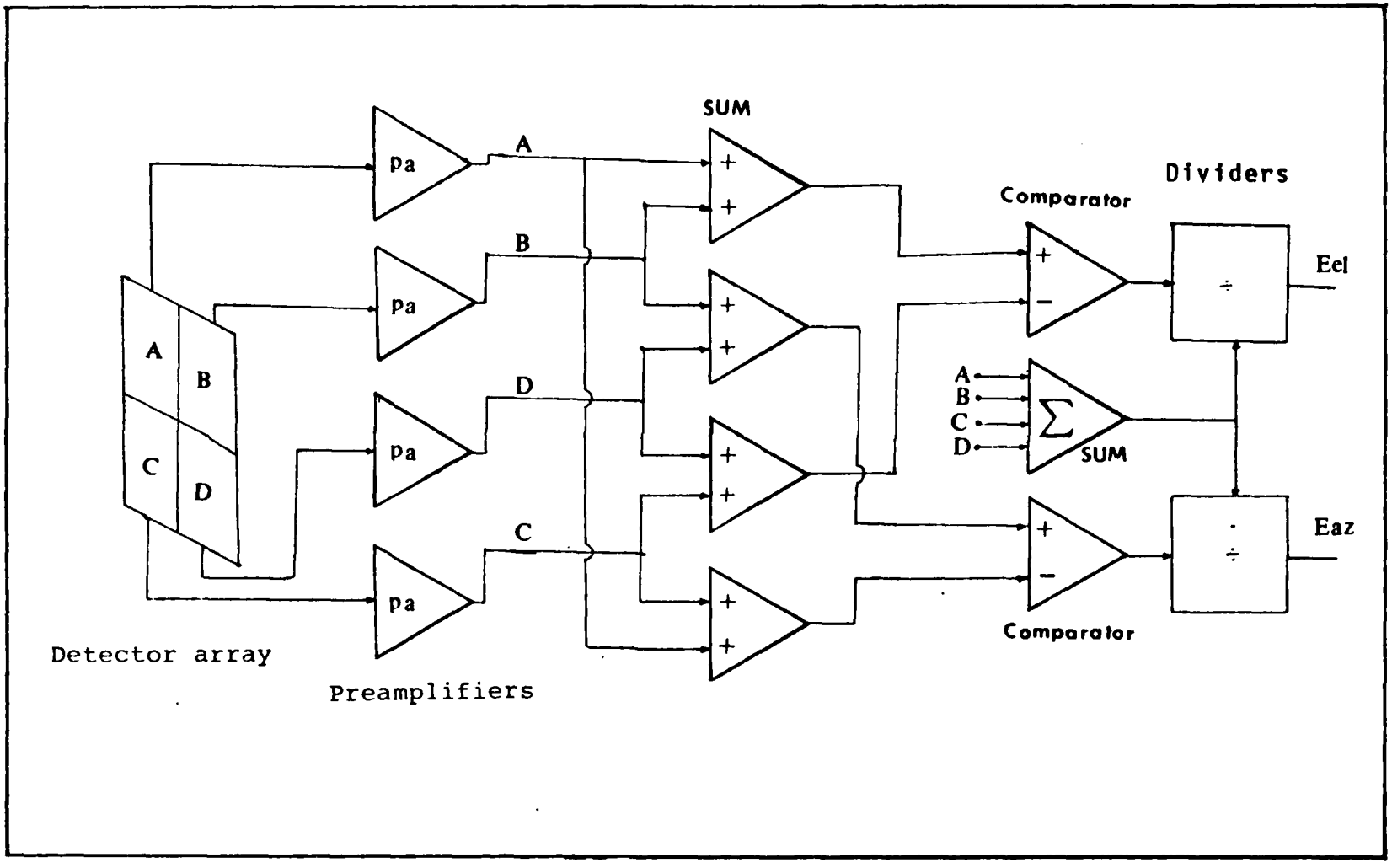

Figure 1.7 Signal Processor for Quadrant Detector Array Strapdown Seeker.

The error signals for the elevation and azimuth axes are calculated as a function of the laser radiation intensity upon each detector.

Elevation error signal:

$$EL = \frac{K1(IA+IB)-(IC+ID)}{IA+IB+IC+ID}$$

Azimuth error signal :

$$AZ = \frac{K2(IA+IC)-(IB-ID)}{IA+IB+IC+ID}$$

Where IA, IB , IC , ID are the incident radiation intensities upon A, B, C, and D detectors. K1 and K2 are the signal processor constants.

Statement of the Problem and Objectives.

The main work on this thesis is to determine the guidance conditions and the accuracy of the laser guided bomb while using a three detector array strapdown seeker, instead of a quadrant detector array seeker. As with the quadrant detector array, the three detectors are connected in an mozaic array configuration which determines the azimuth and elevation error signals in terms of the deviation angles of the centerline of the detectors from the direction of the target. The servo controller device drives the control surfaces according to these error signals, and the bomb is guided onto the flight path toward the target. The complete system is modeled to analyze the performance of this triad detector seeker by a computer algorithm.

The objectives can be summarized as follows :

1) Develop a signal processor to generate the azimuth and the elevation error signals according to the location of the incident laser beam reflected from the target on these three detectors.

2) Develop a computer algorithm to simulate the system. Bomb release position and velocity, target location and movement will be the inputs of the algorithm. The noises and the errors will be generated as random numbers. Also the mean and the variance values of the error and noise sources will be inputs to the algorithm.

3) The computer algorithm will determine the trajectory of the bomb toward the target. The simulation will be tested by different conditions. Then, the stability of the bomb and probability of the destruction of the target will be evaluated under several sets of conditions, for the laser guided bomb constructed with triad detector array strapdown seeker.

Assumptions.

The transfer functions of the laser guided bomb are determined by assuming the bomb is a subsonic flying vehicle. The movements of the bomb are considered in two directions in the body fixed frame by ignoring the rolling movement. The assumptions related with the elements of the system will be given as they are described in following chapters.

Organization.

Chapter II contains the explanation of the laser guided bomb model employed and the developement of the triad detector array strapdown seeker model. Chapter III presents the simulation and the algorithm design of the complete system described as a triad detector array strapdown seeker mounted a generic bomb released from an airplane to destroy a moving or non-moving target designated by a laser. Chapter IV contains the results of the simulation of the guidance of the bomb for several sets of conditions and the modifications on the model implementations. Chapter V summarizes this work and the conclusions determined from the results and also includes the recommendations for future study. The computer algorithm and the trajectory and the error angle plots are found in the apendices.

II. TRUTH MODEL

Introduction.

The simulation of the laser guided bomb which has triad detector array strapdown seeker is based on the truth models of the seeker and the bomb dynamics. Each model includes their noise and error effects. The signal processor for the seeker is developed just for this triad detector array. It determines the commands to guide the bomb to the target. The same seeker may be used both for bomb and missile application by changing the gain values. The complete guidance concept begins from the laser designator.

Designation and Transmission Model.

It is assumed that the laser guided bomb is released from an airplane about 15 to 20 kilometers (Km) from a moving or non-moving target. The target is illuminated by a Nd:YAG uncoded laser designator which deliveres enough energy so that the reflected laser radiation from the target can be seen by the seeker at the maximum slant range of 20 Km. The seeker signal processor has an automatic gain control device, therefore the laser radiation intensity level incident upon detectors is not important unless it is less than the detector threshold radiation value. Only the location of the laser spot on the triad detector array determines the correction signals. For that reason, the atmospheric attenuation of the laser energy from the designator to the

target, then from the target to the seeker, and the attenuation from the target scattering are not considered as a part of this simulation.

The seeker is a sensor for laser radiation. When the target is designated by the laser, reflected radiation provides correct location information of the target according to an inertial frame (Figure 2.1).

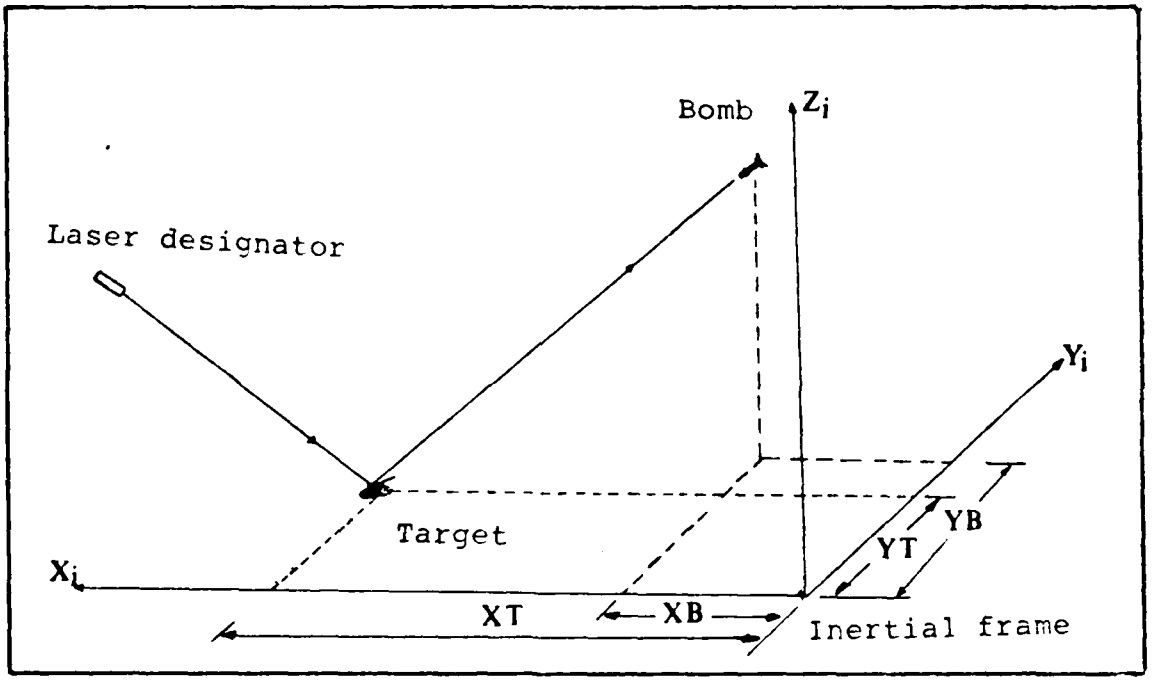

Figure 2.1 Designation Concept of Laser Guidance.

The laser beam is actually aimed to illuminate just a single point on the target, the reference location of the target. The laser designator can be located on the ground or on an airplane. In either case, the person or the mechanization used to maintain the beam on a single point on the target may not provide a fixed reference for the laser seeker eye. Also, erratic target reflections and the

atmospheric turbulence and heat changes can cause jittering of the laser beam. If the top center of the target is assumed to be the desired aimed point and the center of the target frame, the laser spot moves around this point according to the variance values of this total jitting effect on X and Y direction. The probability density function describing the location the laser spot is assumed to be normally distributed (Figure 2.2).

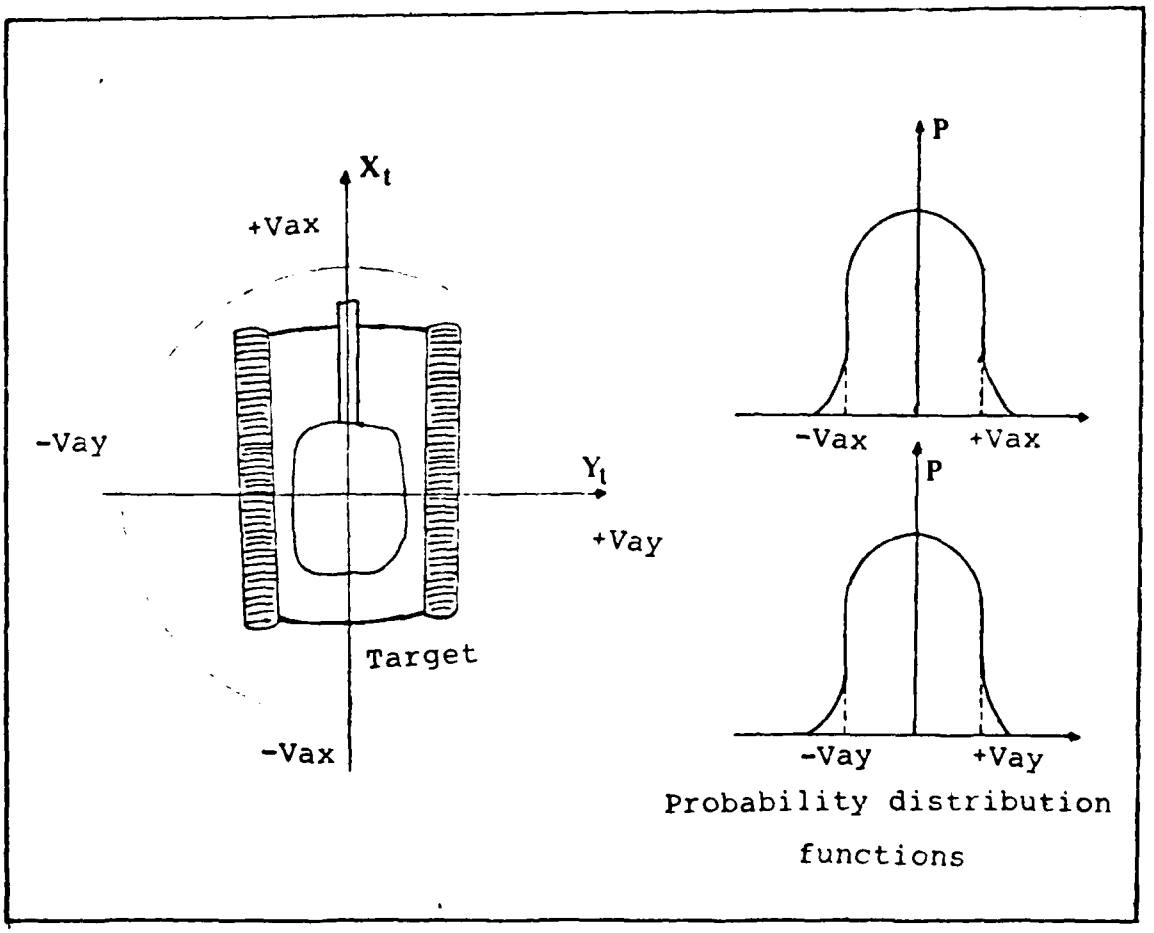

Figure 2.2 Target Induced and Atmospheric Jitter.

The change of location of the laser spot caused by the jitting can be considered as a change of position of the target as seen by the seeker. Actually when the bomb is far from the target, the jitting effect is not significant, but as it comes closer to the target, the jitting has more effect on determining the true location of the target. In addition, the further the laser designator is from the target, the larger the variance of the jitter will be, since there are increased atmospheric effects and larger displacement of the laser spot on the target (Figure 2.3)

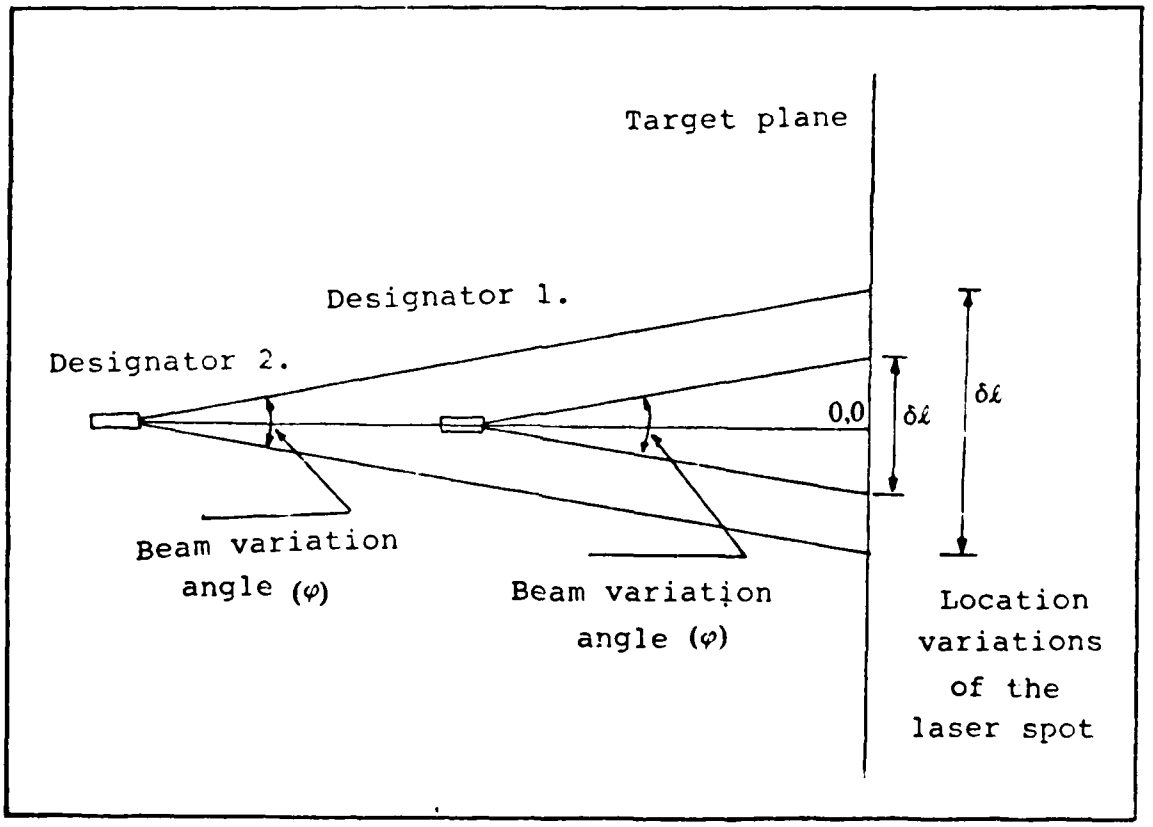

Figure 2.3 The Relation Between the Distance, Beam Variation Angle and the Location Variation.

Seeker Model.

In this simulation, the strapdown seeker used for semi-active laser guidance can be considered in two parts. They are :

1. seeker optics, and
2. seeker electronics.

Seeker optics provide the image of the target on the detectors by transmitting and focusing the laser radiation reflected from the target. Seeker electronics determines the error signals from the location of the laser spot on the triad array. The elements of the triad detector array strapdown seeker are shown in Figure 2.4.

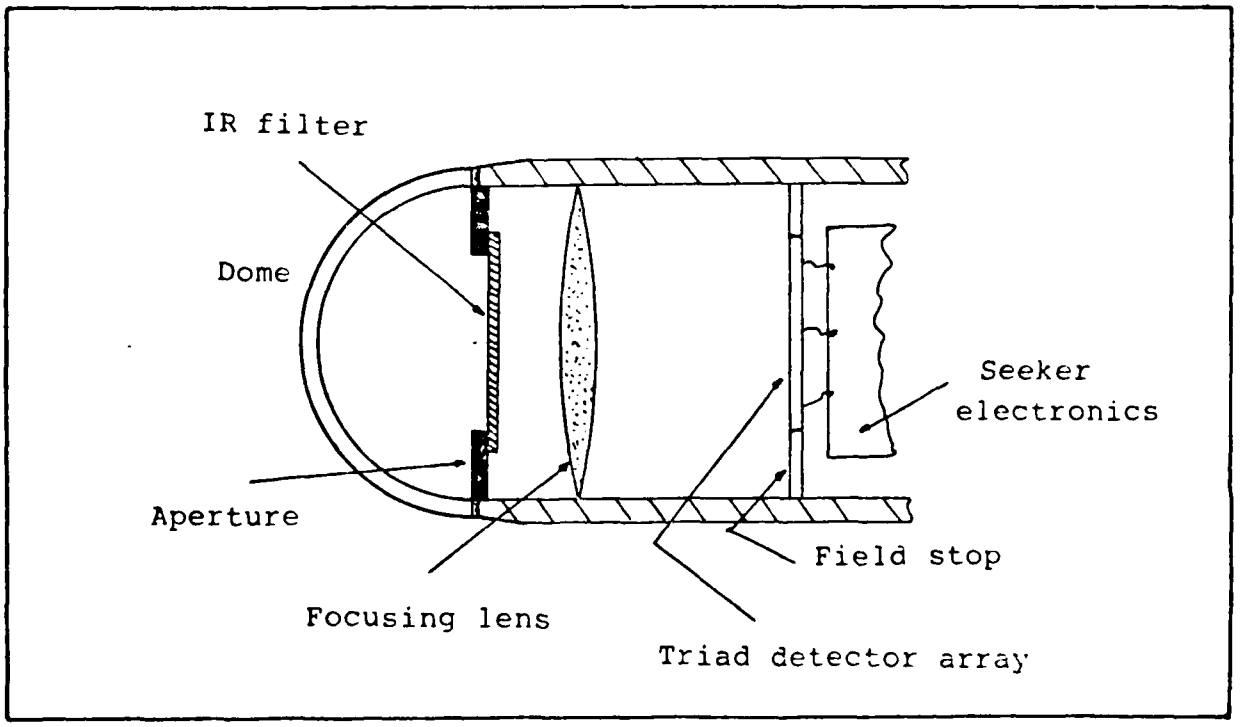

Figure 2.4 The Elements of the Triad Detector Array Strapdown Seeker.

1) Seeker optics.

Dome:

The dome is a semi-spherical window which protects the sensitive elements of the seeker from the small particles in the air. In order to transmit the laser radiation to the detectors without loss of energy, the dome has to be fabricated from special materials that are transmissive in infrared (IR) region. These materials can be germanium or cadmium sulfide, sodium chloride or potassium bromide, since they are transparent at 1.06 μm. radiation, a region where most other materials, including glass are opaque (Ref.10).

Aperture:

The aperture limits the cross section of the image forming energy. Making the aperture smaller makes the image dimmer, without restricting the field of view. The maximum allowed laser radiation on the detectors is adjusted by the aperture in the seeker optics (Ref.8).

IR filter:

The seeker includes an IR filter to reduce noise and excessive radiation in the band of all wavelenghts created by the daylight or the other radiation sources. It allows only 1.06 μm. radiation to be transmitted to the detectors. Also an IR filter can serve as a radiation limiter.

Focusing lens:

This lens converges the incident laser beam on the detector plane to provide a defocused spot. The location of this spot depends on the incident angle of the beam, which

represents the error angles to be corrected (Figure 2.5). The focusing lens has to be fabricated from special materials to be transmissive in IR region.

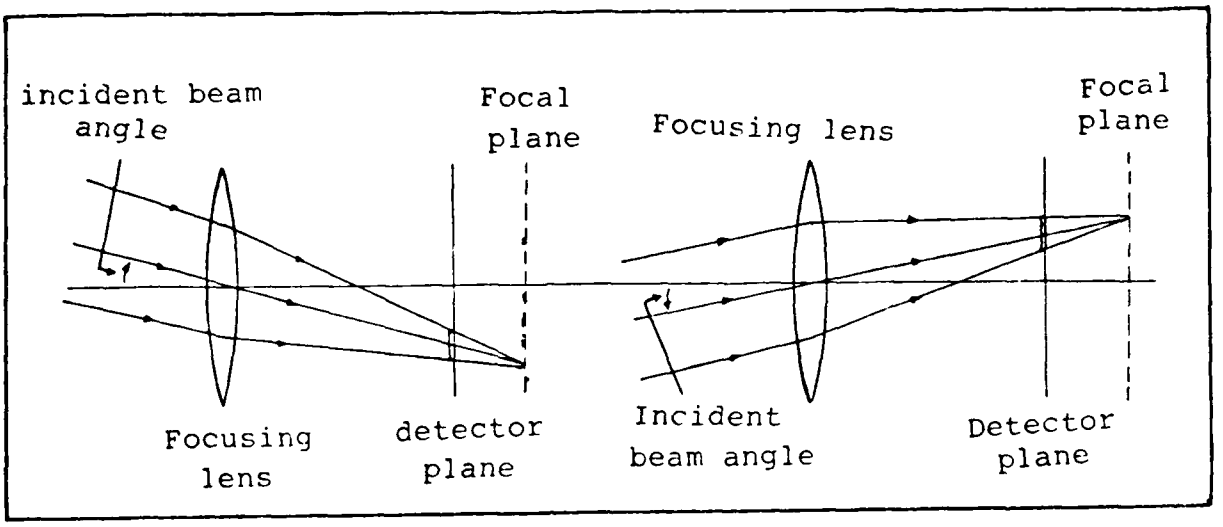

Figure 2.5 Change of the Spot Location on the Detector Plane by Change of Incident Beam Angle.

Field stop:

The field stop limits the angular field or FOV. As the field stop is made smaller, the FOV becomes more narrow, but the amount of light admitted remains the same (Ref.8). In the simulation the diameter of the detector array is assumed to be 3 centimeters (cm.). The field stop is actually the frame of the detector array to establish a 20° total angular FOV (Figure 2.6).

If it is assumed that the bomb is 15 Km away from the target, and the initial pitch angle of the bomb is -45 degrees from the horizon, then it means that seeker can see a target in an ellipse with major axis 7000 m and minor axis 5000 m (Figure 2.7).

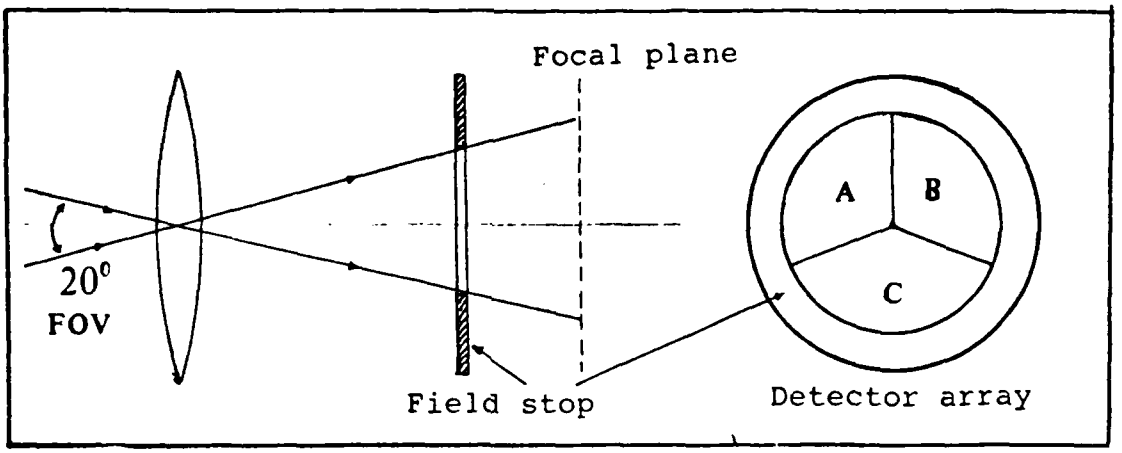

Figure 2.6 Field Stop of the Detector Array and the Relation with the Field of View.

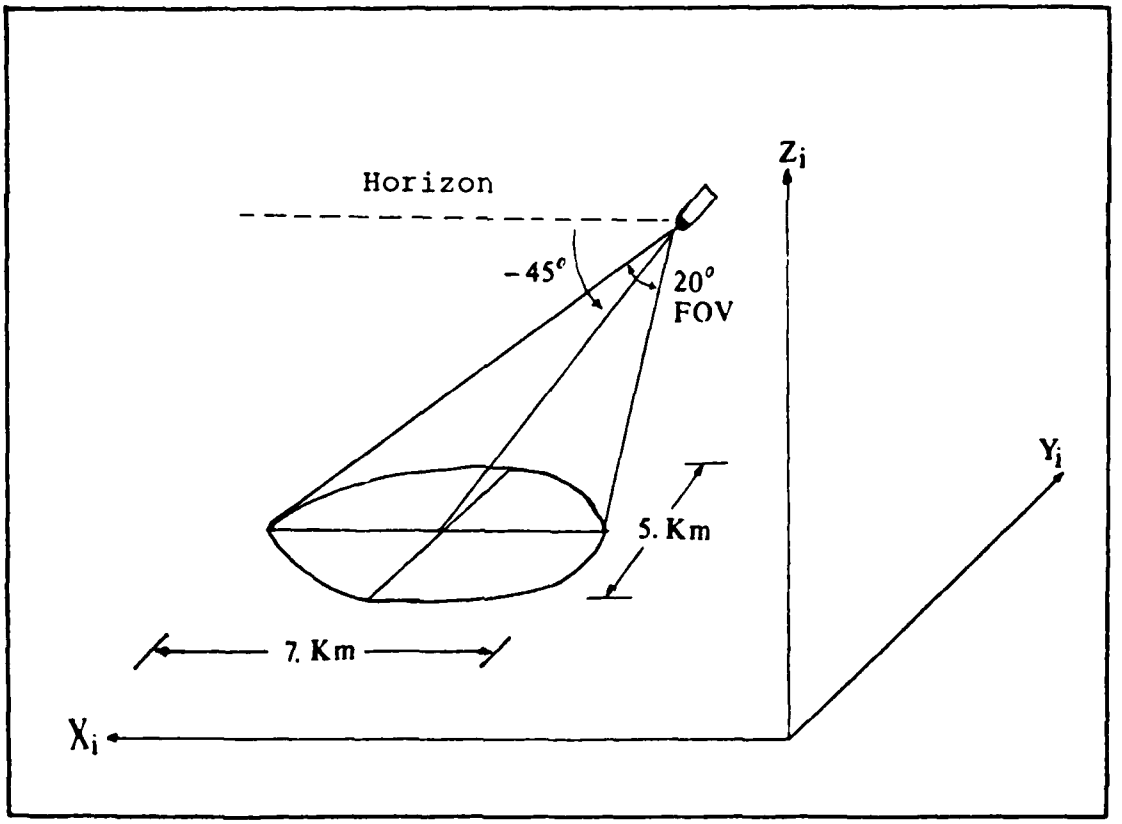

Figure 2.7 Field of View and the Area that FOV Covers.

The lens that is used in the seeker is a converging lens. Thus the lens converges a parallel beam at the focal point. When the incident beam includes more than one wavelenght, each wavelenght is converged to a different focal point. That is called lens aberation. In this simulation, the IR filter prevents the lens aberation, because it is assumed that the filter passes just a single wavelenght 1.06 μm. Because of the manufacturing errors, the lens might be mounted tilted. Therefore instead of converging the zero degree incident beam on the focal point, it focuses this beam at different point (Figure 2.8). This angle can not be more than 0.2 degree but it still causes boresight errors. The simulation includes this error as constant

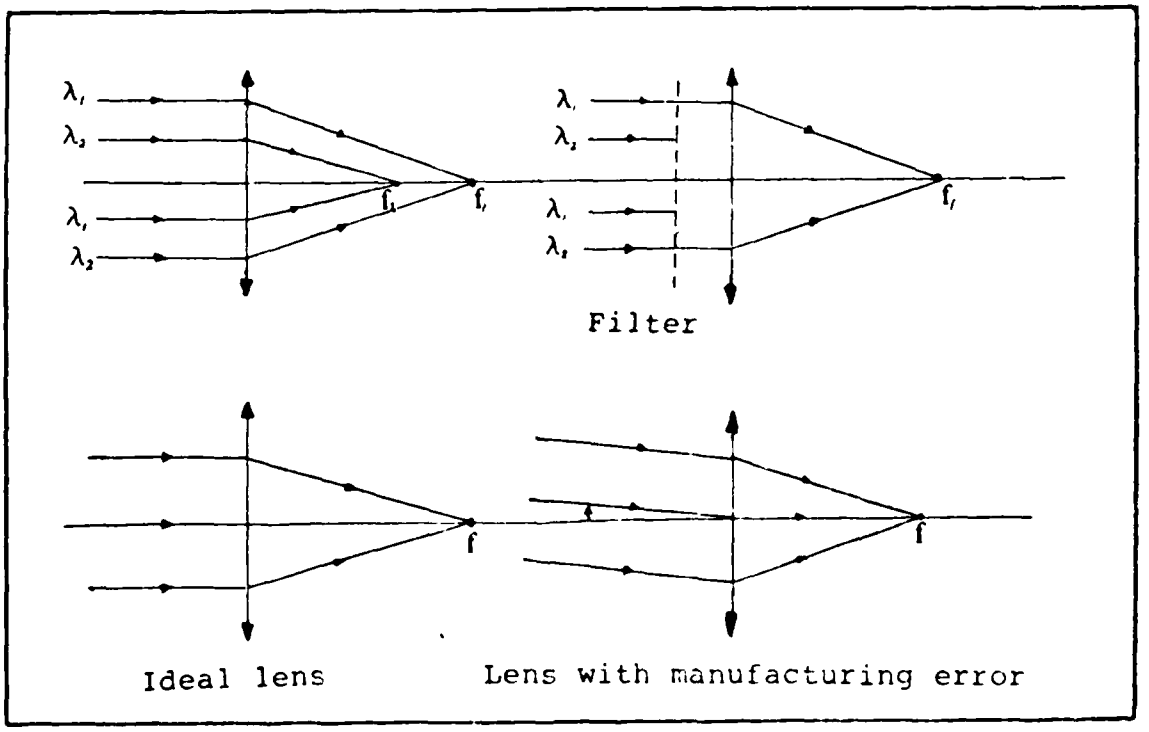

Figure 2.8 Lens Aberation and Boresight Errors.

2) Seeker electronics

Triad Detector Array:

The triad detector array consists of three IR sensitive detectors arranged in circular shape. As shown in Figure 2.9, each detector covers 120 degrees of a circle, and each of them has the same area.

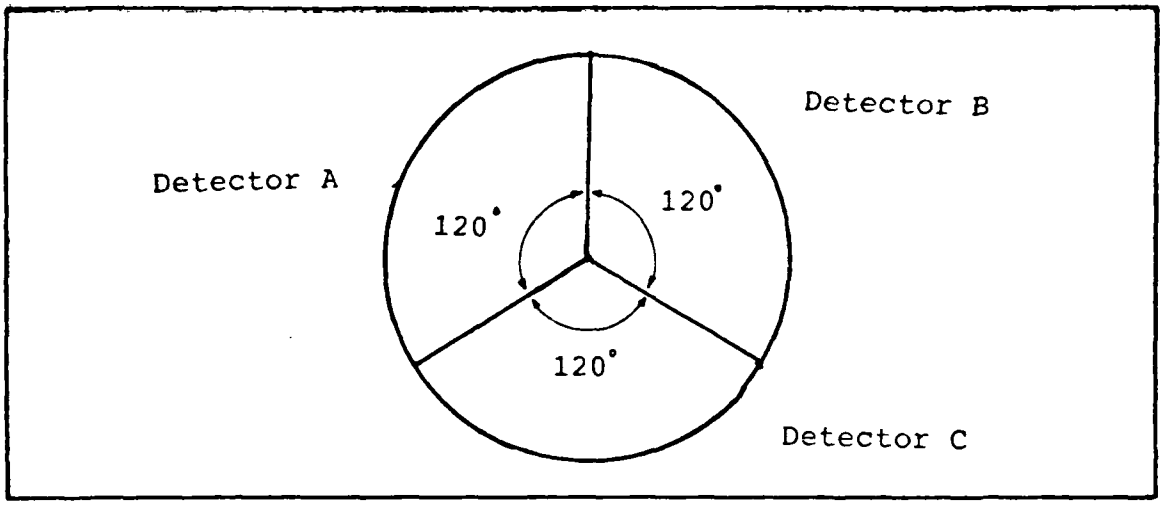

Figure 2.9 Triad Detector Array Configuration.

These detectors are photon detectors and depend on the photovoltaic process to provide the output signal. The photovoltaic effect results from direct conversion of incident photons into conducting electrons within a material. A photon of sufficient energy is absorbed by the photon detector material and excites an electron from a nonconducting state into a conducting state. The "photo excited" electron is then observed through its contribution to an electrical voltage.

To be detected, the photon must have an energy:

$$E > Eexct$$

$$E = \frac{h*c}{\lambda}$$

where Eexct: The electronic excitation energy.

λ : The wavelenght of the photon

h : Plancks constant

c : Speed of the light

Further a photon detector is sensitive only to photons $\lambda<\lambda co$ where co is cut off wavelenght given by (Ref.14)

$$\lambda co = \frac{h*c}{Eexc}$$

where Eexc: Semiconductor band gap

Therefore, in a semi-active laser seeker, when the Nd:YAG laser has been used as a designator, the detectors should have a cut off wavelenght greater than 1.06 μm.

In the simulation, the noises associated with the detectors are assumed to have Gauss-normal distributions. These noises are :

a) Johnson noise: At thermal equilibrium the random motion of the charge carriers in a resistive element generates a random electrical voltage across the element. In a photon detector, this noise effect is not as significant as it is in a thermal detector.

b) Modulation noise: This mechanism is not well understood. As its name implies, it is characterized by the modulation rate of the operation frequency.

c) Background noise: Statistical fluctuations in the rate of generation and in the recombination of charge carriers in the sensitive element result in an electrical noise. These fluctuations can be caused by charge-carrier-photon interactions or by the random arrival rate of photons from the background.

d) Photon noise: It is related to the carrier lifetime and the incident photon wavelenght. Often photon noise can be neglected if the incident radiation is monochromatic (Ref.14)

Signal Processor

The signal processor is specially designed just for a triad detector array strapdown seeker. It takes the voltages produced by the detectors and generates signals proportional to the azimuth and the elevation error angles. As shown in Figure 2.10, each detector has a preamplifier, and the gains of these preamplifiers are automatically adjusted to maintain the total voltage at a specific value. Therefore the control signals are not related with the total laser intensity on the array. However the total intensity can be used to estimate the target range, which can be used to turn off the guidance to avoid uncontrollable maneuvers of the bomb at close range. If the range estimator is set to the initial target range with the initial total intensity on the detector array, then the range can be estimated according to the intensity increase as the bomb gets closer to the target.

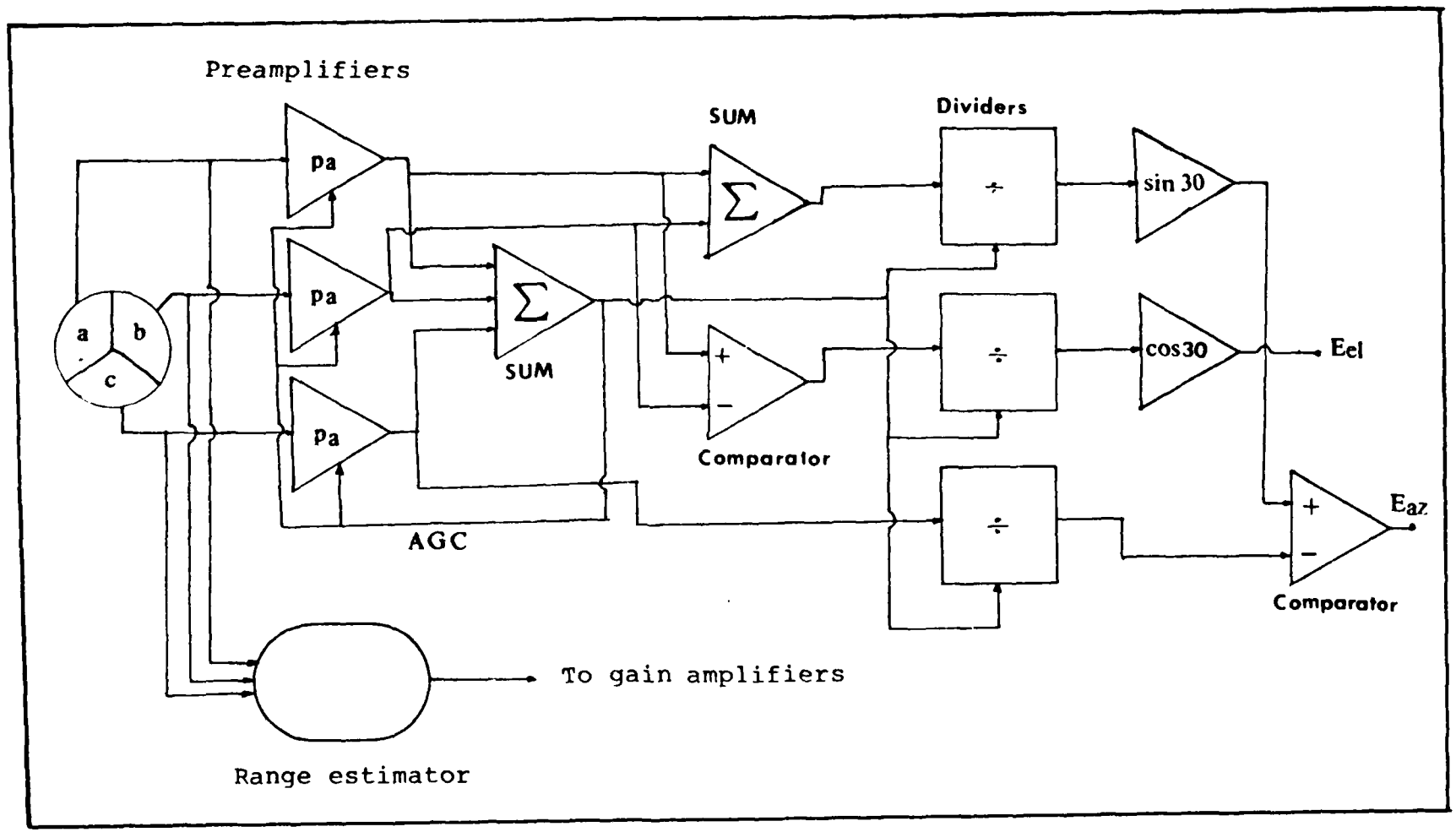

Figure 2.10 Signal Processor for Triad Detector Array Strapdowr. Seeker.

The signal processor generates the azimuth error signal using equation (2.1), and the elevation error signal using equation (2.2) ;

Elevation error signal:

$$Eel = \left(\frac{IA+IB}{IA+IB+IC} * \sin(30) - \frac{IC}{IA+IB+IC}\right) * GAIN \qquad (2.1)$$

Azimuth error signal:

$$Eaz = \left(\frac{IA-IB}{IA+IB+IC} * \cos(30)\right) * GAIN \qquad (2.2)$$

where IA ,IB and IC are the incident laser radiation intensities upon A,B and C detectors respectively. The error signals determined by the signal processor are linear functions of the location of the laser spot on the triad detector array. The conversion process is shown in Figure

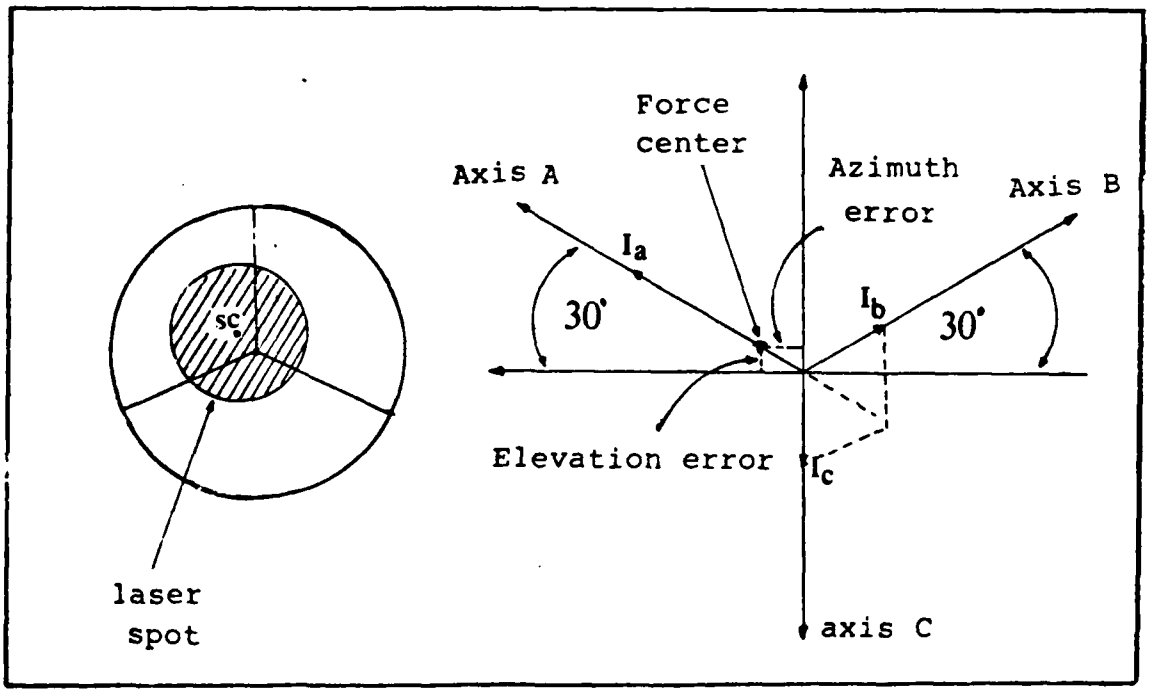

Figure 2.11 Conversion of the Laser Intensities into Error Signals.

The voltage values generated by each detector are considered as the vectors on the three axis a,b,c frame. All three vectors have positive values on their axes. Since detectors can not have negative output voltages, these vectors can not have negative values. The three vectors describe three directions, and each direction represents each detector. The force center of these three vectors is actually the center point of the laser spot. Then, this force center is expressed in the x,y frame of the seeker. The coordinates of the force center are functions of the error angles of the LOS with respect to the body fixed x-axis. Figure 2.12 a,b,c show examples of the function of the signal processor.

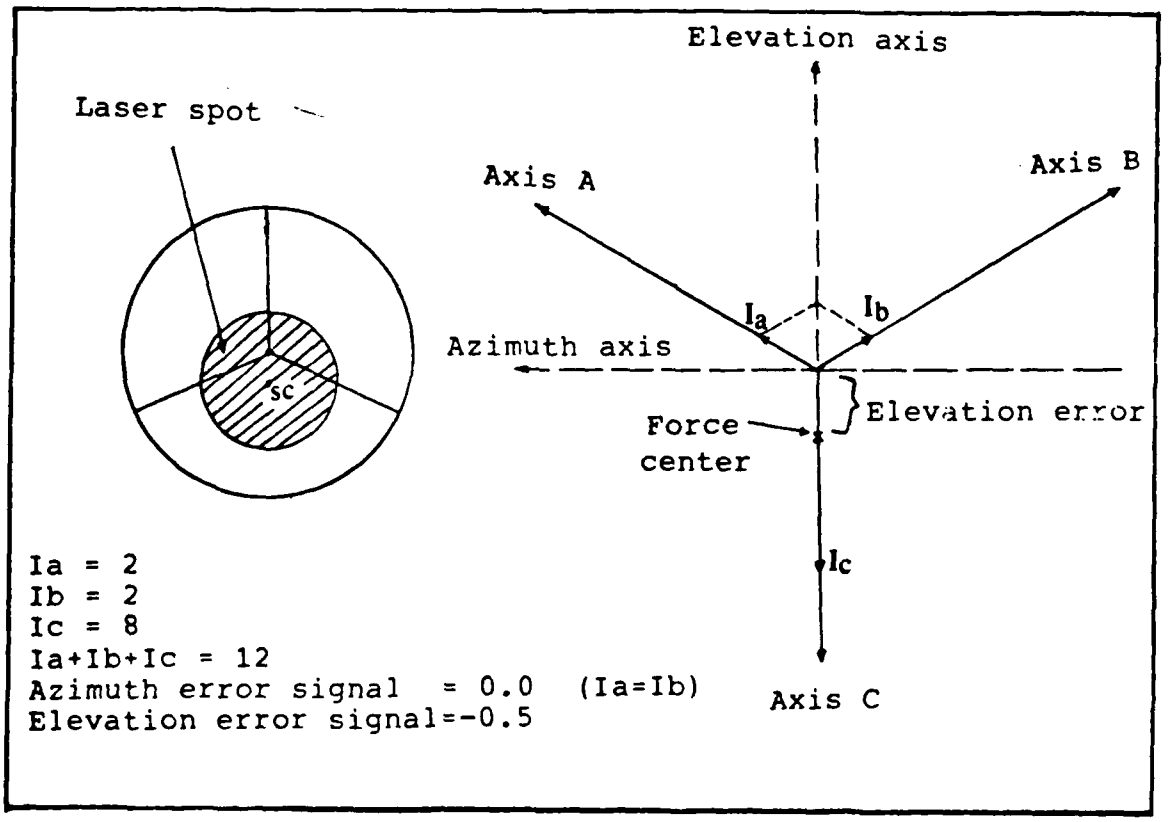

Figure 2.12 a) Signal Processor Function.

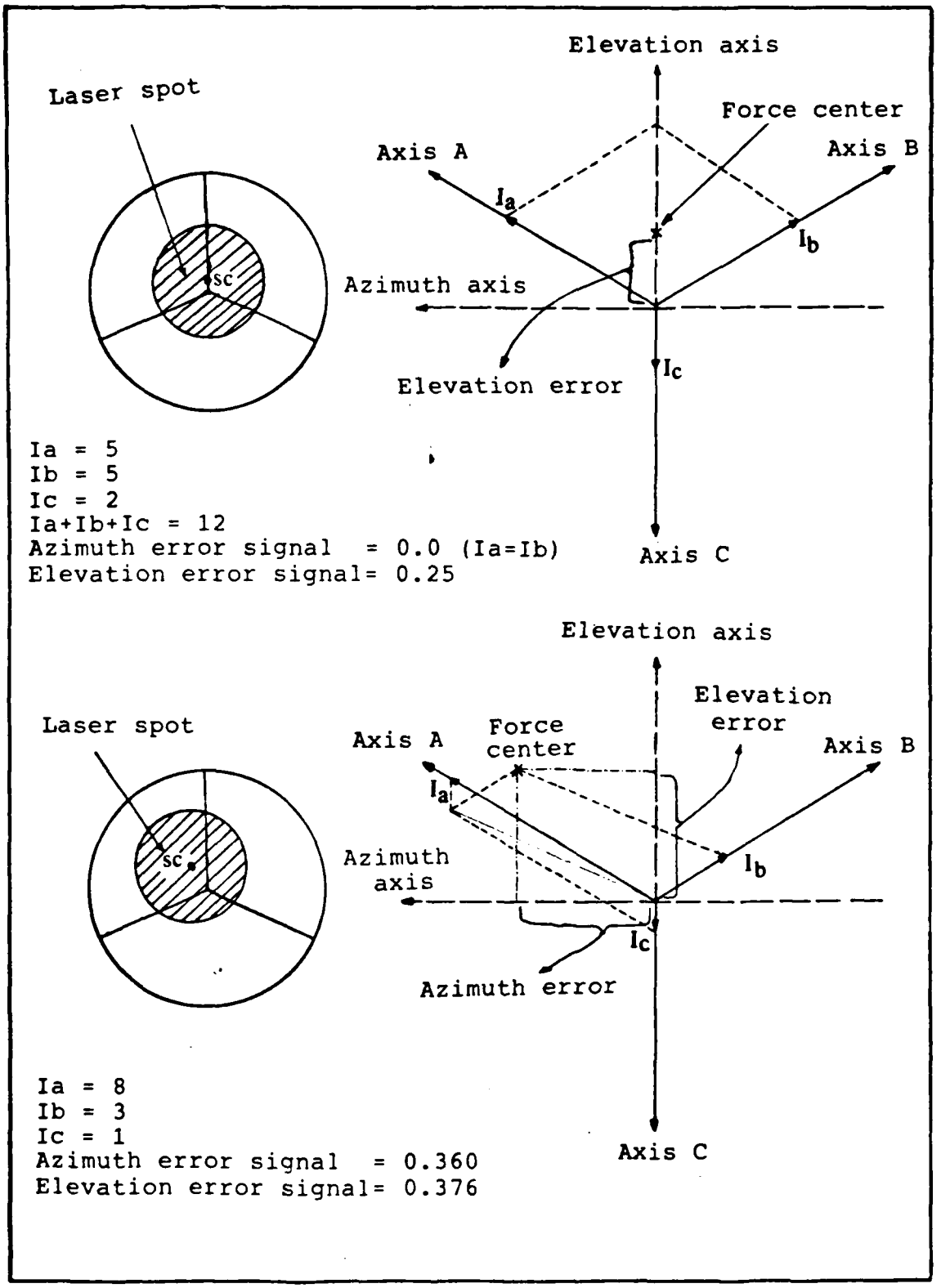

Figure 2.12 b,c Signal Processor Functions According to the Locations or the Laser Spot on Detector Array.

Servo Mechanism.

When the azimuth and elevation error angles are determined, the error signals are generated by the signal processor and are amplified to drive the control surfaces servo mechanisms. There are two servos in the semi-active laser guided vehicle. One is used for pitch angle correction, and the other for yaw angle correction. The error signals multiplied by gains are the inputs of the servo systems. These inputs represent the command angles, θcom and ψcom, respectively. The vertical and horizontal control surface deflections are the outputs of the servo mechanisms (Figure 2.13).

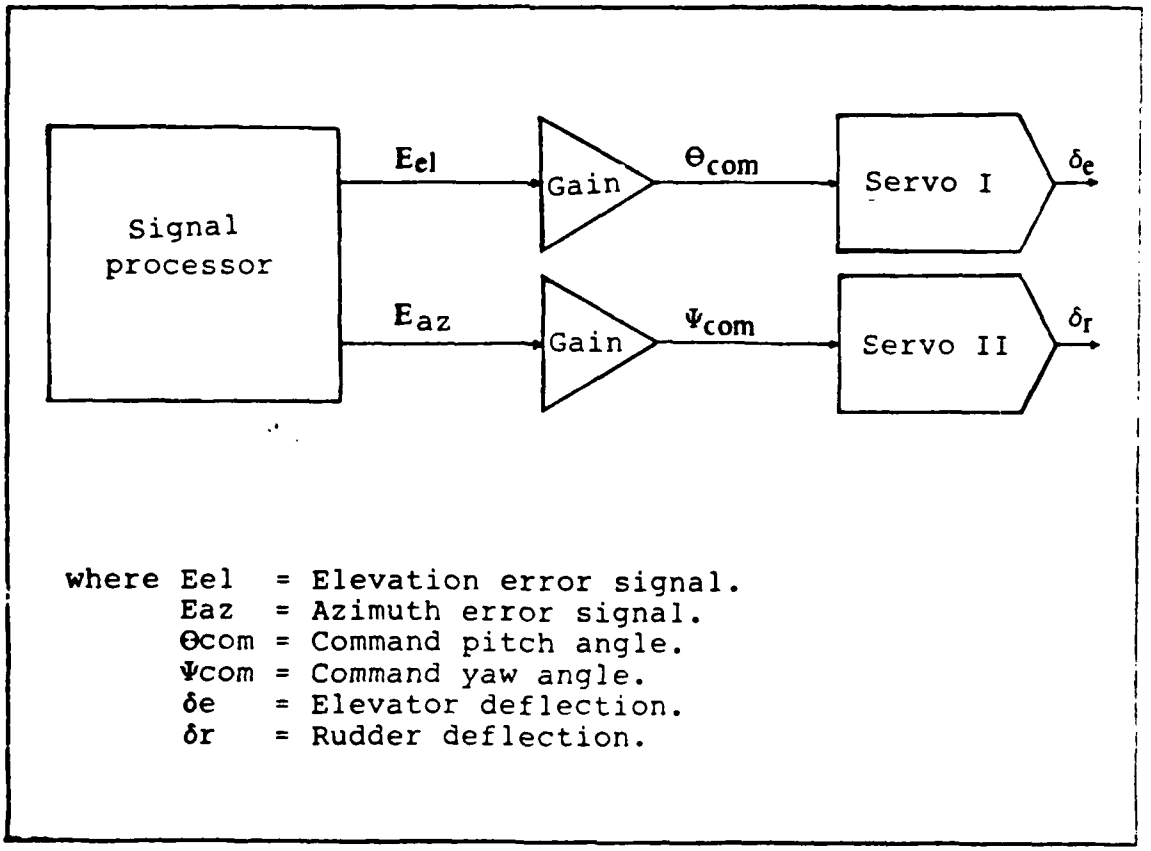

Figure 2.13 Servo Systems of the Laser Guided Bomb.

The transfer functions of both servos are assumed the same and are given by (Ref.13):

$$\frac{\text{Control surface deflection}}{\text{Required angle correction}} = \frac{17.13}{S^2 + 5.713\ S + 17.13}$$

Bomb Dynamic Model.

In this simulation, the weapon is assumed to be an unpowered bomb whose configuration and the body fixed frame are shown in Figure 2.14. The triad detector array strapdown seeker is mounted on the nose of this bomb. The seeker guides the bomb toward the target by using the bomb control surfaces located at the rear of the bomb. In the simulation, the bomb is assumed to have no rolling moment, and it is designed to fly at zero angle of attack when no control is applied.

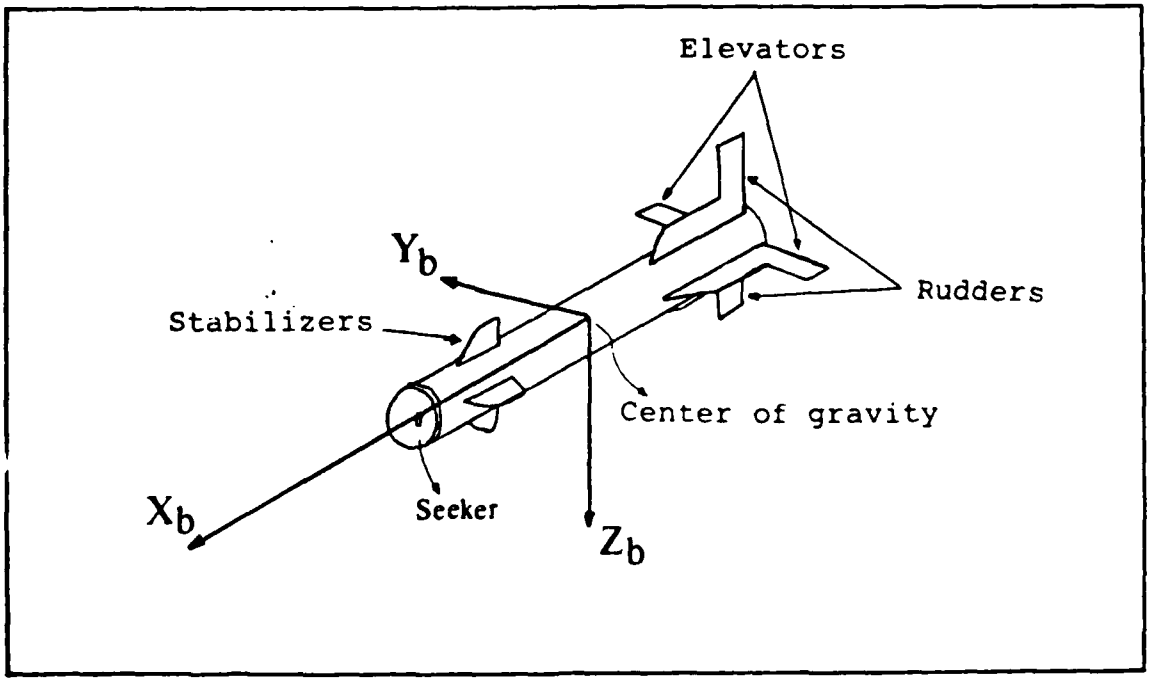

Figure 2.14 Body Fixed Axis Frame of the Bomb.

The actual bomb dynamic equations are not available; they are approxiamated as equations of a flying vehicle by considering the concepts that are known.

Longitudinal dynamics:

In the longitudinal mode, the characteristic equation has two oscillations: one with a high natural frequency and relatively heavy damping, the other with a low natural frequency and very light damping. They are short period and phugoid oscillations, respectively. The short period oscillation consists of variations in angle of attack and pitch angle with very little change in forward velocity. The phugoid oscillation consists of variations in forward velocity and pitch angle with little change in angle of attack, and can be thought of as exchange of potential and kinetic energy (Ref.1). Thus in the longitudinal mode the characteristic equation can be written as combination of these two oscillations ;

$$(S^2 + 2\zeta_p\omega_{np}\, S + \omega_{np}^2)*(S^2 + 2\zeta_s\omega_{ns}\, S + \omega_{ns}^2)$$

where ζ_p : Damping ratio of Phugoid osc.

ω_{np} : Natural frquency of Phugoid osc.

ζ_s : Damping ratio of Short period osc.

ω_{ns} : Natural frquency of Short period osc.

In the simulation, damping ratios and natural frequencies are selected in terms of a subsonic flying vehicle as follows ;

ζ_p : 0.2

ω_{np} : 0.0692 radian/second (rad/s)

ζ_s : 0.352

ω_{ns} : 1.145 rad/s.

Making the nominal angle of attack zero while there is no command makes the nominal flight path angle and pitch angle of the bomb equal. Therefore, the bomb will fly in the direction of the optic axis of the seeker that is actually the body fixed x axis of the bomb. Figure 2.15 shows the angle configurations of the bomb in the longitudinal mode.

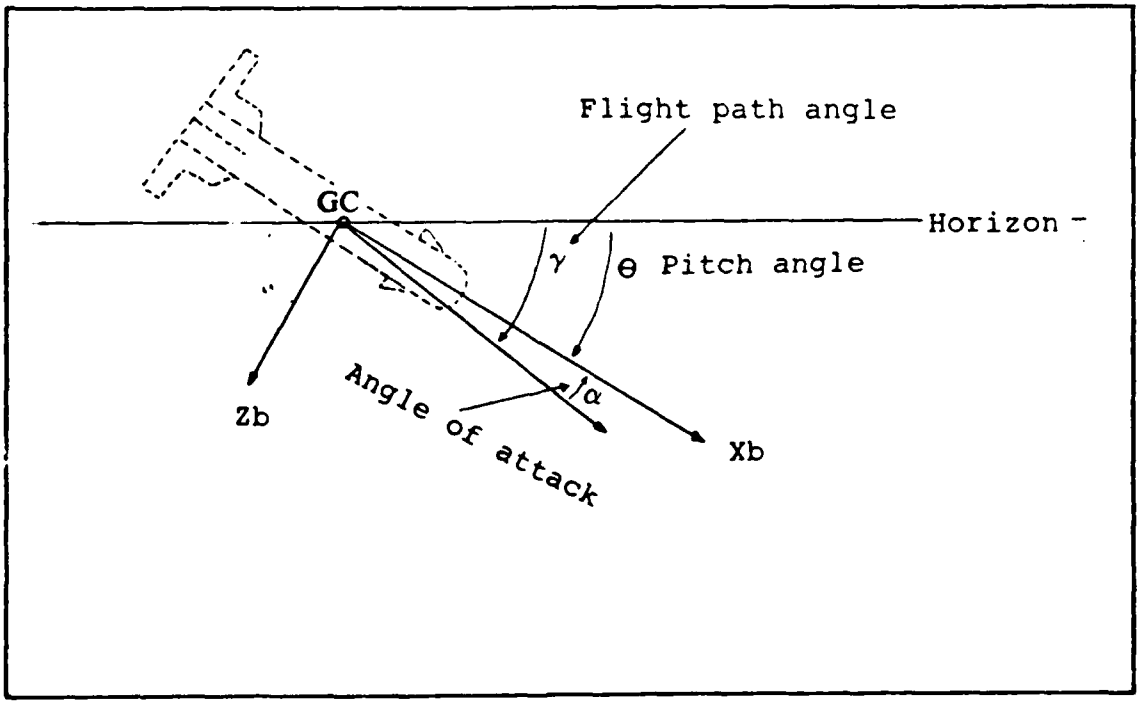

Figure 2.15 Angles of the Longitudinal Mode.

Bomb dynamic equations in the longitudinal mode are selected as follows ;

1) The perturbation of the bomb pitch angle by elevator deflection:

$$\frac{\delta\theta(s)}{\delta e(s)} = \frac{-0.1961877\ (s+0.04)(s+0.8)}{(s^2+0.806s+1.311)(s^2+0.02768s+0.0047886)}$$

2) The change of the true velocity by elevator deflection:

$$\frac{\delta u(s)}{\delta e(s)} = \frac{-0.000559\ (s-45.0)(s+1)}{(s^2+0.806s+1.311)(s^2+0.02768s+0.0047886)}$$

3) The perturbation of the angle of attack by elevator deflection:

$$\frac{\delta\alpha(s)}{\delta e(s)} = \frac{-0.0009\ (s+50)(s^2+0.0063s+0.057)}{(s^2+0.806s+1.311)(s^2+0.02768s+0.0047886)}$$

As shown in Figure 2.16, according to the sign convention, a positive elevator deflection results in a negative steady state pitch angle, in a negative steady state angle of attack, and an increase in steady state velocity perturbations of the bomb.

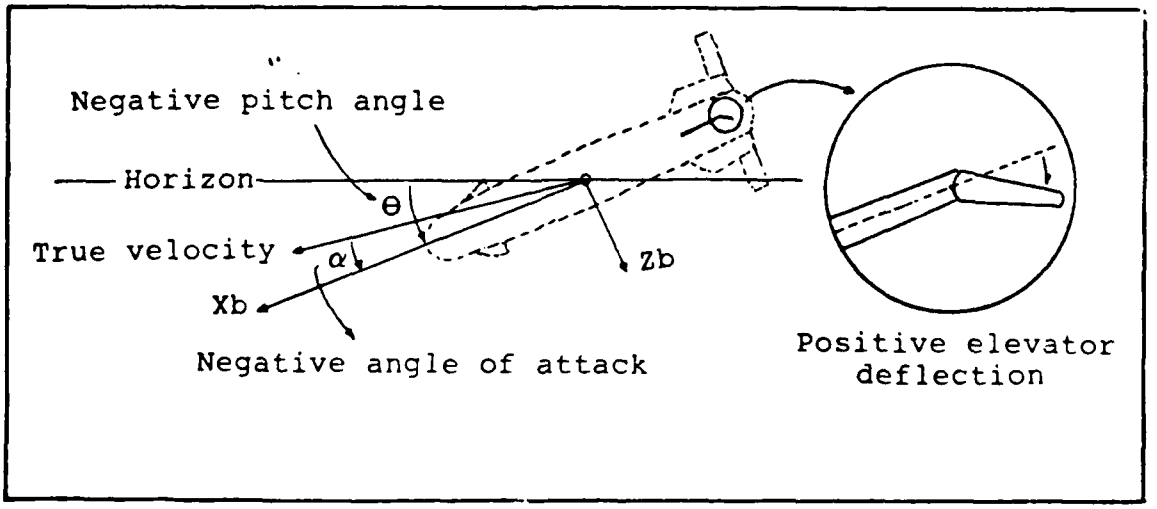

Figure 2.16 Sign Convention for Longitudinal Mode.

In the lateral mode, the bomb dynamic equations are selected as follows;

1) The perturbation of the yaw angle of the bomb by rudder deflection:

$$\frac{\delta\psi(s)}{\delta r(s)} = \frac{-1.63875\ (s+0.8)}{(s^2+0.806s+1.311)}$$

2) The change in the lateral velocity by rudder deflection:

$$\frac{\delta v(s)}{\delta r(s)} = \frac{-0.0873999\ (s-45)(s+1)}{(s^2+0.806s+1.311)}$$

3) The perturbation of the side angle by rudder deflection:

$$\frac{\delta\beta(s)}{\delta r(s)} = \frac{-0.005244\ (s+50)}{(s^2+0.806s+1.311)}$$

As shown in Figure 2.18, according to the sign convention, a positive rudder deflection results in a negative steady state yaw angle, a negative steady state side slip angle and a nagative steady state velocity perturbations.

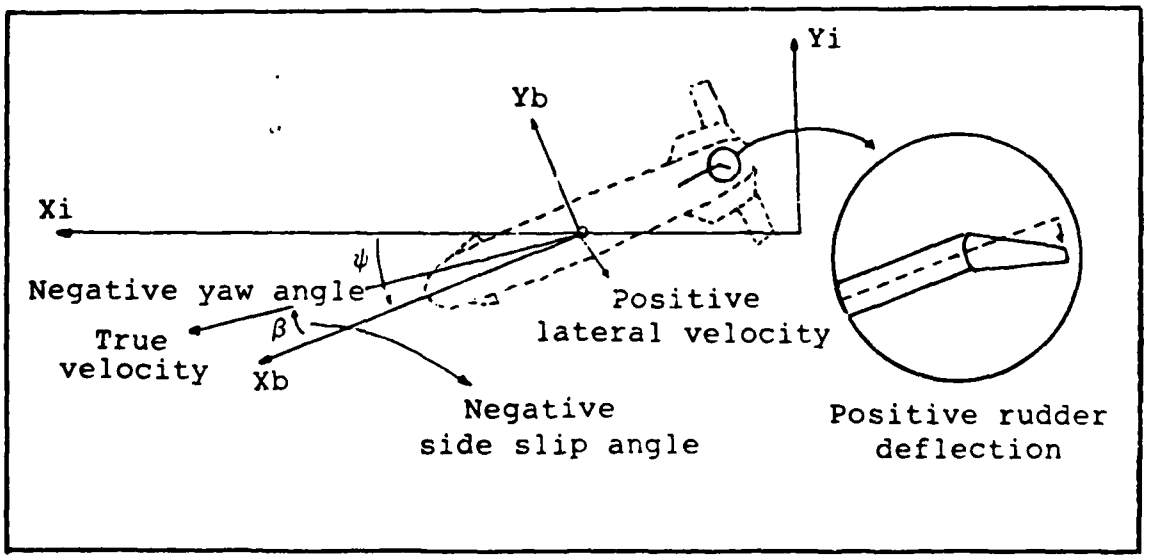

Figure 2.18 Sign Convention for Lateral Mode.

III. COMPLETE SYSTEM SIMULATION AND THE ALGORITHM DESIGN

The three segment detector array strapdown seeker mounted laser guided bomb is modelled according to the considerations explained in Chapter two. In this chapter, the complete system implementation of a computer algorithm to analyse the performance of the triad detector array strapdown seeker will be described. The complete system block diagram is shown in Figure 3.1.

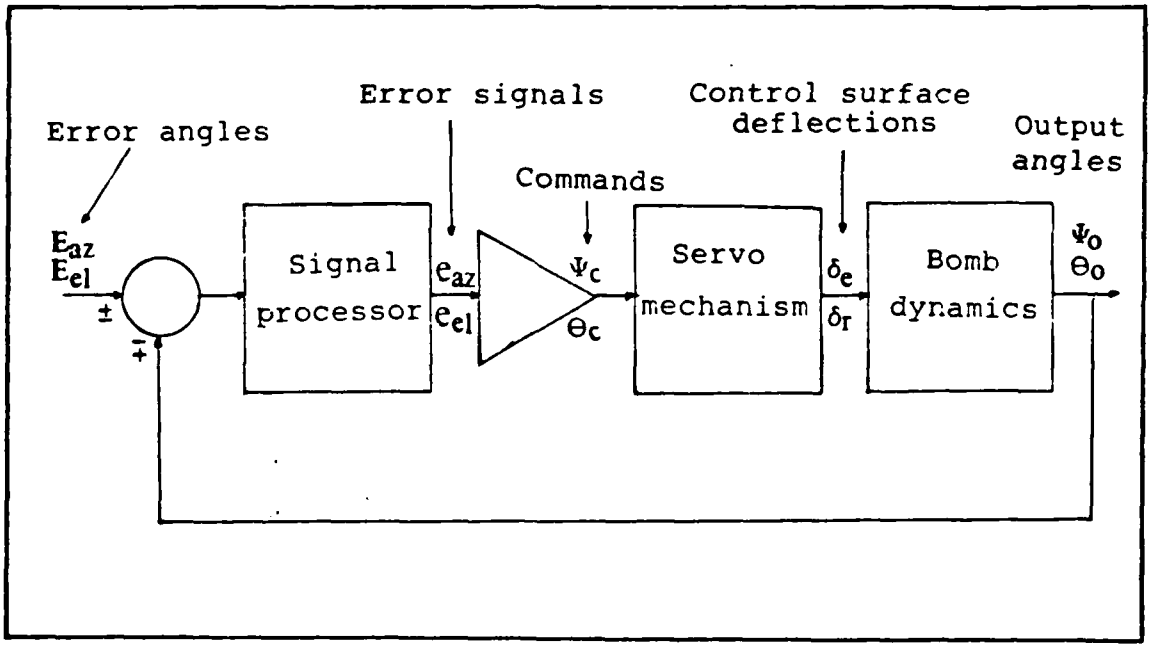

Figure 3.1 Laser Guided Bomb Complete System Block Diagram.

Determining the Error Angles.

The actual input to the system is the reflected laser radiation from the target. However, the detector array and the seeker electronics interpret this input as two error

angles between the target LOS and the body fixed x axis of the bomb. Therefore, the error angles can be considered as the inputs of the system. As stated before, the reflected beam location on the triad detector array is used to generate these error angles. Since, the beam location depends on the error angles between the body fixed x axis of the bomb and the target LOS that represents the nominal trajectory, as shown in Figure 3.2, error angles are determined from the bomb release position, bomb pitch and yaw angles and the target location.

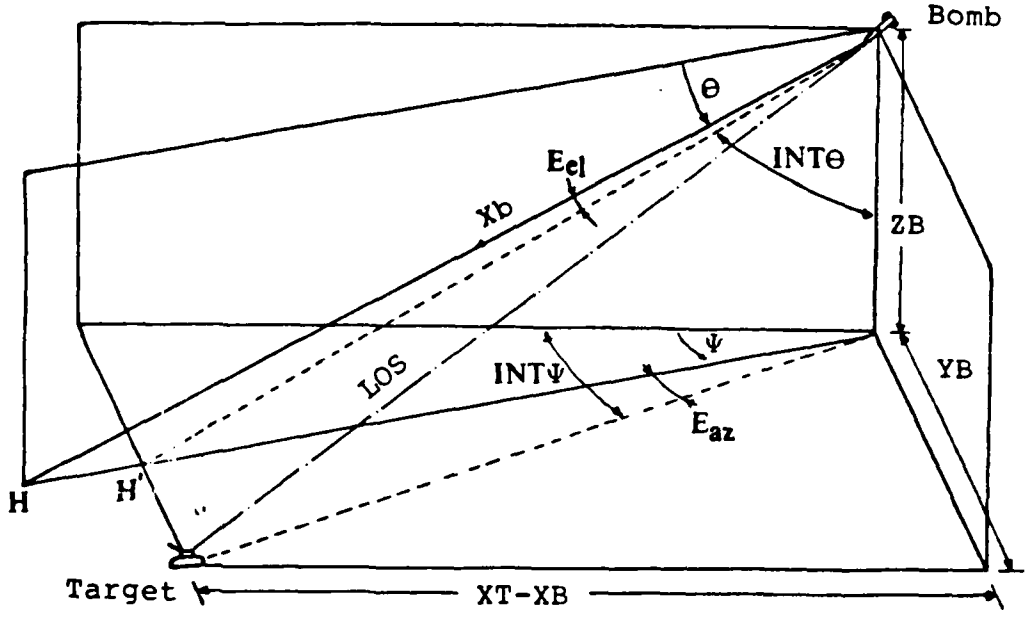

where XB,YB,ZB : Position of the bomb.
XT,YT : Position of the target.
Eel,Eaz : Elevation and azimuth error angles.
INTΘ : Intermediate longitudinal angle.
INTΨ : Intermediate lateral angle.
Θ, Ψ : Bomb pitch and yaw angles.

Figure 3.2 Scheme Geometry and the Description of the Error Angles.

Since, the position (XB,YB,ZB), the pitch and the yaw angles of the bomb (θ,ψ), and the target location (XT,YT) are known initially, the error angles are calculated as:

Elevation error angle:

$$Eel = -(90 + \theta - INT\theta) \tag{3.1}$$

$$\text{where} \quad INT\theta = \arctan \frac{(XT-XB)/\cos\theta}{ZB} \tag{3.2}$$

Azimuth error angle:

$$Eaz = INT\psi - \psi \tag{3.3}$$

$$\text{where} \quad INT\psi = \arccos \frac{XT-XB}{\sqrt{(YB-YT)^2 + (XT-XB)^2}} \tag{3.4}$$

It is assumed that XT is always greater than XB, therefore the intermediate longitudinal angle INTθ is always positive as seen in Equation (3.2). The nominal bomb pitch angle is negative throughout the flight. According to these considerations, if the x-axis of the bomb is above the LOS, the elevation error angle is negative; similarly, if the x-axis of the bomb is below that line, the elevation error angle is positive (Figure 3.3). The intermediate lateral angle INT is always positive according to the Equation (3.4). However, if YT is greater than YB, INTψ must be negative to maintain sign convention for azimuth error angle calculation. Therefore in the computer algorithm, INTψ is replaced with -INTψ when YT is greater than YB. The yaw angle of the bomb may be either negative or positive according to the bomb release position. In either case, if the x axis of the bomb is on the right of the LOS, the

azimuth error angle is negative, and if the x-axis of the bomb is on the left of the LOS, the azimuth error angle is positive (Figure 3.4).

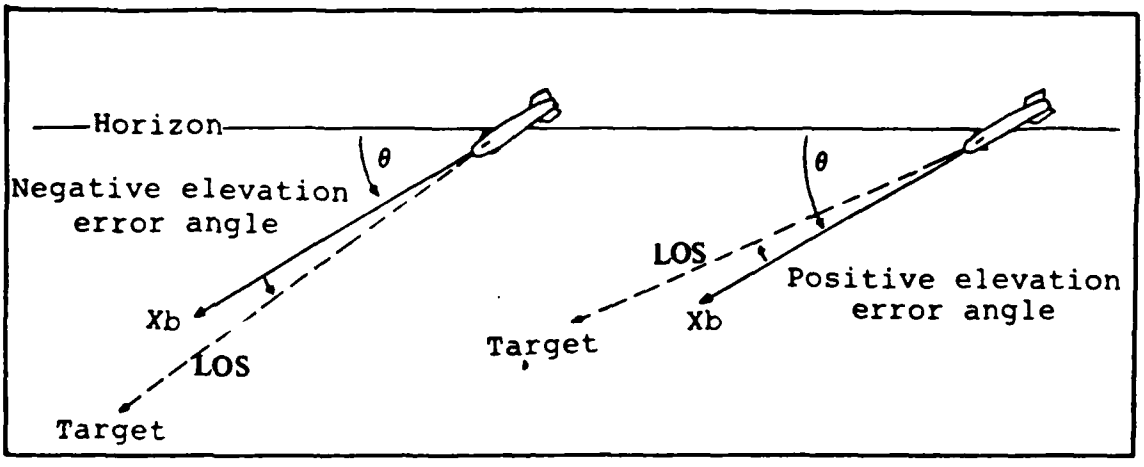

Figure 3.3 Sign Convention for Elevation Error Angle.

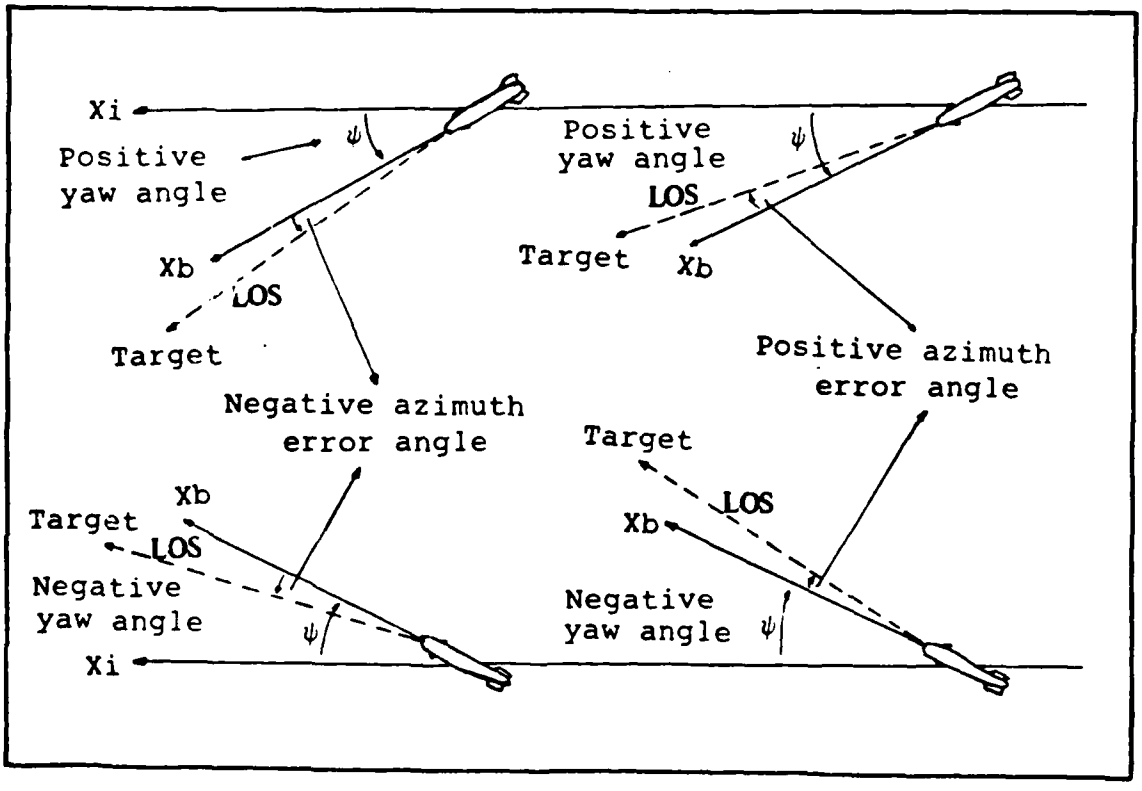

Figure 3.4 Sign Convention for Azimuth Error Angle.

When the bomb is released from an airplane, the x-axis of the bomb may not be pointed toward the target. It is desired the bomb guides itself toward a trajectory that is a line from the bomb to the target (the LOS). As the bomb or the target moves, this line, the nominal trajectory changes. The error angles are measured from this nominal trajectory (Figure 3.5). Therefore the guidance commands also change since they depend on these error angles.

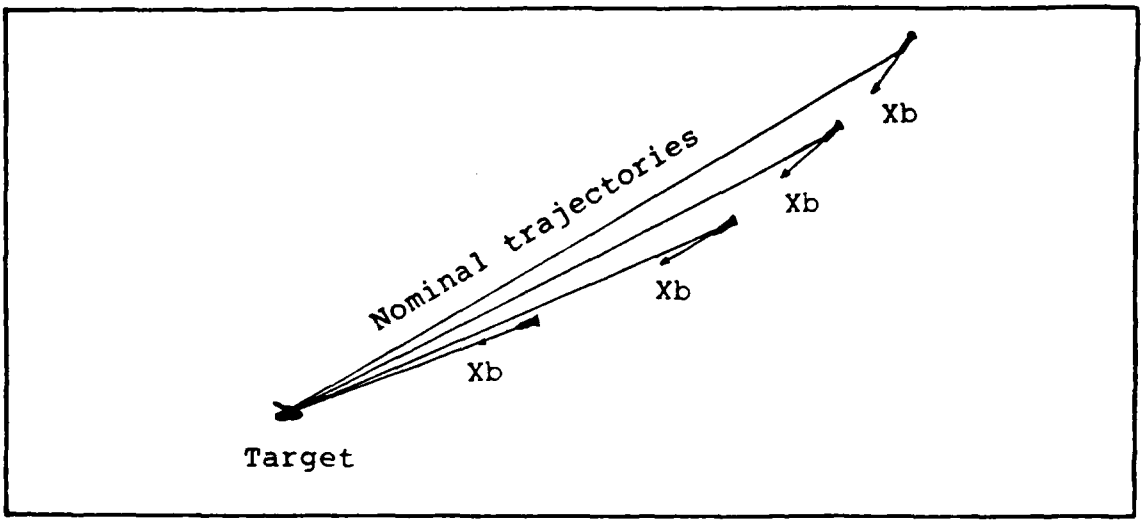

Figure 3.5 Nominal Trajectory in the Longitudinal Mode.

In the seeker, since there is no position information, error angles are not calculated from the positions of the target and the bomb. The seeker optics focus the reflected laser beam on the triad array so that the location is actually a function of the error angles. In the computer algorithm, the true error angles are found from the positions of the bomb and the target to determine the laser spot location on the triad array (Figure 3.6).

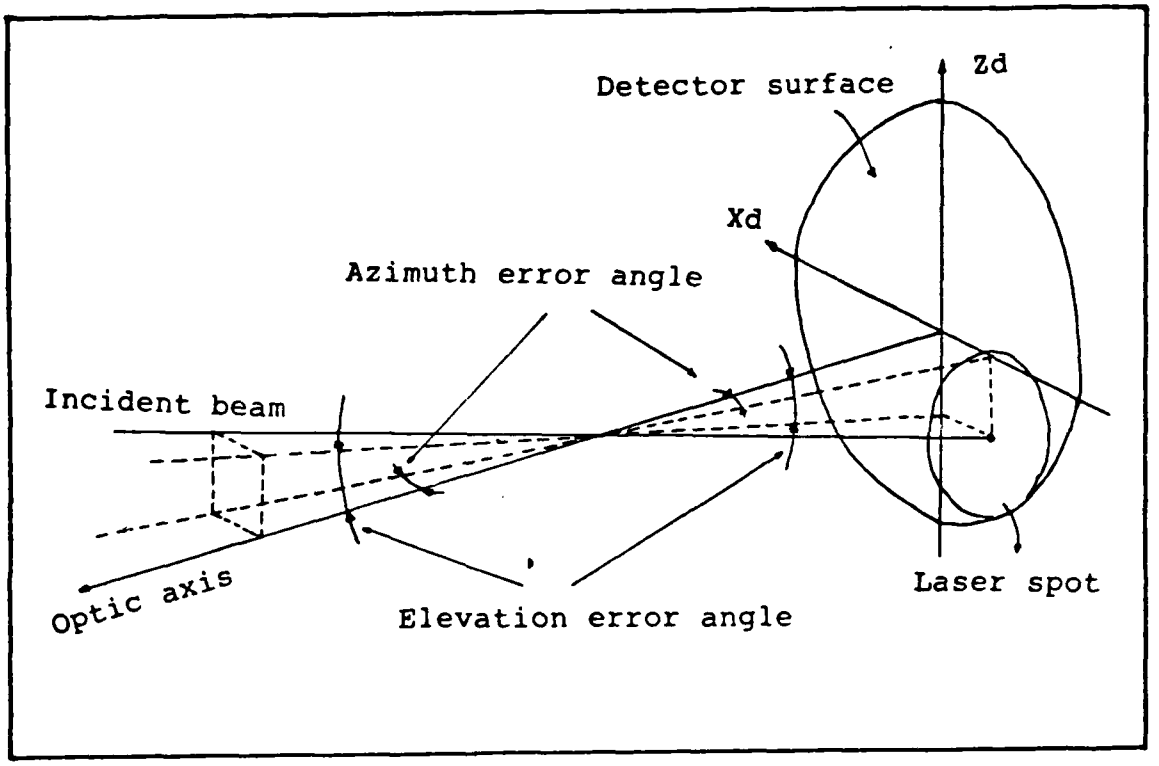

Figure 3.6 Error Angles and the Relation with the Laser Spot Location on Detector Array.

Detector Simulation.

When the error angles are calculated, the location of the centroid of the laser spot is calculated relative to the detector frame using the Equations (3.5)and (3.6).

The position of the center of the laser spot:

$$xd = d * \tan(Eaz) \qquad (3.5)$$

$$zd = d * \tan(Eel) \qquad (3.6)$$

where Eaz is the azimuth error angle, Eel is the elevation error angle and d is the distance between the focusing lens and the detector plane. Since the diameter of the detector array is 3 cm, a distance, d, of 8.5 cm is chosen to assure 20 total angular FOV (Figure3.7).

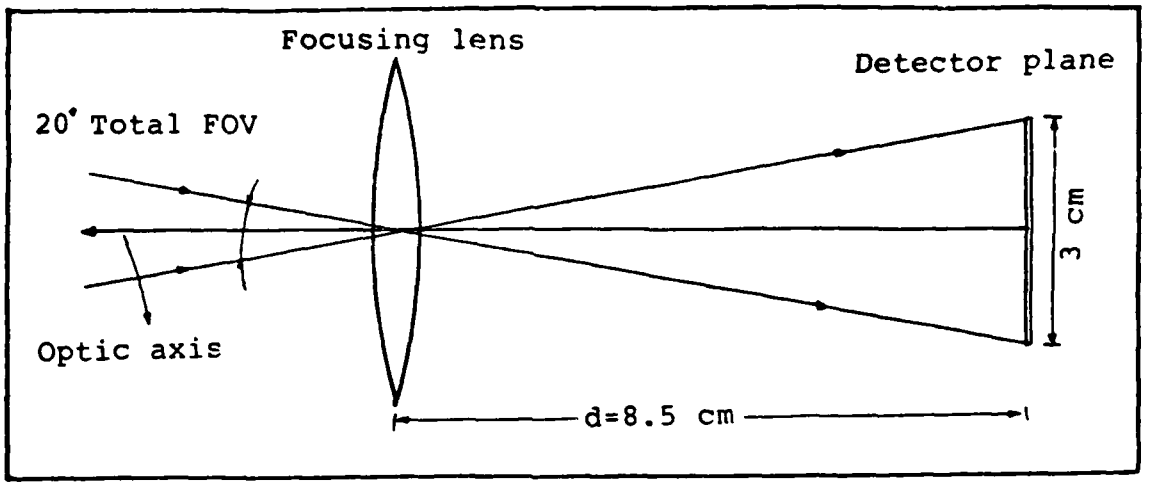

Figure 3.7 Angular Field of View.

The surface of the triad detector array is simulated by placing a circle with a radius of 64 units at the center of a 256 by 256 matrix array (Figure 3.8). Then as seen in Figure 3.9, this circle is divided into three parts, each covering 120 area to determine the surfaces of the detector A,B and C. The detector array may be constructed as a square, but a circular shape is used to make the areas of the three detectors the same.

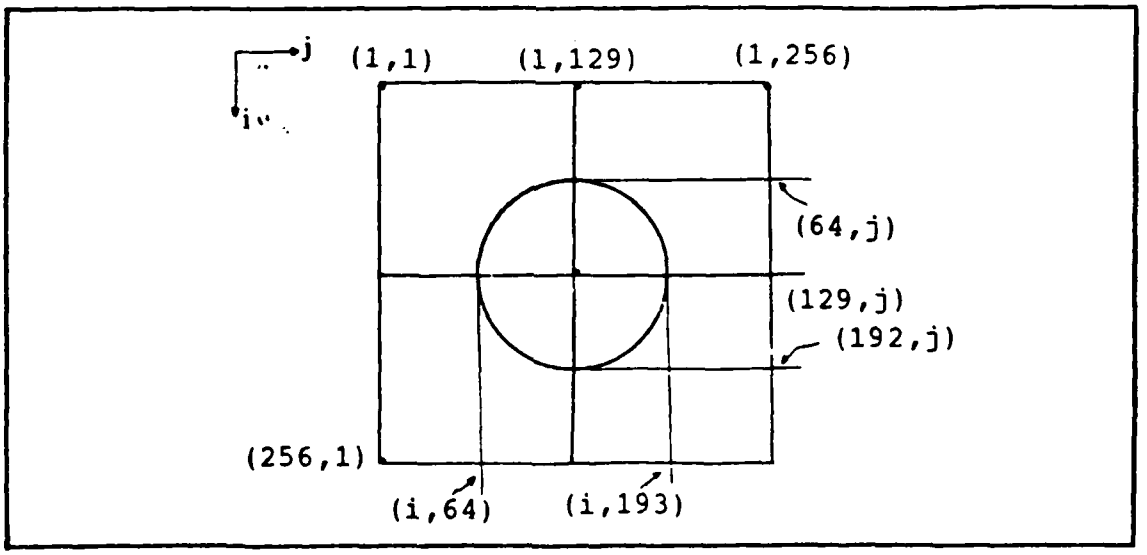

Figure 3.8 Placement of the Triad Detector Array on 256 by 256 Matrix Array.

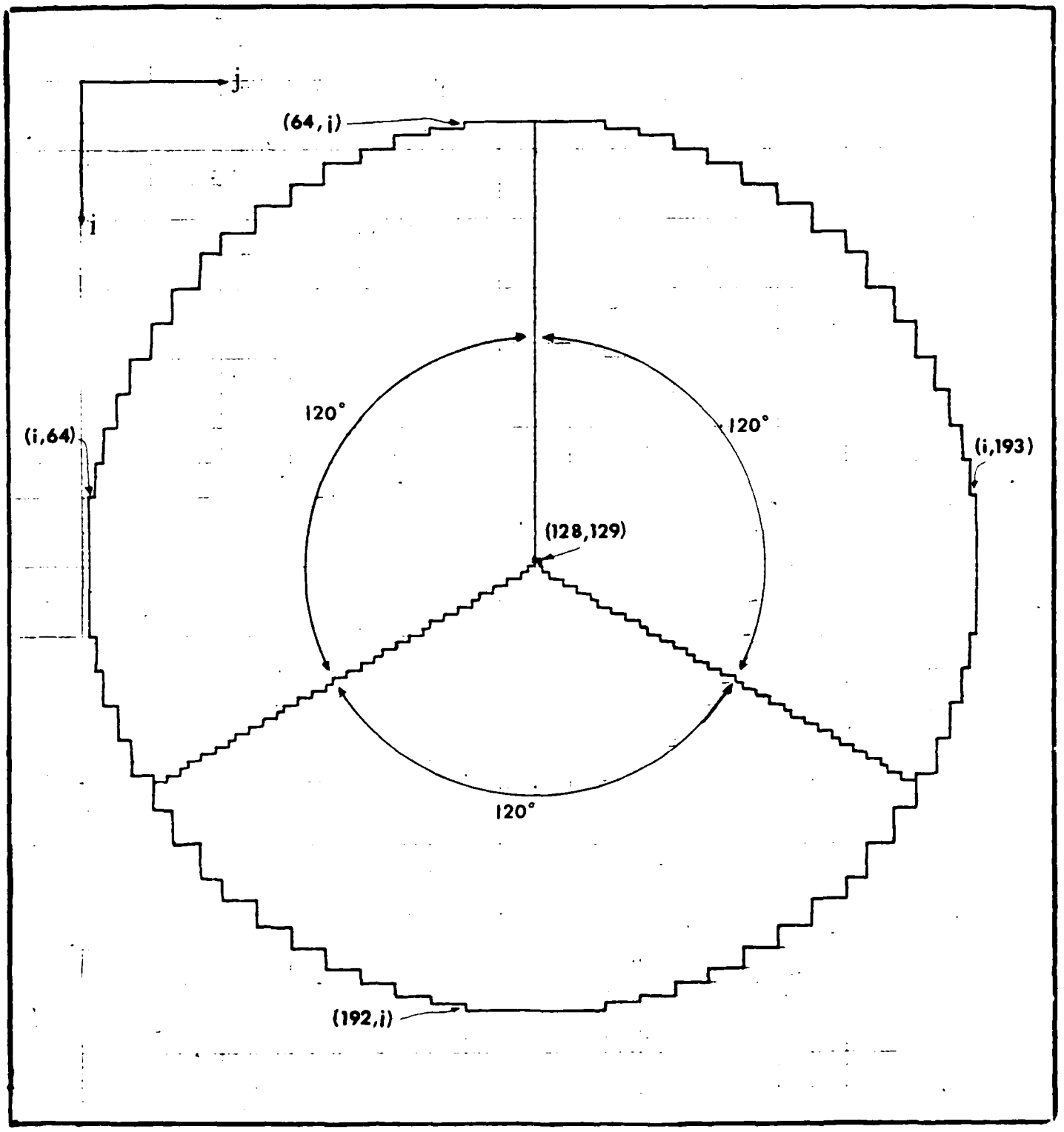

Figure 3.9 Triad Detector Array Surface Simulation.

Laser Spot Simulation.

The position of the centroid of the laser spot with respect to the detector frame is converted into the (i,j) position in the 256 X 256 matrix array by the Equation (3.6) and (3.7), assuming the center point of the detector array (128,129) as the reference.

$$i=128+d*\tan(Eel) \qquad (3.6)$$

$$j=129+d*\tan(Eaz) \qquad (3.7)$$

It is assumed that the designator laser is operating on a single mode, TEM.. that represents the transverse intensity distribution of the laser beam as Gaussian. Therefore the intensity of the reflected beam from the target coming on the detector array is modelled to have Gauss-normal distribution (Figure 3.10). The laser spot intensity distribution is simulated as a 32 unit square radius circle that has relative intensity values according to the Gauss-normal distribution as shown in Figure 3.11.

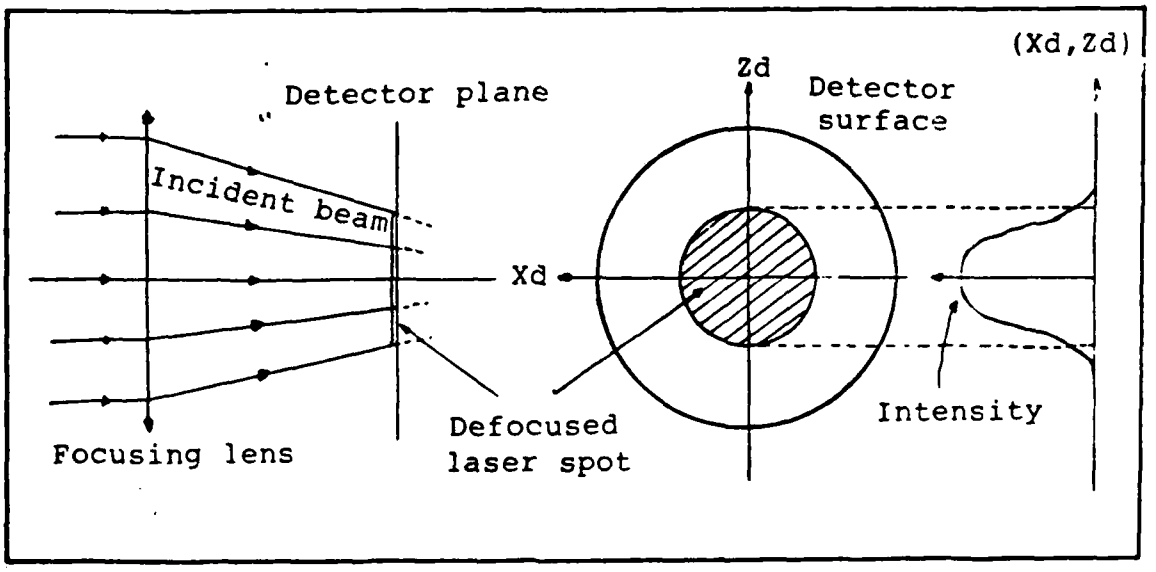

Figure 3.10 Laser Spot Intensity Distribution on Detector Array.

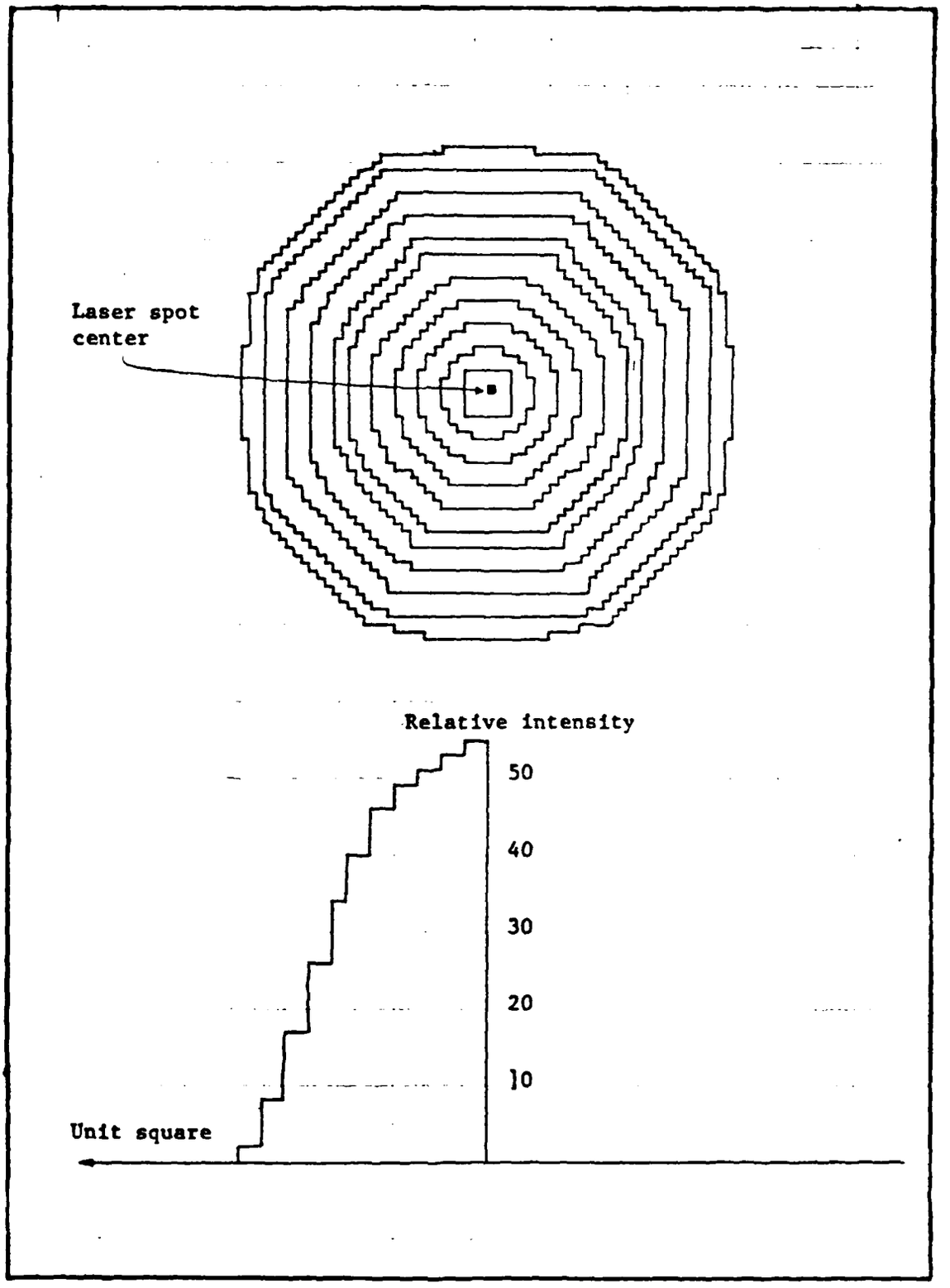

Figure 3.11 Laser Spot Intensity Simulation.

The location of the center of the laser spot is determined in terms of i and j values in the 256 X 256 matrix array. The laser spot center is represented by the reference square as shown in Figure 3.11. Then the squares covered by the laser spot are assigned intensity values according to the distribution described in Figure 3.11. The intensity distribution is modelled such that the relative intensities on three detectors will be the same when the centroid of the laser spot is at (128,129)th of the matrix array. In this case the error signals will be zero. If the centroid of the laser spot is not at (128,129) coordinates, there are error angles to be corrected, and error signals are produced which are a function of the intensity of each detector. The intensity values of the detector A, B and C are calculated by adding the intensity values of the squares covered by the laser spot in each detector surface.

Signal Processor.

The function of the signal processor is to produce error signals associated with the error angles. The signal processor is represented by the Equations (2.1) and (2.2) given in Chapter II. The total voltage produced by the detector array stays the same throughout the flight since an AGC device is employed. For this reason, relative intensities are considered as the normalized output voltages of the preamplifiers, and remain same throughout the flight.

The Simulation of the Bomb Dynamics and the Servo Systems.

Longitudinal dynamics:

The signal processor output of the elevation error signal is multiplied by the gain to determine the elevation command signal that is the input of the elevation servo mechanism. This correction signal is considered as the command pitch angle perturbation, θ_{com}, that should reduce the elevation error angle to zero, but transients delay this realization. The characteristics of these transients are functions of the damping ratio and the natural frequency of the servo and bomb dynamics. As shown in Figure 3.12, the servo responds to the commanded pitch angle and provides an elevator deflection (δe). An elevator deflection produces perturbations in the pitch angle, angle of attack and the true velocity.

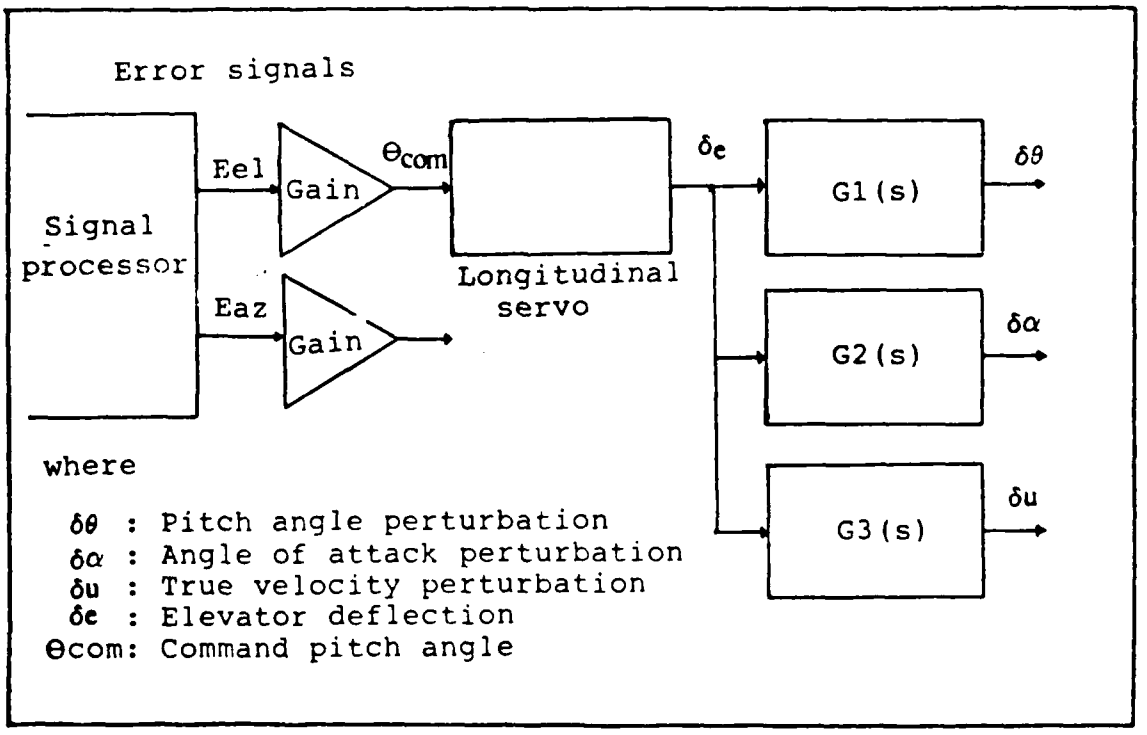

Figure 3.12 Longitudinal Outputs of the System.

The transfer functions between the elevator deflection, δe, and the system outputs in longitudinal mode are converted into canonic controllable form as follows:

$$G_1(s) = \frac{\delta\theta(s)}{\delta e(s)} = \frac{-.1961877s^2 - .1647977s - .006278}{s^4 + .8337s^3 + 1.338s^2 + .04015s + .006278} \qquad (3.8)$$

The Equation (3.8) will be in the form of:

$$\dot{\underline{X}} = \underline{Ac}\ \underline{X} + \underline{B}\ u$$

where

$$\dot{\underline{X}} = \begin{bmatrix} \dot{X}_1 \\ \dot{X}_2 \\ \dot{X}_3 \\ \dot{X}_4 \end{bmatrix} = \begin{bmatrix} \dot{\delta\theta} \\ \ddot{\delta\theta} \\ \dddot{\delta\theta} \\ \delta\theta'''' \end{bmatrix}$$

$$\underline{Ac} = \begin{bmatrix} 0 & 1 & 0 & 0 \\ 0 & 0 & 1 & 0 \\ 0 & 0 & 0 & 1 \\ -.006278 & -.04015 & -1.338 & -.8337 \end{bmatrix}$$

$$u = \delta e$$

The matrix B is formed by dividing the nominator of the $G_1(s)$ by the denominator of the $G_1(s)$ (Ref.13)

$$G_1(s) = b_1 s^{-1} + b_2 s^{-2} + b_3 s^{-3} + b_4 s^{-4} + b_5 s^{-5} + \ldots\ldots$$

$$\underline{B} = \begin{bmatrix} b_1 \\ b_2 \\ b_3 \\ b_4 \end{bmatrix} = \begin{bmatrix} 0 \\ -.1961877 \\ -.001236 \\ .257251 \end{bmatrix}$$

The output matrix can be expressed in terms of selected state variables as :

$$Y = \underline{C} \cdot \underline{X}$$

where $$\underline{C} = \begin{bmatrix} 1 & 0 & 0 & 0 \end{bmatrix}$$

$$y = X_1 = \delta\theta$$

The servo transfer function is converted into canonic controllable form in the same manner :

Servo equation $$\frac{\delta e}{\theta com} = \frac{17.13}{s^2 + 5.713s + 17.13} \qquad (3.9)$$

$$\dot{\underline{X}} = \begin{bmatrix} 0 & 1 \\ -17.13 & 5.713 \end{bmatrix} \cdot \underline{X} + \begin{bmatrix} 0 \\ 17.13 \end{bmatrix} \cdot u$$

where $$\underline{X} = \begin{bmatrix} \delta e \\ \dot{\delta} e \end{bmatrix}$$

$$u = \theta com$$

The servo transfer function and the $G_1(s)$ are cascaded into one canonic controllable form. The input of the system .com is included as one of the states to of the system, because the differential equation solver routine, DGEAR requires that the system be expressed as first order differential equations. In the simulation, the system matrix associated with the command pitch angle and the bomb pitch angle perturbation is in the form :

$$\begin{bmatrix} \dot{K}_1 \\ \dot{K}_2 \\ \dot{K}_3 \\ \dot{K}_4 \\ \dot{K}_5 \\ \dot{K}_6 \\ \dot{K}_7 \end{bmatrix} = \begin{bmatrix} 0 & 0 & 1 & 0 & 0 & 0 & 0 \\ 0 & 0 & 0 & 1 & -.196187 & 0 & 0 \\ 0 & 0 & 0 & 0 & -.001236 & 0 & 0 \\ -.006278 & -.04015 & -1.338 & -.8337 & .257251 & 0 & 0 \\ 0 & 0 & 0 & 0 & 0 & 1 & 0 \\ 0 & 0 & 0 & 0 & -17.13 & -5.713 & 17.13 \\ 0 & 0 & 0 & 0 & 0 & 0 & 0 \end{bmatrix} \begin{bmatrix} K_1 \\ K_2 \\ K_3 \\ K_4 \\ K_5 \\ K_6 \\ K_7 \end{bmatrix}$$

where $K_1 = \delta\theta$

$K_2 = \delta\dot{\theta}$

$K_3 = \delta\ddot{\theta}$

$K_4 = \delta\dddot{\theta}$

$K_5 = \delta e$

$K_6 = \delta\dot{e}$

$K_7 = \theta_{com}$

The transfer functions of the elevator deflection with the angle of attack and the true velocity perturbations are also converted into canonic controllable form, then augmented with the servo transfer function. The seventh states of the canonic forms are the inputs of the equations as command pitch angle. The change of the command input, between the time t_i and $t_i+\Delta t$ is assumed zero. This means that the input is a step of magnitude θcom for $t\epsilon(t_i, t_i+\Delta t)$. As shown in Figure 3.13, the θcom is a piecewise continuous step function.

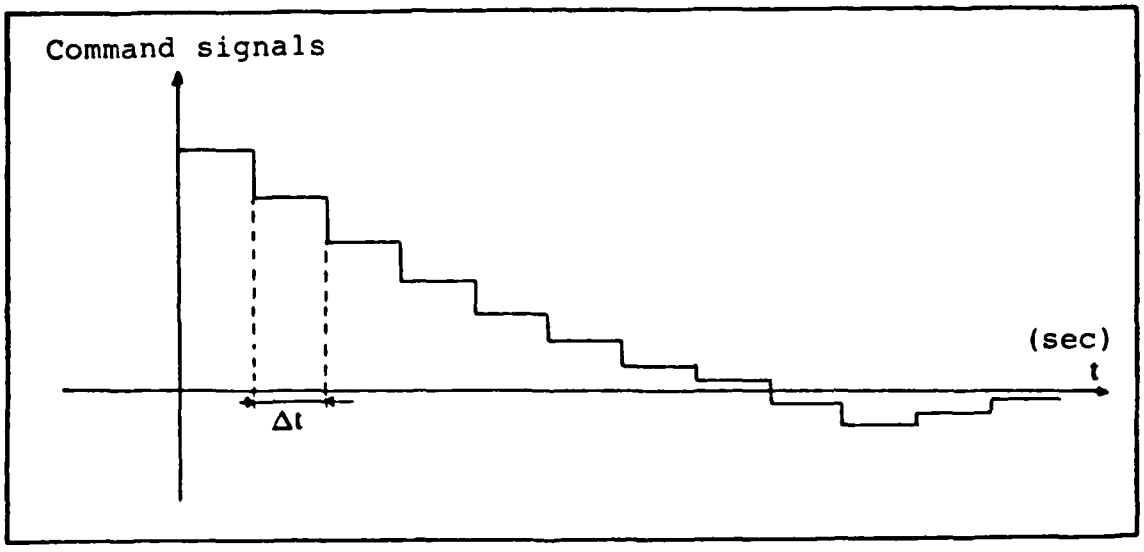

Figure 3.13. Possible Changes in Commands.

The transfer function of the angle of attack perturbation for a given elevator deflection is :

$$G_2(s) = \frac{\delta\alpha(s)}{\delta e(s)} = \frac{-.0009s^3 - .04501s^2 - .000335s - .002565}{s^4 + .8337s^3 + 1.338s^2 + .004015s + .006278} \quad (3.9)$$

If Equation (3.9) is cascaded with the servo transfer function in canonic controllable form, it becomes :

$$\begin{bmatrix} \dot{L}_1 \\ \dot{L}_2 \\ \dot{L}_3 \\ \dot{L}_4 \\ \dot{L}_5 \\ \dot{L}_6 \\ \dot{L}_7 \end{bmatrix} = \begin{bmatrix} 0 & 1 & 0 & 0 & -.0009 & 0 & 0 \\ 0 & 0 & 1 & 0 & -.044259 & 0 & 0 \\ 0 & 0 & 0 & 1 & .037768 & 0 & 0 \\ -.006278 & -.04015 & -1.338 & -.8337 & .252028 & 0 & 0 \\ 0 & 0 & 0 & 0 & 0 & 1 & 0 \\ 0 & 0 & 0 & 0 & -17.13 & -5.713 & 17.13 \\ 0 & 0 & 0 & 0 & 0 & 0 & 0 \end{bmatrix} \begin{bmatrix} L_1 \\ L_2 \\ L_3 \\ L_4 \\ L_5 \\ L_6 \\ L_7 \end{bmatrix}$$

where $L_1 = \delta\theta$

$L_2 = \delta\dot{\theta}$

$L_3 = \delta\ddot{\theta}$

$L_4 = \dddot{\delta\theta}$

$L_5 = \delta e$

$L_6 = \dot{\delta} e$

$L_7 = \theta_{com}$

The transfer function of the true velocity perturbation of the bomb for a given elevator deflection is :

$$G_3(s) = \frac{\delta u(s)}{\delta e(s)} = \frac{-.000559s^3 + .024596s + .025155}{s^4 + .8337s^3 + 1.338s^2 + .04015s + .006278} \qquad (3.10)$$

Again it is cascaded with the servo transfer function in the canonic controllable form to give :

$$\begin{bmatrix} \dot{M}_1 \\ \dot{M}_2 \\ \dot{M}_3 \\ \dot{M}_4 \\ \dot{M}_5 \\ \dot{M}_6 \\ \dot{M}_7 \end{bmatrix} = \begin{bmatrix} 0 & 1 & 0 & 0 & 0 & 0 & 0 \\ 0 & 0 & 1 & 0 & -.000559 & 0 & 0 \\ 0 & 0 & 0 & 1 & .025062 & 0 & 0 \\ -.006278 & -.04015 & -1.338 & -.8337 & .005008 & 0 & 0 \\ 0 & 0 & 0 & 0 & 0 & 1 & 0 \\ 0 & 0 & 0 & 0 & -17.13 & -5.713 & 17.13 \\ 0 & 0 & 0 & 0 & 0 & 0 & 0 \end{bmatrix} \begin{bmatrix} M_1 \\ M_2 \\ M_3 \\ M_4 \\ M_5 \\ M_6 \\ M_7 \end{bmatrix}$$

where $M_1 = \delta u$

$M_2 = \dot{\delta u}$

$M_3 = \ddot{\delta u}$

$M_4 = \dddot{\delta u}$

$M_5 = \delta e$

$M_6 = \dot{\delta e}$

$M_7 = \theta com$

Lateral dynamics:

The azimuth error signal provided by the signal processor is amplified by the lateral gain to produce the azimuth correction signal. The gain value for lateral mode may not be the same as it is in the longitudinal mode. The azimuth correction signal is considered as the command yaw angle .com. The lateral servo drives the control surfaces and the bomb responds to this input in three ways : Perturbations in the bomb yaw angle, side slip angle and the lateral velocity (Figure 3.14).

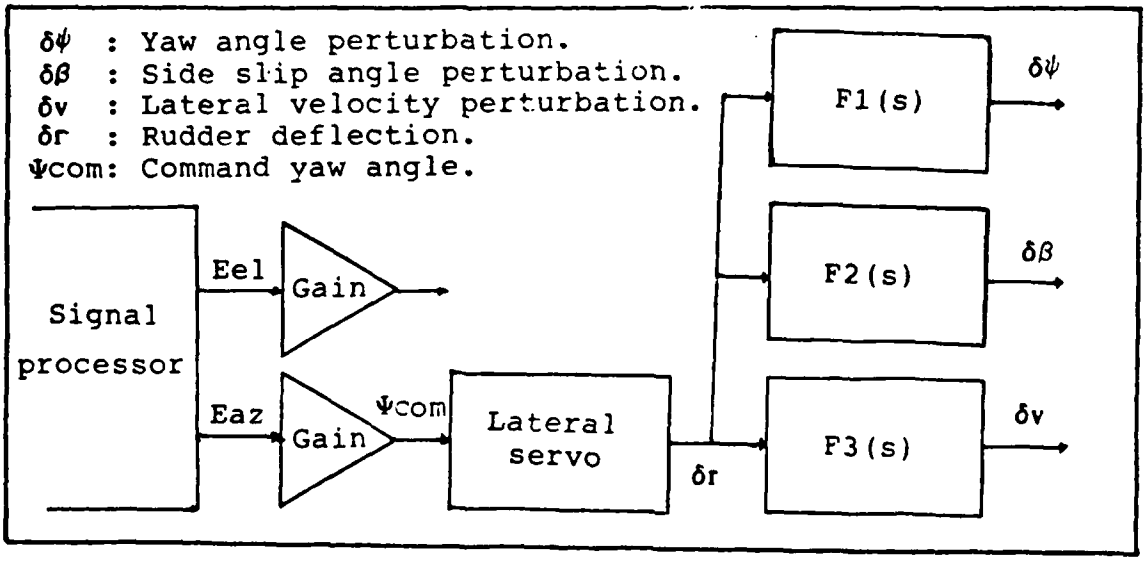

Figure 3.14 Lateral Outputs of the System.

The transfer functions between the lateral control surface, the rudder, and the system outputs are converted into canonic controllable form as follows :

$$F_1(s) = \frac{\delta\Psi(s)}{\delta r(s)} = \frac{-1.63875s-1.311}{s^2 + 0.806s + 1.311} \qquad (3.11)$$

Equation (3.11) can be written in the form :

$$\dot{\underline{X}} = \underline{Ac}\,\underline{X} + \underline{B}\,u$$

where $$\underline{X} = \begin{bmatrix} X_1 \\ X_2 \end{bmatrix} = \begin{bmatrix} \delta\Psi(s) \\ \delta\dot{\Psi}(s) \end{bmatrix}$$

$$\underline{Ac} = \begin{bmatrix} 0 & 1 \\ -1.311 & -.806 \end{bmatrix}$$

$$u = \delta r$$

The matrix B is then found by dividing the nominator of the $F_1(s)$ by the denominator of the $F_1(s)$.

$$F_1(s) = b_1 s^{-1} + b_2 s^{-2} + b_3 s^{-3} + \ldots\ldots\ldots$$

$$\underline{B} = \begin{bmatrix} b_1 \\ b_2 \end{bmatrix} = \begin{bmatrix} -1.63875 \\ 0.00983 \end{bmatrix}$$

The output matrix can be written in terms of selected state variable as :

$$Y = \underline{C}\,\underline{X}$$

where $\underline{C} = \begin{bmatrix} 1 & 0 \end{bmatrix}$, Thus $y = X_1 = \delta\Psi$

The same servo transfer function used in the longitudinal mode and $F_1(s)$ are cascaded to produce a canonic controllable form. The command yaw angle, ψcom, is considered the fifth state of the system and assumed to be a step function like the command pitch angle described in Figure 3.13. The transfer function of the ψcom and the yaw angle perturbation is expressed in the matrix equation as :

$$\begin{bmatrix} \dot{P}_1 \\ \dot{P}_2 \\ \dot{P}_3 \\ \dot{P}_4 \\ \dot{P}_5 \end{bmatrix} = \begin{bmatrix} 0 & 1 & -1.63875 & 0 & 0 \\ -1.311 & -.806 & .009833 & 0 & 0 \\ 0 & 0 & 0 & 1 & 0 \\ 0 & 0 & -17.13 & -5.713 & 17.13 \\ 0 & 0 & 0 & 0 & 0 \end{bmatrix} \cdot \begin{bmatrix} P_1 \\ P_2 \\ P_3 \\ P_4 \\ P_5 \end{bmatrix}$$

where $P_1 = \delta\psi$

$P_2 = \delta\dot{\psi}$

$P_3 = \delta r$

$P_4 = \delta\dot{r}$

$P_5 = \psi$com

The transfer functions of the side slip angle and the lateral velocity perturbations with the rudder deflection are converted into canonic controllable form and cascaded with the servo state model. The transfer function of the rudder deflection and the side slip angle perturbation is :

$$F_2(s) = \frac{\delta\beta(s)}{\delta r(s)} = \frac{-.005244s - .2622}{s^2 + .806s + 1.311} \qquad (3.13)$$

It is cascaded with the servo transfer function in the canonic controllable form as follows ;

$$\begin{bmatrix} \dot{R}_1 \\ \dot{R}_2 \\ \dot{R}_3 \\ \dot{R}_4 \\ \dot{R}_5 \end{bmatrix} = \begin{bmatrix} 0 & 1 & -.005244 & 0 & 0 \\ -1.311 & -.806 & -.257973 & 0 & 0 \\ 0 & 0 & 0 & 0 & 0 \\ 0 & 0 & -17.13 & -5.713 & 17.13 \\ 0 & 0 & 0 & 0 & 0 \end{bmatrix} \cdot \begin{bmatrix} R_1 \\ R_2 \\ R_3 \\ R_4 \\ R_5 \end{bmatrix}$$

where $R_1 = \delta\psi$

$R_2 = \delta\dot{\psi}$

$R_3 = \delta r$

$R_4 = \delta\dot{r}$

$R_5 = \psi_{com}$

The transfer function of the lateral velocity perturbation for a rudder deflection is :

$$F_3(s) = \frac{\delta v(s)}{\delta r(s)} = \frac{-.087399s^2 - 3.845595s - 3.393299}{s^2 + 0.806s + 1.311} \qquad (3.14)$$

Equation (3.14) is cascaded with the servo transfer function in the canonic controllable form as follows :

$$\begin{bmatrix} \dot{Q}_1 \\ \dot{Q}_2 \\ \dot{Q}_3 \\ \dot{Q}_4 \\ \dot{Q}_5 \end{bmatrix} = \begin{bmatrix} 0 & 1 & -3.775151 & 0 & 0 \\ -1.311 & -.806 & -.775642 & 0 & 0 \\ 0 & 0 & 0 & 1 & 0 \\ 0 & 0 & -17.13 & -5.713 & 17.13 \\ 0 & 0 & 0 & 0 & 0 \end{bmatrix} \begin{bmatrix} Q_1 \\ Q_2 \\ Q_3 \\ Q_4 \\ Q_5 \end{bmatrix}$$

where $Q_1 = \delta\psi$

$Q_2 = \delta\dot{\psi}$

$Q_3 = \delta r$

$Q_4 = \delta\dot{r}$

$Q_5 = \psi_{com}$

The six state equations in the canonic controllable form that describe the bomb dynamics in the longitudinal and the lateral modes are solved by a computer simulation algorithm, using an IMSL differential equation solver routine called DGEAR. The solutions of the state equations are the perturbations in the states of the bomb between the time t and t+ Δt. For each time ti, the perturbations calculated at ti+Δt are added to the initial conditions at ti to determine the conditions for the next step. The calculation step size (Δt) is selected as 0.15 second to be able to observe the changes of the system responses by considering the maximum natural frequency of the system. The position of the bomb for each time ti is calculated according to the bomb responses. As shownn in Figure 3.15, the angles and the velocity components that are known at time ti are used to find the position of the bomb at time ti+1.

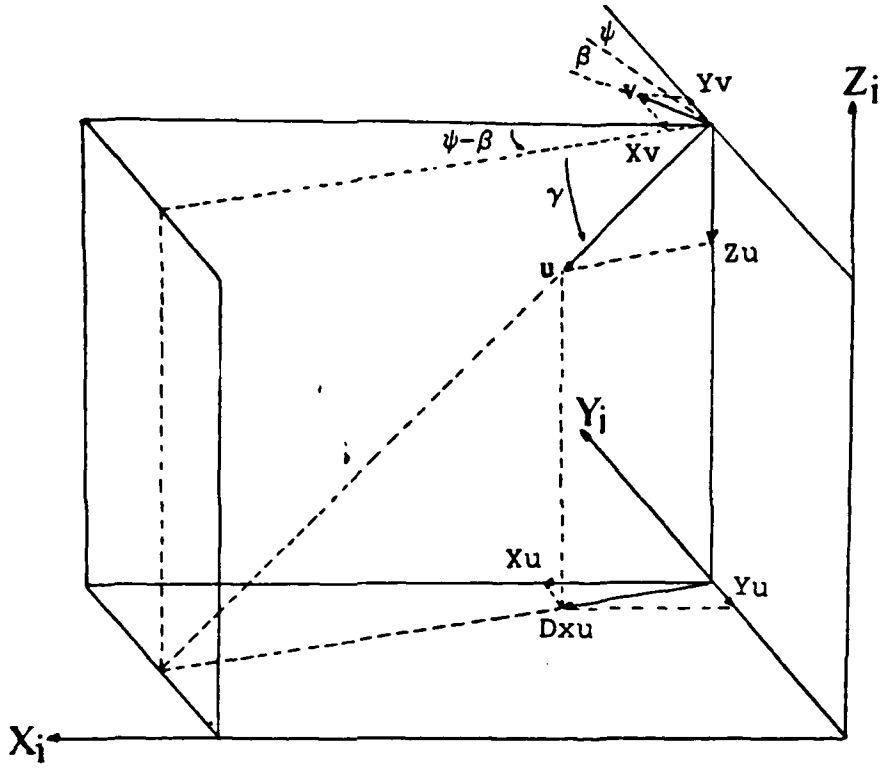

where γ : Flight path angle
Dxu : True velocity projectile on x,y plane
u : True velocity of the bomb
v : Lateral velocity of the bomb
β : Side slip angle
Xu,Yu,Zu : True velocity components
Xv,Yv : Lateral velocity components

Figure 3.15 Velocity Components of the Bomb.

The calculation of the bomb position at time ti+ Δt as follows:

True velocity projected on the inertial X-Y plane :

$$Dxu = u * \cos\gamma$$

True velocity components on the inertial X,Y and Z axes :

$$Xu = Dxu * \cos(\psi - \beta)$$

$$Yu = Dxu * \sin(\psi - \beta)$$

$$Zu = u * \sin\gamma$$

Lateral velocity component on the inertial X and Y axes :

$$Xv = v * \sin(\psi - \beta)$$

$$Yv = v * \cos(\psi - \beta)$$

The total velocity components on the inertial X,Y and Z axes

$$Velx = Xu + Xv$$

$$Vely = Yu + Yv$$

$$Velz = Zu$$

Then the position of the bomb at time ti+ t:

$$Xb_{i+1} = Xb_i + Velx * \Delta t$$

$$Yb_{i+1} = Yb_i + Vely * \Delta t$$

$$Zb_{i+1} = Zb_i + Velz * \Delta t$$

where Δt=0.15 seconds.

When the position of the bomb at time ti+Δt is found, it is used as the initial conditions for the next calculation step. This procedure goes on throughout the flight. Finally, when the altitude, Zb, reaches zero, the X and Y position of the bomb dtermine the impact point on the ground.

If it is assumed that the target is moving, in addition to the target location, true target speed and the angle between the target velocity and the inertial X axis have to be provided to the computer algorithm as inputs. The position of the target for each time ti is calculated according to these inputs (Figure 3.16), as

Target velocity components on inertial X and Y axes :

$$Vtx = Vt * \cos(a)$$

$$Vty = Vt * \sin(a)$$

The position of the target at time ti+1 :

$$Xt_{i+1} = Xt_i + Vtx * \Delta t$$

$$Yt_{i+1} = Yt_i + Vty * \Delta t$$

where Δt=0.15 seconds.

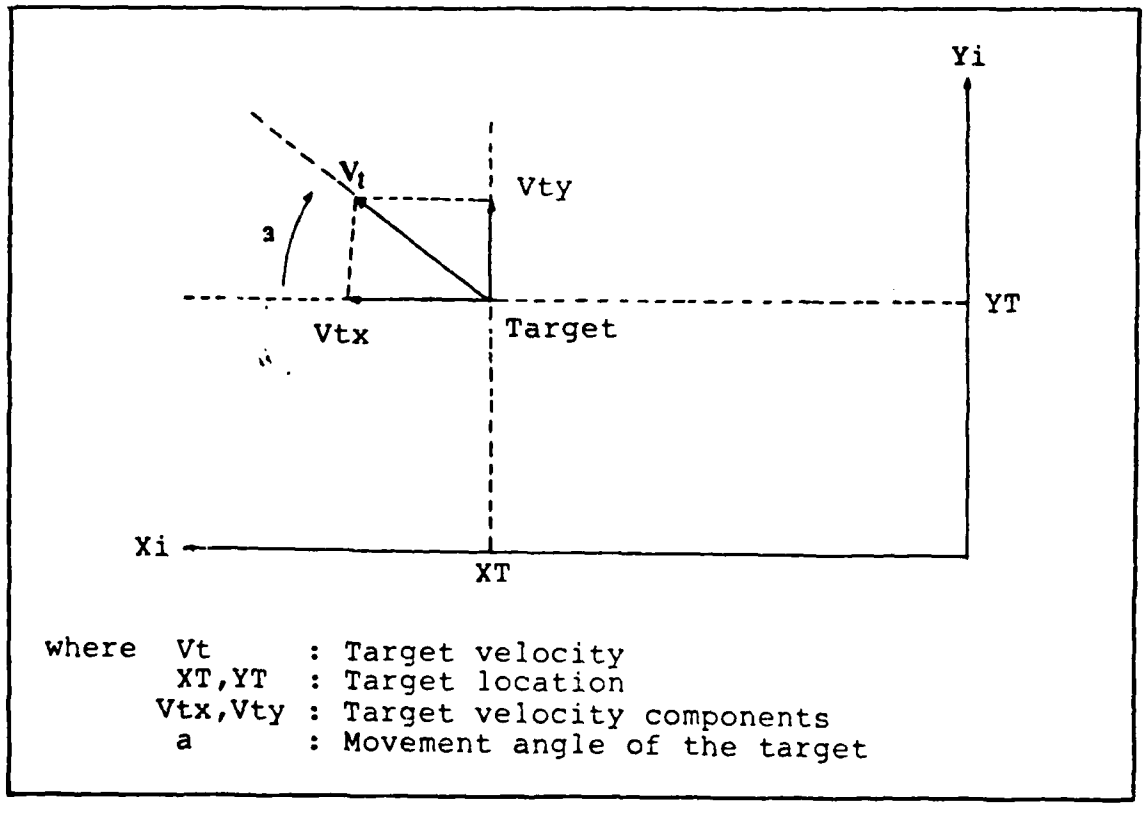

Figure 3.16. Velocity Components of the Target.

IV RESULTS

Introduction

This chapter presents the discussion of the results of the simulation program designed in Chapter III for the laser guided bomb with triad detector array strapdown seeker. The simulation is tested for both moving and nonmoving targets. Trajectory and the error angle plots are included in the appendices section.

General Performance of the Triad Detector Array Seeker

The performance evaluation of the triad detector array strapdown seeker is done with respect to both the trajectory and the impact point of the bomb. The seeker provides information about the error angles by producing signals that are functions of the error angles. The maneuvers of the bomb are determined by the servo driving signals known as pitch and yaw command signals and the bomb dynamics.

The simulation of the triad detector array depends on the integration of discrete pixels. Therefore the sensitivity of the detector array is a function of these pixels. The angular resolution of one pixel of the detector surface in the vertical and horizontal direction, represents a 0.002727 radian (0.1562456°) change in the error angles. Thus the sensitivity of the detector array to change of location of the laser spot is 0.002727 rad. If the laser spot location change is less than this value, it can not be

measured by the detector array.

The seeker signal processor is capable of producing error signals that are linear functions of the error angles. But the linearity of the signal processor depends on the location of the laser spot on the detector array. If the laser spot is not completely within the detector array, the error signals produced by the signal processor are not linear functions of the error angles (Figure 4.1). However, the detector still provides error signals that can be used by the signal processor as long as any portion of the laser spot is on the detector array.

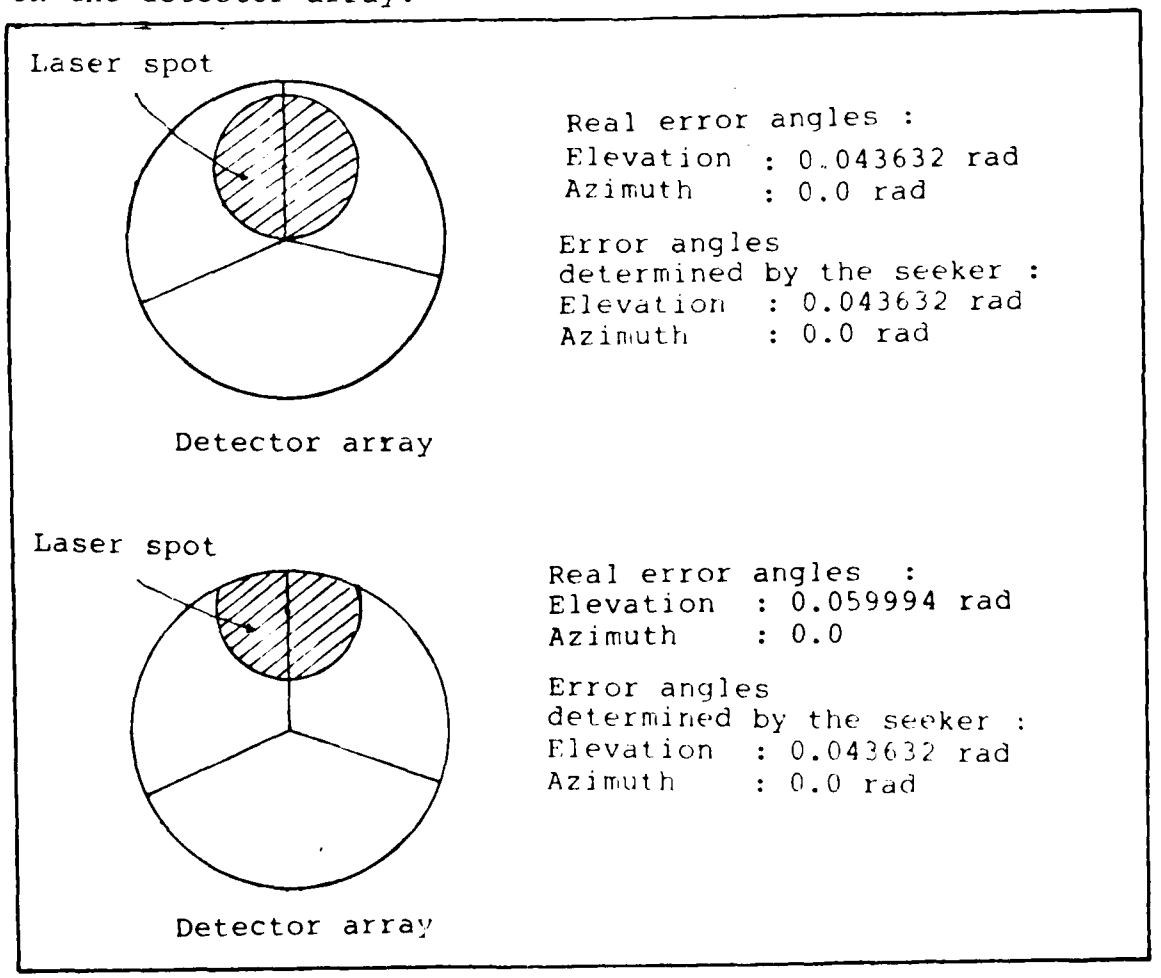

Figure 4.1. The Relation Between the Error Angles Measured by the Seeker and the Laser Spot Location.

According to the explanation above, the operation curve of the triad detector array strapdown seeker can be described as shown in Figure 4.2. When the real error angles are larger than 0.087265 rad (≈5°), the measured error angles are actually smaller than the real error angles. As error angles enter the linear range the seeker measures the exact error angles within ± one half pixel. Then the command signals are produced by multiplying the error signals with the gains. The determination of the longitudinal and lateral gains are discussed in the trajectory evaluation in this chapter.

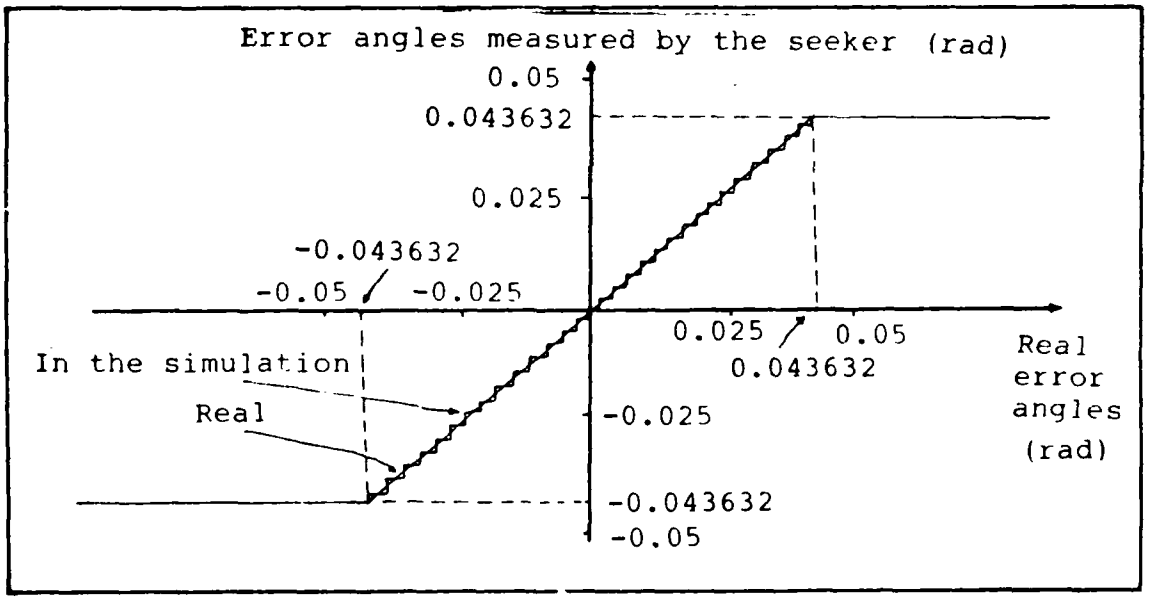

Figure 4.2 The Operation Curve of the Triad Detector Array Strapdown Seeker

Trajectory Evaluation and the Determining the Gains

The bomb is released from an airplane with initial error angles. It is desired that these error angles will be

corrected before the bomb impacts the ground. In the longitudinal mode, when the bomb is very far from the target, the gain is set to 1.8, to provide stable operation. Since the system type is zero, the proper gain provides stable response for the bomb. Any rate feedback compensation added to the system requires the use of additional hardware. For that reason, a rate compensator is not added to the guidance scheme. If the longitudinal gain is smaller than 1.8, the bomb never catchs the nominal trajectory, since the provided correction is not enough. On the other hand, if the longitudinal gain is larger than 1.8 the respond of the bomb becomes unstable as the bomb approaches the target (Figure 4.3).

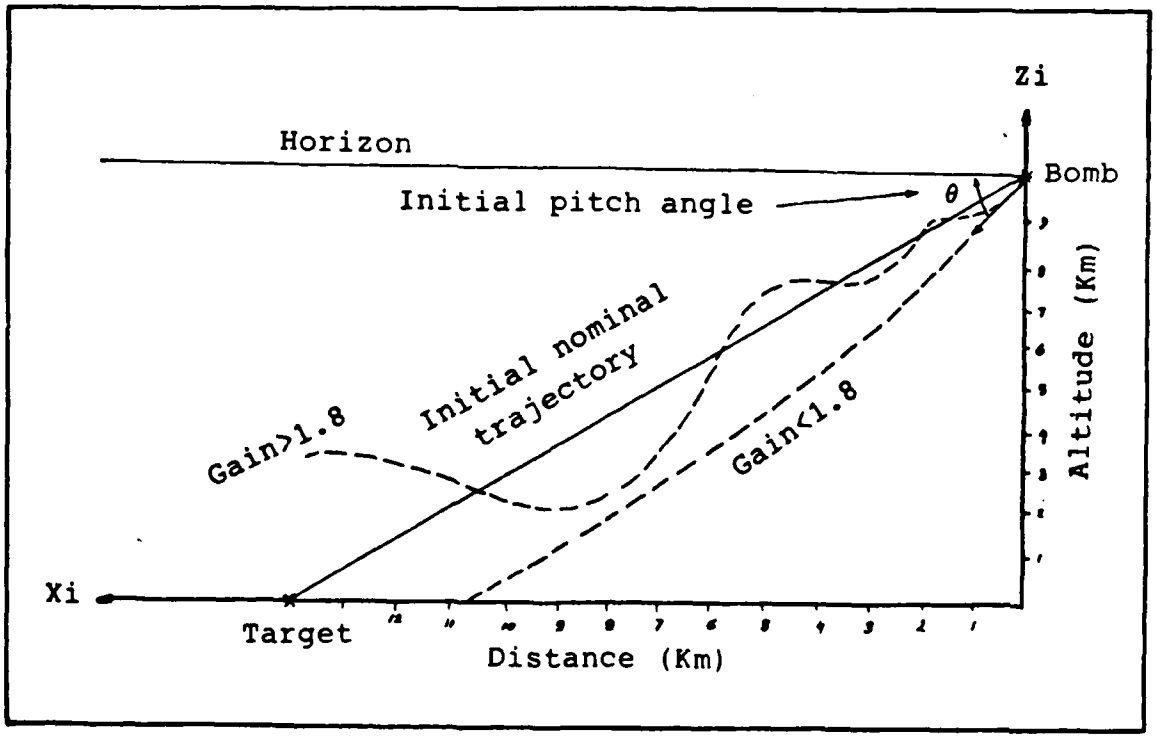

Figure 4.3 The Responses of the Bomb for Extreme Gains in Longitudinal Mode.

The same evaluation can be made for the lateral mode of the bomb. This time, when the lateral gain is set to 0.8, the stable operation can be achieved. As shown in Figure D.1, D.2 in Apendix D (longitudinal trajectory and elevation error plots for the bomb equations described in Chapter II) the initial elevation error angle is corrected and held at a small negative value within the first one fourth of the flight. However, as the bomb gets closer to the target, the error angle created by the change of the nominal trajectory can not be corrected. More than 50 values were evaluated for the longitudinal gain until it was obvious that the bomb equations actually did not describe the system properly. The response of the bomb in the longitudinal mode is dominated by the phugoid mode as the bomb approaches the target and the response is very slow. Also the bomb gets closer to the target, the change of the nominal trajectory is much more rapid than the change of the bomb pitch angle (Figure 4.4).

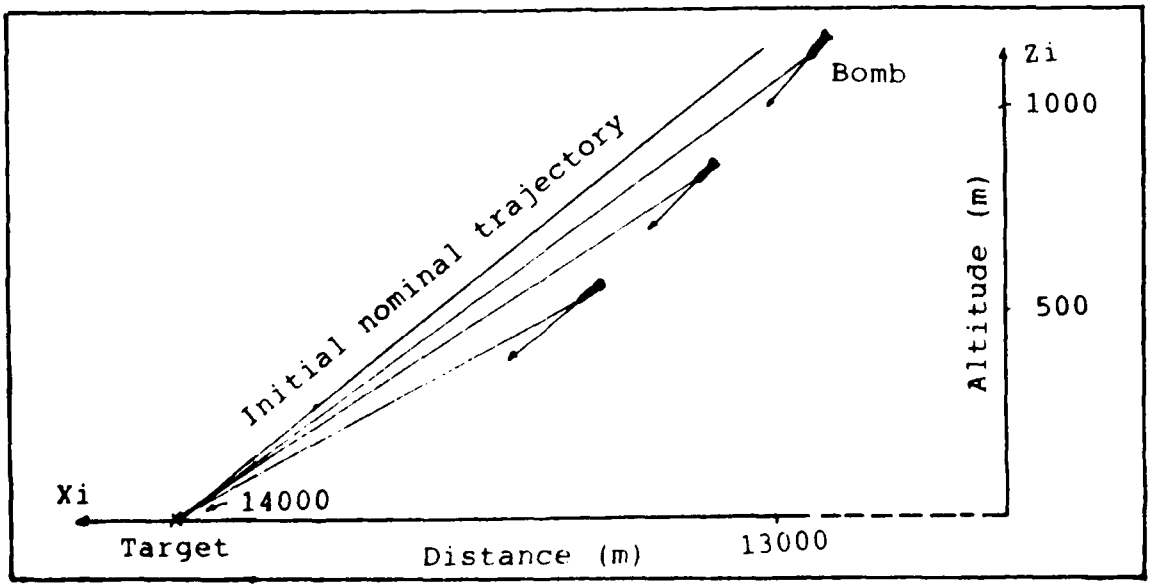

Figure 4.4 Change of the Nominal Trajectory at Final Phase.

At this range the bomb pitch angle changes toward the nominal trajectory, but slow response causes the elevation error angle to increase rapidly (Figure 4.5). Therefore, the elevation error angle in the last one fourth of the flight can not be corrected with this bomb model.

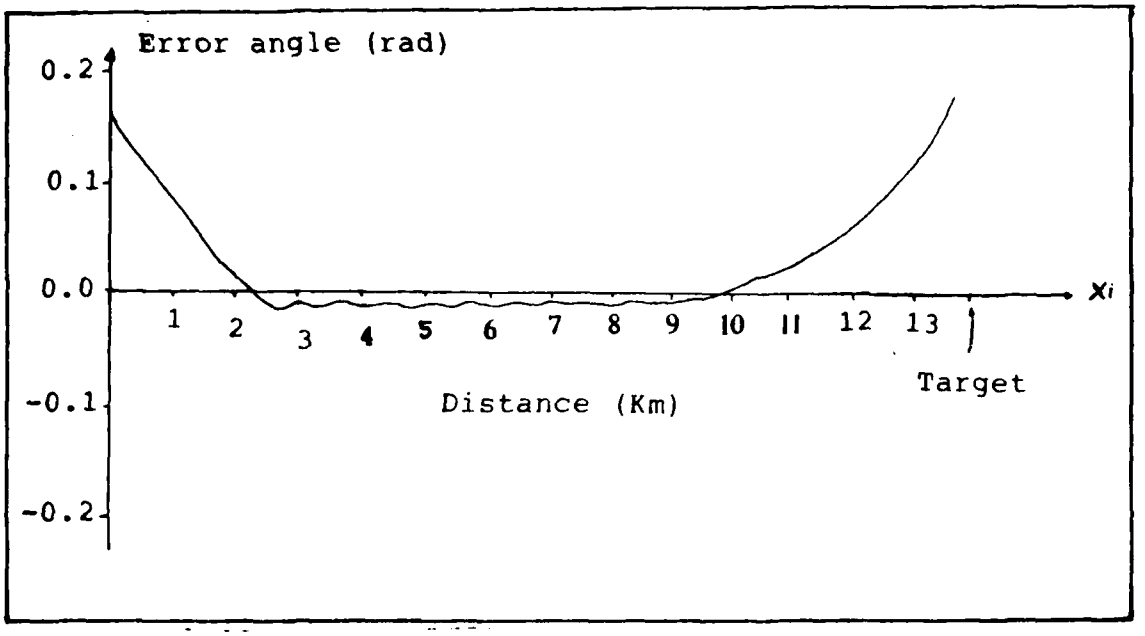

Figure 4.5 Increase in Elevation Error Angle in Close Range.

Before assuming a new set of equation for the bomb dynamics, the longitudinal gain is increased throughout the flight, beginning from 1.8, to make the response of the bomb faster as the bomb gets closer to the target. This improves the response of the bomb, but the bomb still can not return to the nominal trajectory. Also the gain increase causes the system to move into unstable region (Figure 4.6). Beginning from that point, the bomb does not respond to the commands as desired because the system is unstable. In the lateral mode of the bomb, there is no phugoid effect. Therefore, the

lateral nominal trajectory is followed with a small azimuth error throughout the flight (Figure 4.7).

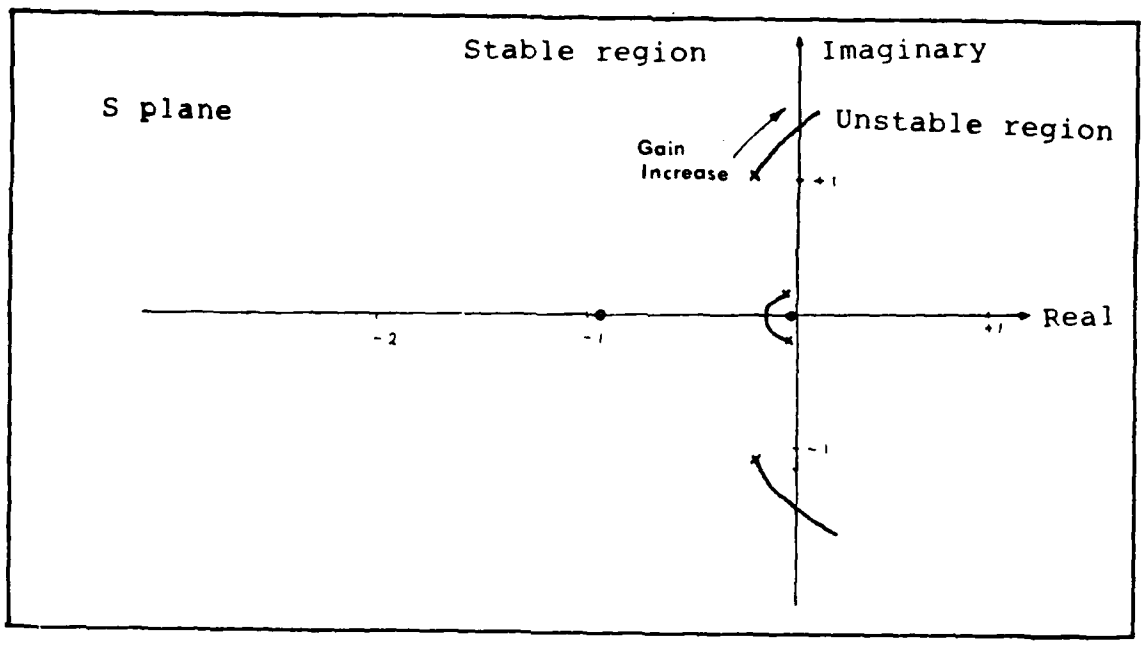

Figure 4.6 Root Locus for the Transfer Function of the Pitch Angle with Elevator Deflection.

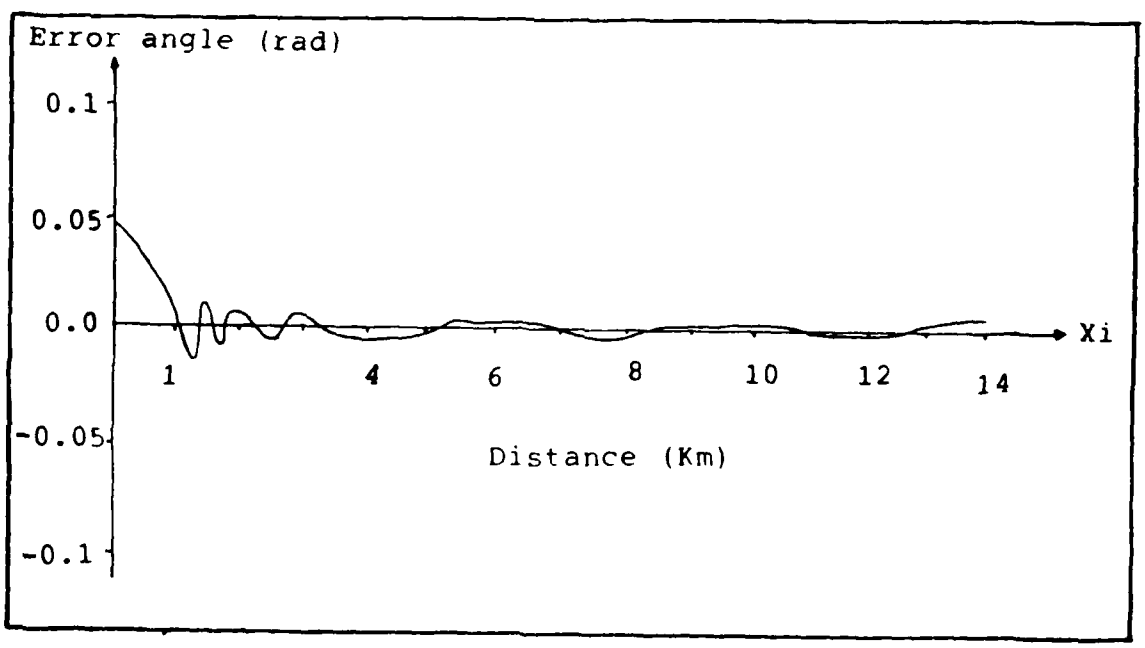

Figure 4.7 Azimuth Error Angle Throughout Flight.

Impact Point Evaluation

It is obvious that the triad detector array strapdown seeker does not correct the position offset with the bomb equations described in Chapter II. Therefore, it is expected that the impact point of the bomb is not close to the target location. The bomb is released from 10000.0 m altitude and a 500.0 m lateral offset (inertial y axis) with -45° initial pitch angle and 0° initial yaw angle. The target is located 14000.0 m on inertial x axis, 4500.0 m on inertial y axis. If there is no guidance the bomb will hit the ground at 10000.0 m on x axis. Table I shows that the triad detector array strapdown seeker provides guidance, however, the reasons described above cause the bomb not to reach the target location.

Table I. Statistics of Results for Bomb Dynamics 1.

Bomb release conditions					
XB	YB		ZB	Ψinitial	Θinitial
0.0	4000.0 m		10000.0 m	0.0°	-45°
Target initial conditions				Final target location	
XT	YT	Vt	a	X	Y
14000.0 m	4500.0 m	0.0 m/s	0.0°	14000.0 m	4500.0 m
Bomb impact point				Difference	
No noise	13801.0 m		4490.0 m	-199.0 m	-10.0 m
Noise level I	13790.0 m		4492.0 m	-210.0 m	-8.0 m
Noise level II	13785.0 m		4493.0 m	-215.0 m	-7.0 m

Because of the confidential nature of the real bomb data, realistic bomb equations can not be provided. Also, developing equations for a real bomb is itself a thesis subject. For that reason, other bomb equations are assumed that give faster response than the bomb described in Chapter II does. For the second bomb dynamics, the short period and the phugoid modes, damping ratios and natural frequencies are selected as follows :

Short period :

$\zeta_s = 0.7$

$\omega_{ns} = 1.3$ rad/sec

Phugoid mode :

$\zeta_p = 0.352$

$\omega_{np} = 1.145$ rad/sec

The longitudinal and the lateral dynamic equations are given in Appendix B.

Trajectory Evaluation and Determining the Gains (2).

With the modified bomb dynamic equations, faster response is achieved. For that reason, longitudinal gain of 0.02 is enough to provide stable operation. As seen in Figure 4.8, the initial elevation error angle is corrected within the first one fourth of the flight and kept at a small constant negative value. This negative elevation error angle shows that the bomb is flying with a positive angle of attack (Figure 4.9). Because of the bomb dynamics

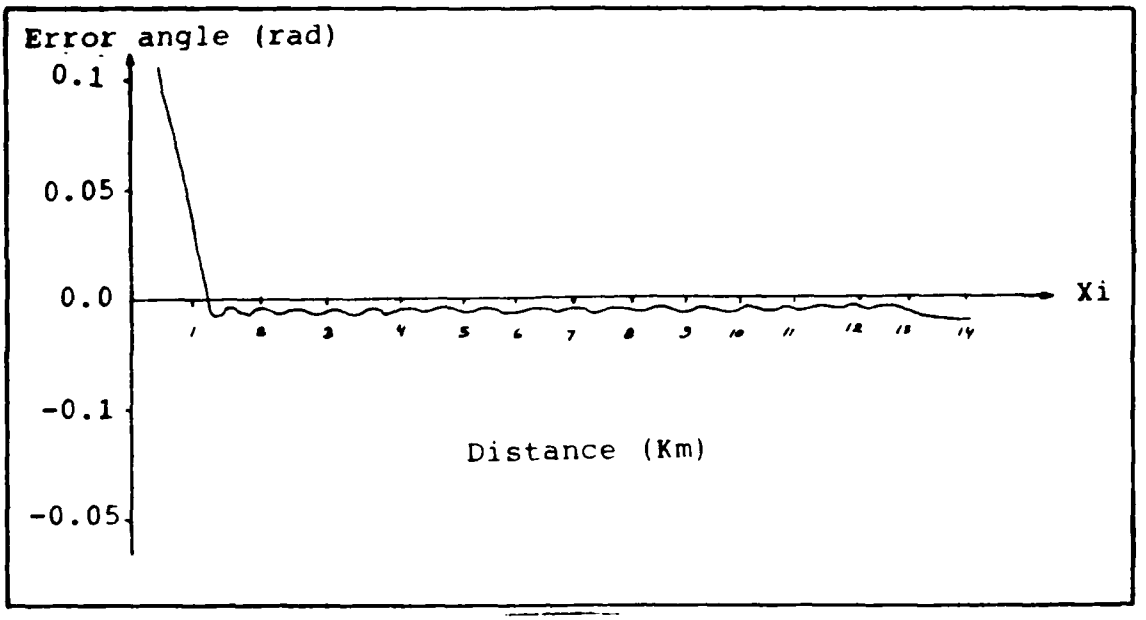

Figure 4.8 Elevation Error Angle for Bomb Dynamics 2.

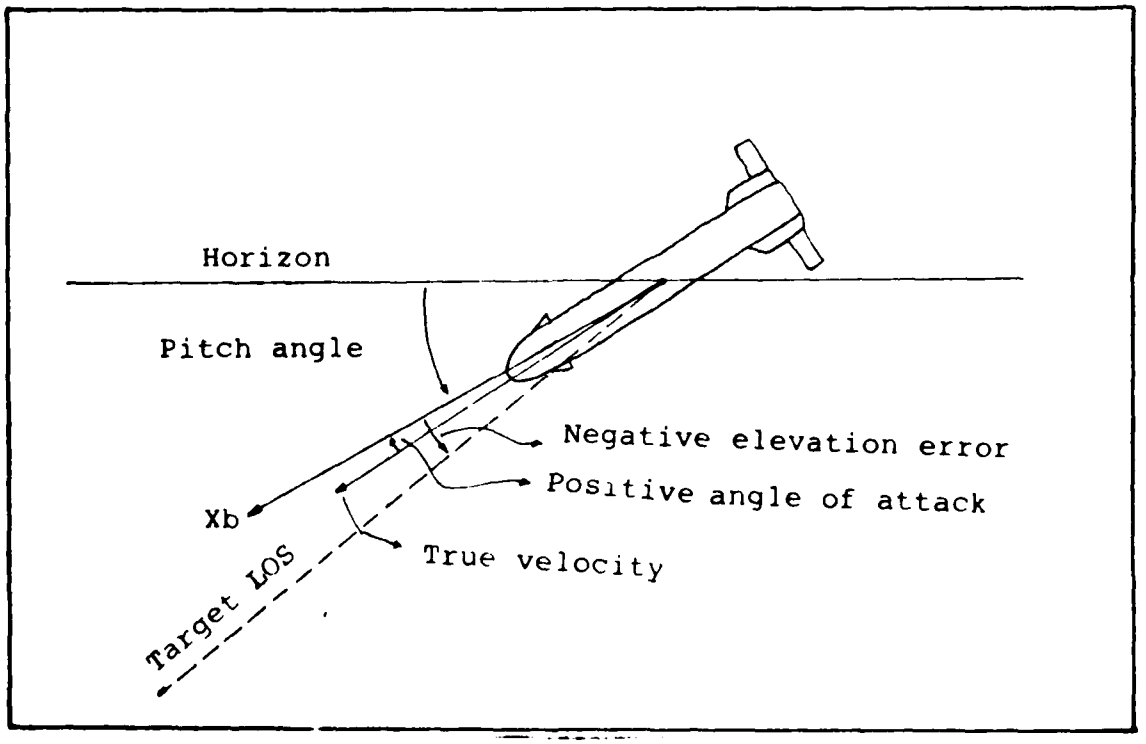

Figure 4.9 Flying Conditions in Longitudinal Mode for Bomb Dynamics 2.

and the small longitudinal gain, this angle of attack is maintained throughout the flight. The same result is seen for the lateral gain of 0.8. This lateral gain provides stable operation, but the azimuth error angle is kept at a nearly constant small positive value (Figure 4.10). This indicates a side slip angle. Actually, if the gains are increased, these angles can be reduced to zero. However, larger gains drive the system into unstable region earlier in the flight. When the noises and the errors are added to the system, the triad detector array strapdown seeker guides the bomb into the nominal trajectory, and the error angles are kept small (Appendix E).

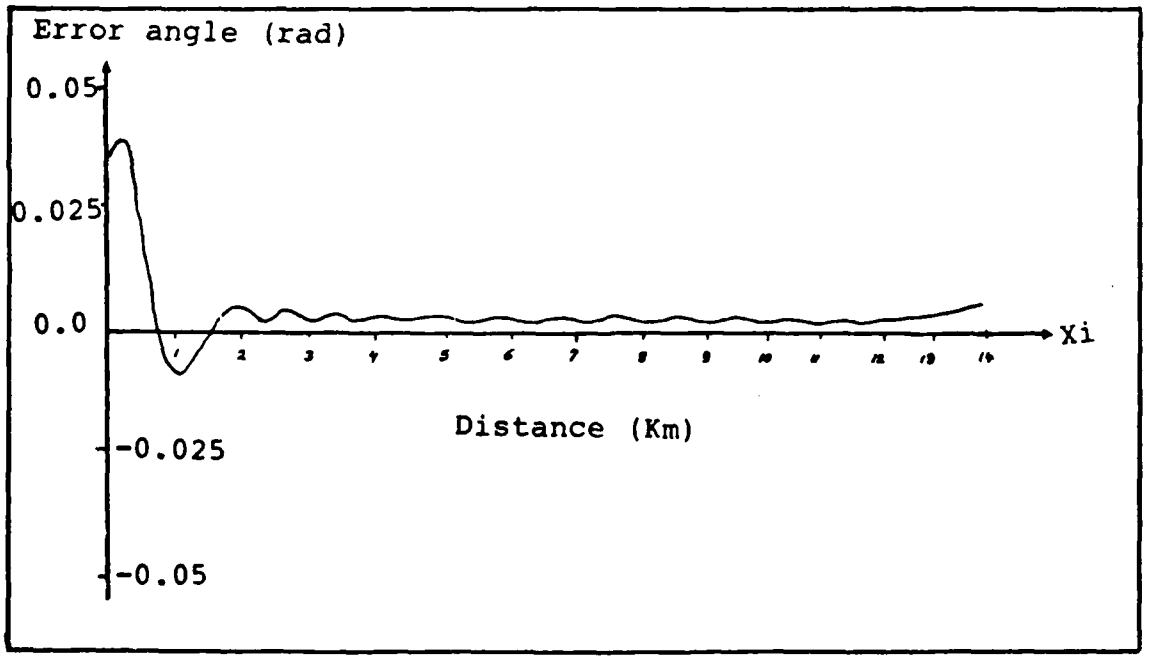

Figure 4.10 Azimuth Error Angle for Bomb Dynamics 2.

Impact Point Evaluation (2).

When the bomb is tested under no noise conditions, as shown in Figures E.1, E.3 in Appendix E, the impact point of the laser guided bomb is 1.46 m beyond the target on the longitudinal axis (Xi) and 2.0 m to the left of the target on the lateral axis (Yi) using modified bomb equations. Actually, as the bomb gets closer to the target, two problems are encountered. First, the laser spot on the detector array is getting larger. Even, the laser spot can completely cover the detector surface. Once the laser spot covers the entire detector, the error signals produced by the seeker are not related to the error angles. The solution used to overcome this problem is to shut off the detector 250 m from the target to avoid unwanted maneuvers of the bomb. The second problem is the oscillation seen before entering the blind range. The rapid change of the error angles, because of the close range causes this oscillation in the longitudinal mode (Figure 4.11). The bomb is undergoing this oscillation

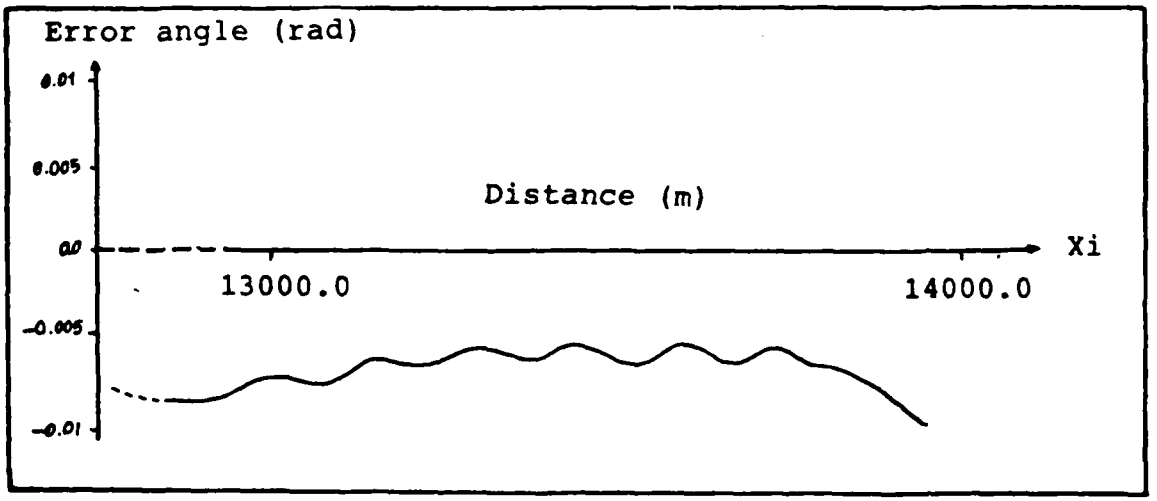

Figure 4.11 Close Range Oscillation in Longitudinal Mode.

even before 250 m. This oscillation is related with the bomb configuration and resulting bomb dynamics. Thus the turning off the detector at any range may not be the real solution of these problems. Even if noise and the errors are added to the system and if the target is assumed to be larger than a two meter by two meter object, the destruction of the target can be achieved while the target is not moving (Table II).

Table II. Statistics of Results for Bomb Dynamics 2.

Bomb release conditions					
XB	YB	ZB	Ψinitial	Θinitial	
0.0 m	4000.0 m	10000.0 m	0.0°	-45°	
Target initial conditions				Target final location	
XT	YT	Vt	a	x	y
14000.0 m	4500.0 m	0.0 m/s	0.0°	14000.0 m	4500.0 m
Bomb impact point				Difference	
	x	y		x	y
No noise	14001.46 m	4498.0 m		+1.46 m	-2.0 m
Noise level I	14002.33 m	4499.0 m		+2.33 m	-1.0 m
Noise level II	13996.51 m	4501.0 m		-3.49 m	+1.0 m

If the target is moving, the trajectory of the bomb changes toward the target position (Appendix F). However, since the seeker is strapdown, there is no information about the target LOS rate. Therefore, the bomb never achieves a destruction on the moving targets even in a no noise conditions (Table III).

Table III. Statistics of Results for Moving target.

Bomb release conditions				
XB	YB	ZB	Ψinitial	Θinitial
0.0 m	4000.0 m	10000.0 m	0.0°	-45°

Target initial conditions			
XT	YT	Vt	a
14000.0 m	4500.0 m	14 m/sec	+45°
14000.0 m	4500.0 m	-12 m/sec	+45°
14000.0 m	4500.0 m	-10 m/sec	+45°

Noise level	Bomb impact point (m)		Final target location (m)		Difference (m)	
	x	y	x	y	x	y
0	14657.7	5199	14686	5186	-28.43	13
0	13465.2	3967	13448.7	3946	16.5	21
0	13618.2	4097.9	13582.5	4082.2	35.6	15.7
I	13681.5	4189.7	13674.3	4174.4	7.2	15.3
II	13678.4	4188.9	13674.6	4174.2	3.8	14.7

V CONCLUSIONS AND RECOMMENDATIONS

Introduction.

The triad detector array strapdown seeker designed in Chapter II is used in the simulation of the laser guided bomb. The signal processor is developed just for this triad detector array to produce the error signals for guidance. The complete guidance law for a laser guided bomb is simulated in a computer algorithm to evaluate the triad detector array strapdown seeker performance for nonmoving and moving targets in Chapter III. The simulation is run to determine and evaluate the impact point and the longitudinal and lateral trajectories of the bomb. This chapter presents the conclusions drawn from the results and the recommendations for expanding on the work done for this study.

Conclusions.

The signal processor design for triad detector array sensor performed well in producing error signals related to the error angles. The mathematical function of the signal processor converts the intensity values on detector surface into error signals. This is done by taking the intensities on each detector as vectors in three axis frame and evaluating the force center in azimuth and elevation axes in detector frame. If the second bomb dynamics are used to evaluate the triad detector array strapdown seeker, an

accuracy of 2.5 m is achieved in both X and Y direction of the inertial frame. Even in the high noise and large error conditions, this accuracy has been reached while the target is not moving. If the target is moving, the impact point of the bomb is never closer to the target than 20.0 m. Actually in the mowing target case, the nominal trajectory is followed, but at close range the bomb can not respond fast enough to follow the changing nominal trajectory. The guidance applied to the bomb is pursuit guidance. It is provided just from the measurements of the immediate error angles. Since there is neither information about the target LOS rate, no target position estimator, the bomb can not easily destroy moving targets while using this controller design.

In the simulation of the laser guidance with triad detector array strapdown seeker, the nominal trajectory is captured in the first one fourth of the flight. Loss of the seeker at midflight, if the wind effect is not large, does not decrease the accuracy of the bomb significantly. The results of the simulation show that the triad detector array can provide the necessary information about the error angles of the bomb from the target LOS while using the signal processor designed in Chapter II. With the accuracy achieved from this simulation, the triad detector array strapdown seeker can be used for nonmoving enemy targets without endangering the aircraft and personel.

In the simulation, since the limited sources and time

AD-A159 215 LASER GUIDANCE WITH TRIAD DETECTOR ARRAY STRAPDOWN SEEKER(U) AIR FORCE INST OF TECH WRIGHT-PATTERSON AFB OH SCHOOL OF ENGINEERING N KASIKCIOGLU JUN 85 2/2

UNCLASSIFIED AFIT/GE/ENG/85J-3 F/G 17/7 NL

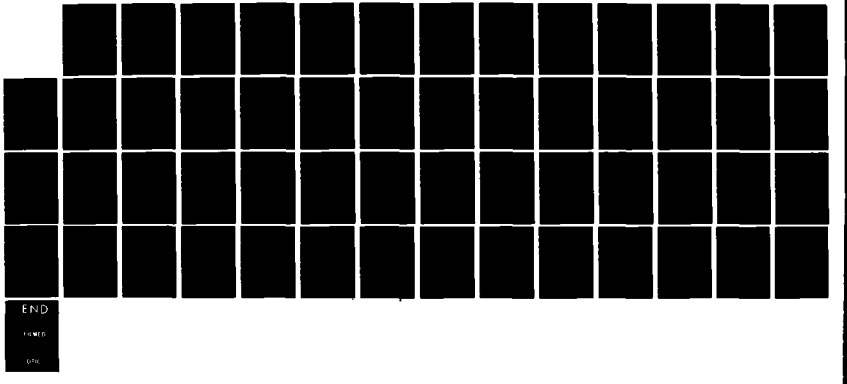

END

FILMED

DTIC

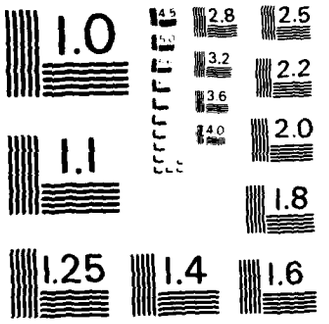

limited the Monte Carlo evaluation of the system, the impact point error mean and variance could not be determined.

Recommendations

Based on the results and the insight gained from this work, the following recommendations are made to guide future studies on the laser guidance with triad detector array strapdown seeker.

1) Use realistic bomb dynamic equations instead of assumed equations to evaluate the seeker in real life.

2) The impact point error mean and variance should be determined by testing the algorithm using a Monte Carlo simulation.

3) The triad detector array sensor can be mounted on two axis gimbal system or estimates of LOS rates to provide target LOS rate made for use in proportional guidance system.

4) The simulation should be modified to test the triad detector array seeker in different atmospheric conditions.

5) In the simulation for this thesis, the seeker has to acquire the target before it is released from an airplane. A searching scheme should be added to allow the bomb to be released before target acquisition.

6) The laser designator can be made coded and the signal processor is designed to recognise the designator code for destroying more than one targets in the same battle field.

Bibliography

1. Blakelock, John H. Automatic Control of Aircraft and Missiles. New York: John Wiley & Sons, Inc., 1965.

2. Clemow, J. Short Range Guided Weapons. London: Temple Press Limited, 1961.

3. Ehrich R. D., Vergez P. "Strapdown Seeker Technology for the Terminal Guidance of Tactical Weapons," AGARD-CP-292 Guidance and Control Aspects of Tactical Air-Launched Missiles. Neuilly Sur Seine, France: AGARD, October 1980. (AD AO92 606)

4. Heaston R. J., Smoots C. W. "How Smart Weapons Work," GACIAC HB-83-01, Vol. 1, Precision Guided Munitions. Chicago: GACIAC IIT Research Institue, May 1983.

5. Hobbs, Marvin. Basics of Missile Guidance and Space Technique. Volume 1, 2 vols. New York: John F. Rider Publisher, Inc., 1959.

6. Maybeck, Peter S. Stochastic Models Estimation and Control. Volume 1, 3 vols. New York: Academic Press, Inc.,1979.

7. Mc Aleese, Frank. The Laser Experimenter's Handbook. U.S.A.: Tab Books, Inc., 1979.

8. Meyer, Jurgen R. Introduction to Classical and Modern Optics. 2nd ed. New Jersey: Prentice-Hall, Inc., 1984.

9. "Military Ground-Based Laser designators," Lasers and Applications. September 1983, pp. 59-61.

10. O'shea C., Callen R., Rhodes W. Introduction to Lasers and Their Applications. 2nd ed. U.S.A.: Addison-Wesley Publishing Company, Inc., 1978.

11. Pressley, Robert. Handbook of Lasers. Cleveland, Ohio: The Chemical Rubber Co., 1971.

12. Safford, E. The Fiberoptics and Laser Handbook. U.S.A.: Tab Books, Inc., 1984.

13. Weston, Andrew C. "Dual-Seeker Measurement Processing for Tactical Missile Guidance," Master's Thesis, Air Force Institue of Technology, 1982.

14. Wolfe William, Zissis George. The Infrared Handbook. Washington: United States Goverment Printing Office, 1978.

Appendix A

Computer Algorithm Block Diagram

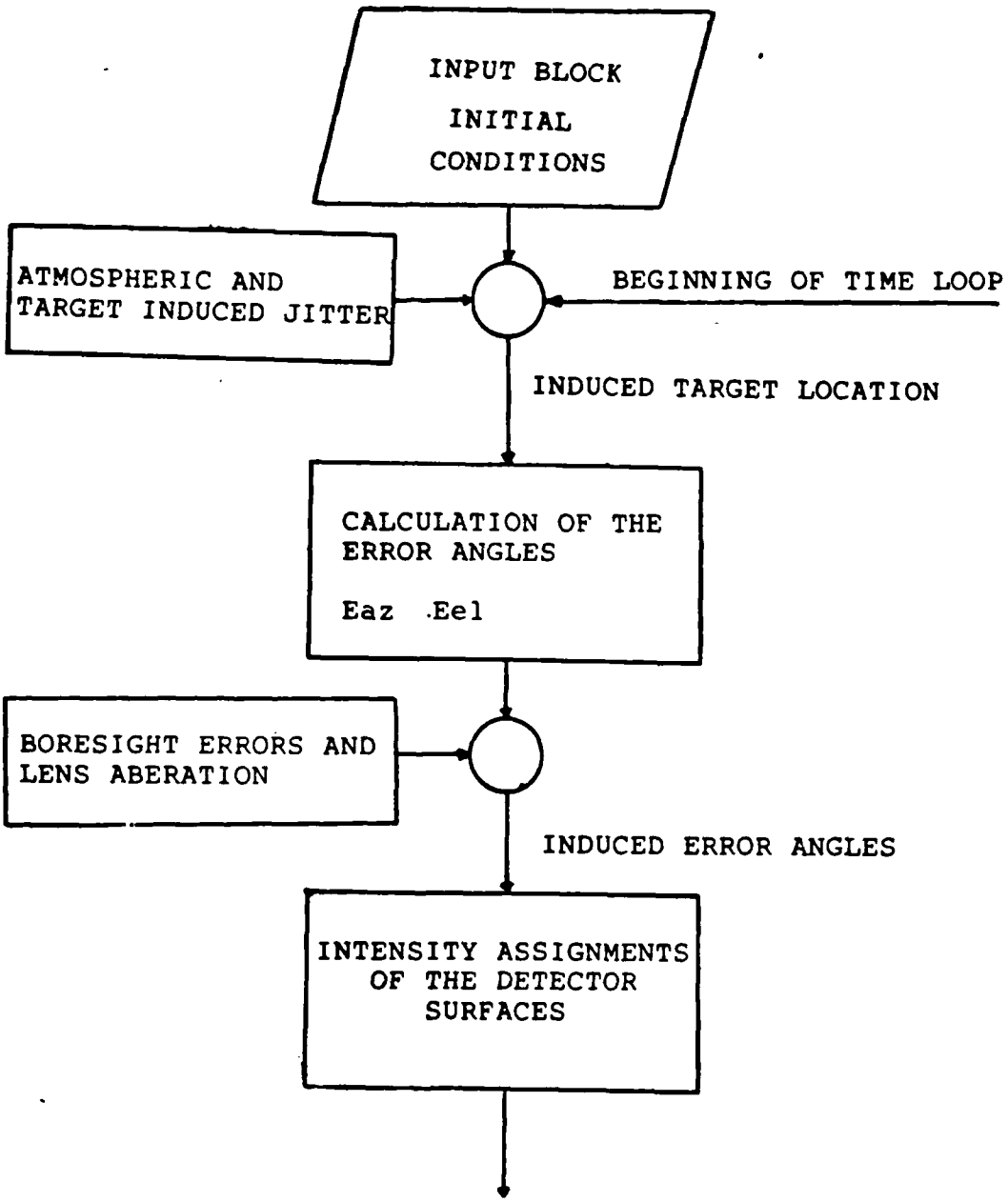

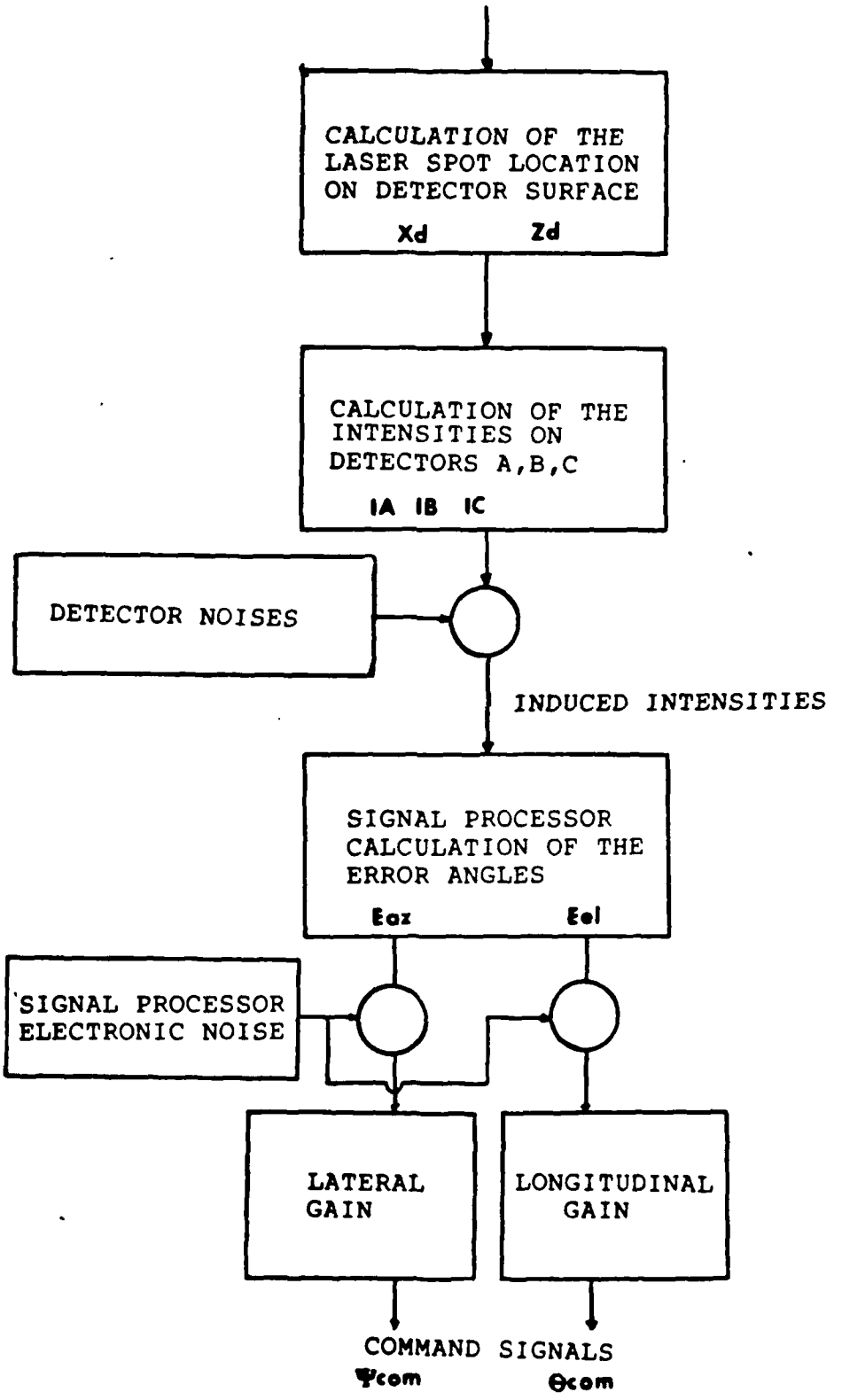
CALCULATION OF THE LASER SPOT LOCATION ON DETECTOR SURFACE
Xd Zd
CALCULATION OF THE INTENSITIES ON DETECTORS A,B,C
IA IB IC
DETECTOR NOISES
INDUCED INTENSITIES
SIGNAL PROCESSOR CALCULATION OF THE ERROR ANGLES
Eaz Eel
SIGNAL PROCESSOR ELECTRONIC NOISE
LATERAL GAIN
LONGITUDINAL GAIN
COMMAND SIGNALS
Ψcom
Θcom

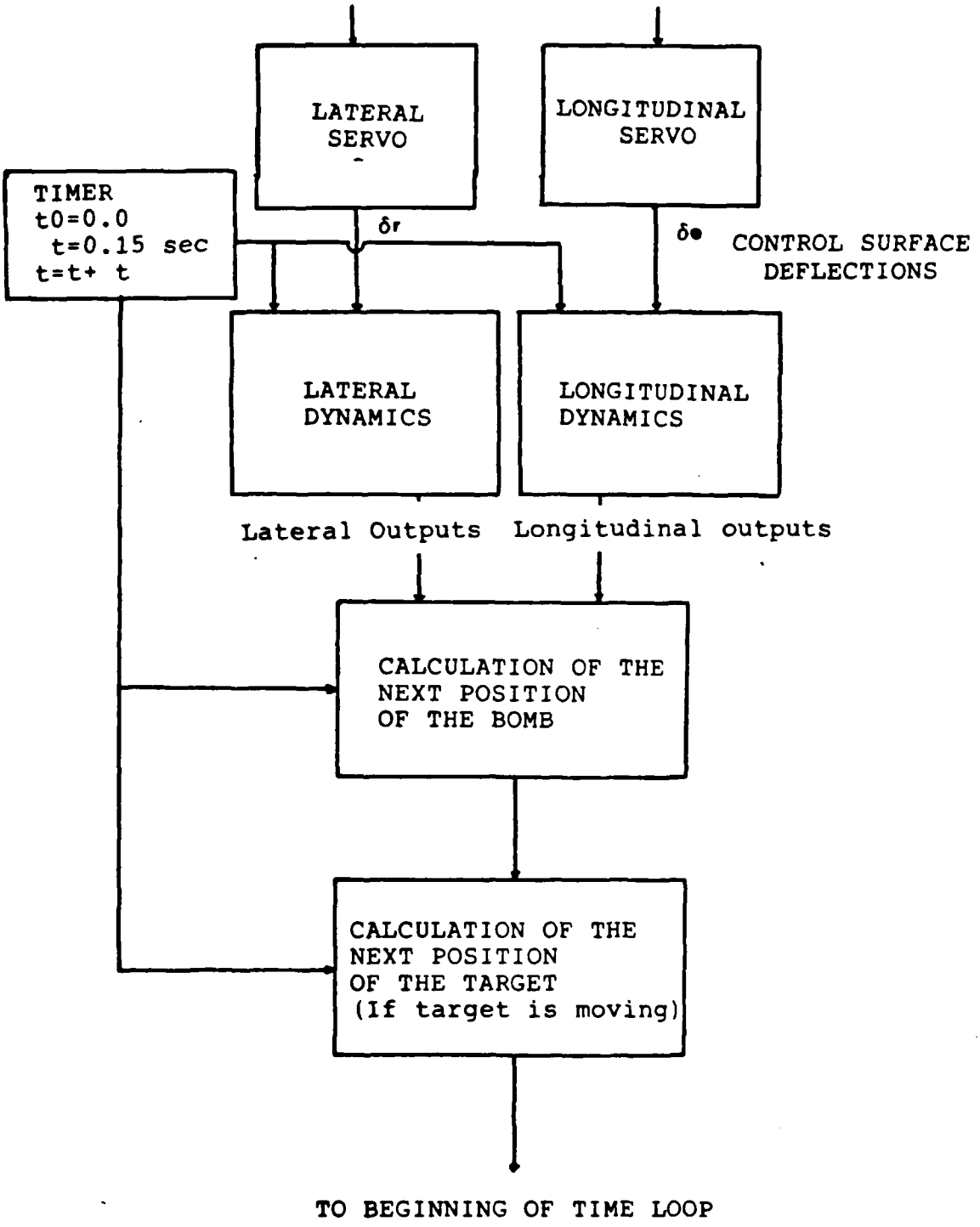
LATERAL SERVO
LONGITUDINAL SERVO
TIMER
t0=0.0
t=0.15 sec
t=t+ t
δr
δe
CONTROL SURFACE DEFLECTIONS
LATERAL DYNAMICS
LONGITUDINAL DYNAMICS
Lateral Outputs
Longitudinal outputs
CALCULATION OF THE NEXT POSITION OF THE BOMB
CALCULATION OF THE NEXT POSITION OF THE TARGET (If target is moving)
TO BEGINNING OF TIME LOOP

Appendix B

Bomb Dynamic Equations 2

Longitudinal dynamic equations :

The transfer function of the pitch angle perturbation for elevator deflection :

$$\frac{\delta\theta(s)}{\delta e(s)} = \frac{-70\ s}{s^4+2.626s^3+4.468s^2+3.748s+2.216} \qquad (B.1)$$

The transfer function of the true velocity perturbation for elevator deflection :

$$\frac{\delta u(s)}{\delta e(s)} = \frac{-0.196878s^2+8.667022s+8.864}{s^4+2.626s^3+4.468s^2+3.748s+2.216} \qquad (B.2)$$

The transfer function of the angle of attack perturbation for elevator deflection :

$$\frac{\delta\alpha(s)}{\delta e(s)} = \frac{-0.3s^3-15.003s^2-0.1116s-0.855}{s^4+2.626s^3+4.468s^2+3.748s+2.216} \qquad (B.3)$$

Lateral dynamic equations :

The transfer function of the yaw angle perturbation for rudder deflection :

$$\frac{\delta\psi(s)}{\delta r(s)} = \frac{-2.1125s-1.69}{s^2+1.82s+1.69} \qquad (B.4)$$

The transfer function of the lateral velocity perturbation for rudder deflection :

$$\frac{\delta v(s)}{\delta r(s)} = \frac{-0.1127s^2+4.9588s+5.0715}{s^2+1.82s\ 1.69} \qquad \text{(B.5)}$$

The transfer function of the side slip angle perturbation for rudder deflection :

$$\frac{\delta \beta(s)}{\delta r(s)} = \frac{-0.00676s-0.338}{s^2+1.82s+1.69} \qquad \text{(B.7)}$$

The second bomb dynamic equations are converted into canonic controllable form and augmented with the servo transfer function (Equation 3.9) by following the method explained in Chapter III.

Appendix C

Input Block, Initial Conditions

XT : Initial target location on axis X (m).

YT : Initial target location on axis Y (m).

XB : Initial bomb position on axis X (m).

YB : Initial bomb position on axis Y (m).

ZB : Initial bomb altitude (m).

θ_i : Initial bomb pitch angle (rad).

ψ_i : Initial bomb yaw angle (rad).

u : Bomb true velocity (m/sec).

Vt : Target velocity (m/sec).

a : Target movement direction (rad).

JMEX : Jitter mean on X axis of target frame (m).

JMEY : Jitter mean on Y axis of target frame (m).

JVAX : Jitter variance on X axis of target frame (m).

JVAY : Jitter variance on Y axis of target frame (m).

LEAZ : Lens placement error on azimuth axis of seeker (rad).

LEEL : Lens placement error on elevation axis of seeker (rad).

DEME : Detector noise mean (noise/(intensity+noise)).

DEVA : Detector noise variance (noise/(intensity+noise)).

SPME : Signal processor noise mean (noise/(noise+signal)).

SPVA : Signal processor noise variance(noise/(noise+signal)).

DSEED: Random generator seed number.

GAINT: Longitudinal gain.

GAINP: Lateral gain.

APPENDIX D

Bomb trajectory and error angle plots for

Bomb Dynamics 1

Input File1

XT : 14000.0

YT : 4500.0

XB : 0.0

YB : 4000.0

ZB : 10000.0

θi : -.7853982

ψi : 0.0

u : 260

Vt : 0.0

a : 0.0

JMEX : 0.0

JMEY : 0.0

JVAX : 0.0

JVAY : 0.0

LEAZ : 0.0

LEEL : 0.0

DEME : 0.0

DEVA : 0.0

SPME : 0.0

SPVA : 0.0

DSEED: 234324334

GAINT: 1.8

GAINP: 0.8

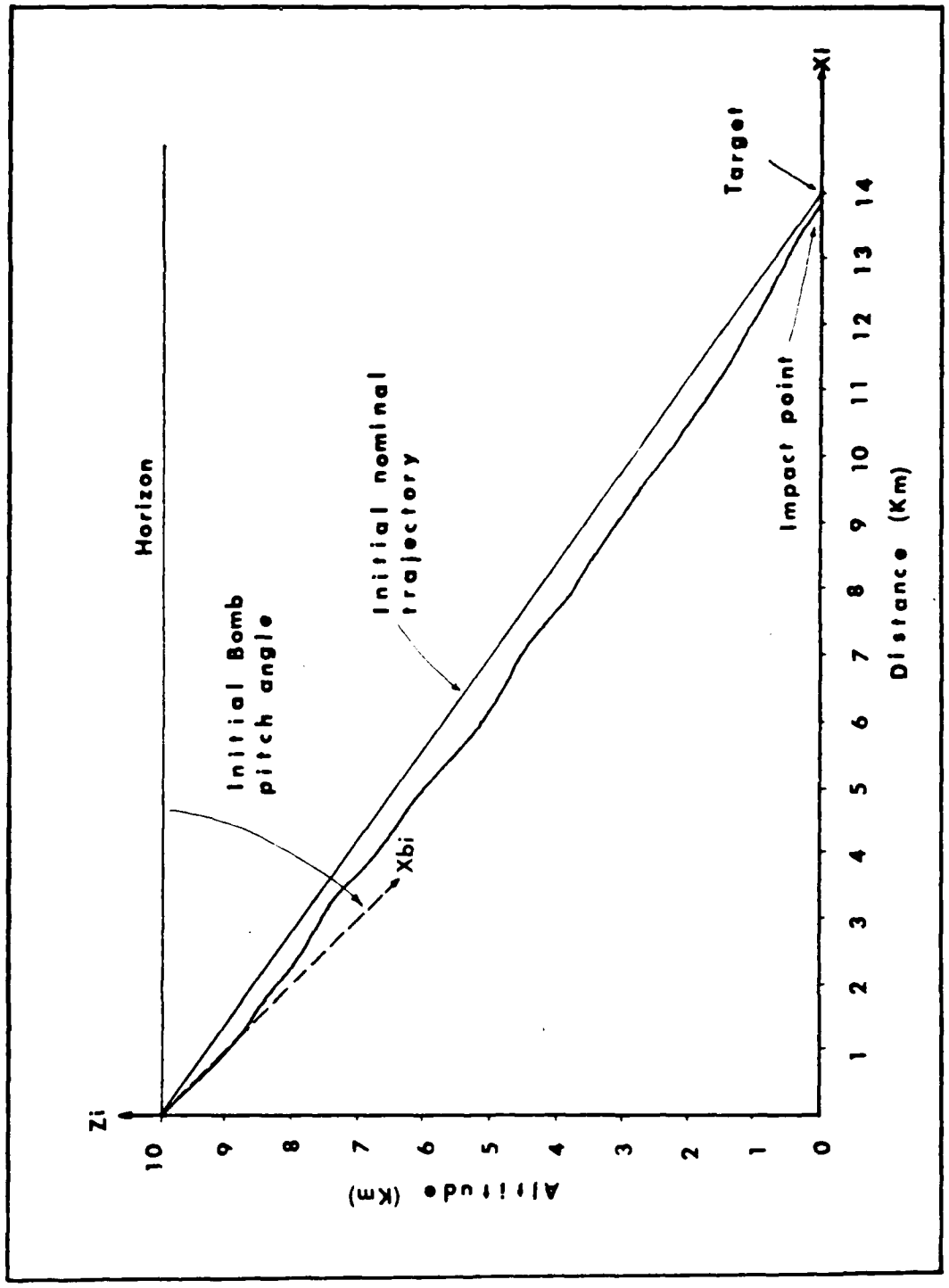

Figure D.1. Longitudinal Trajectory for Inputs in File 1.

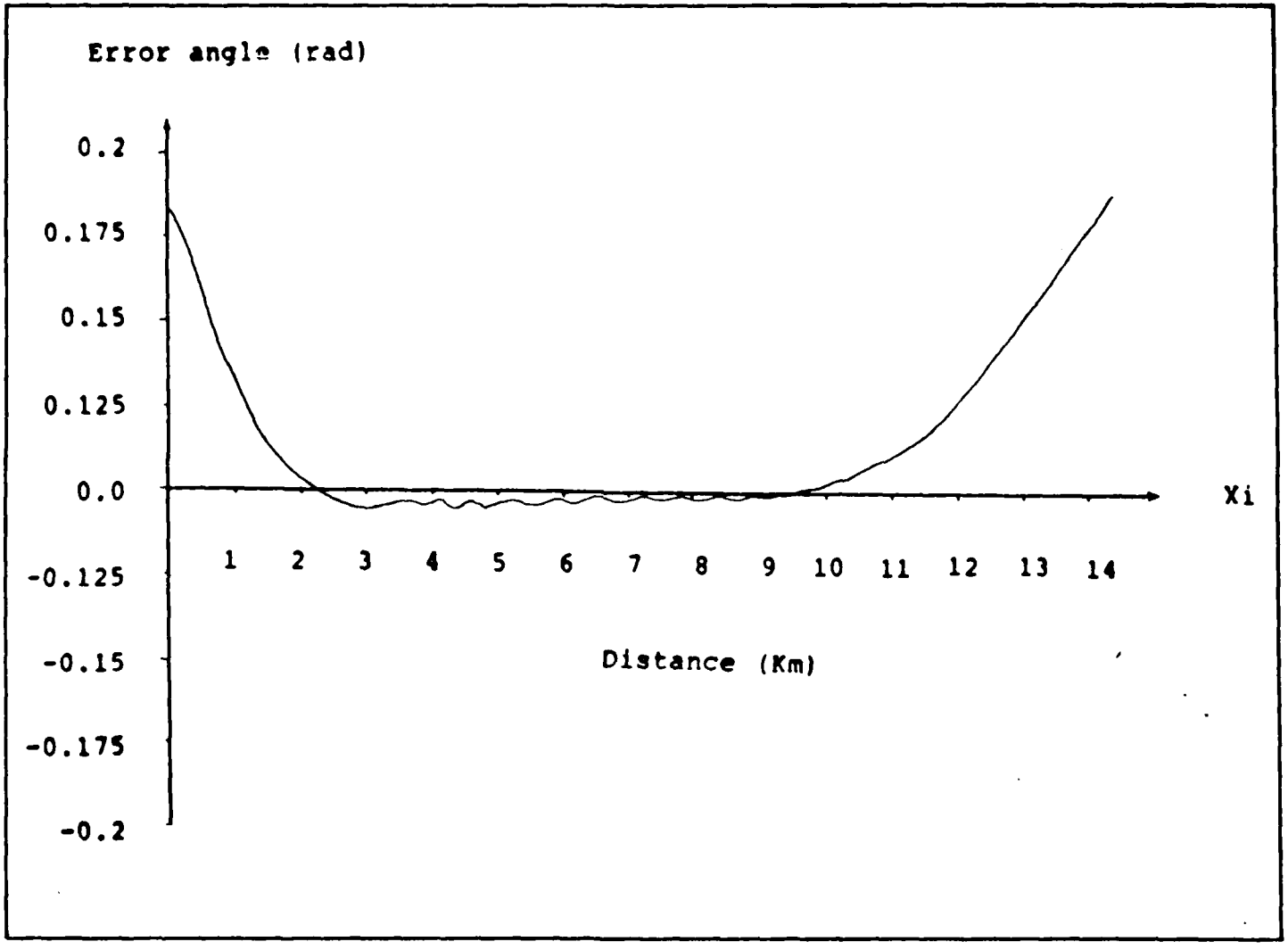

Figure D.2. Elevation Error Angle for Inputs in File 1.

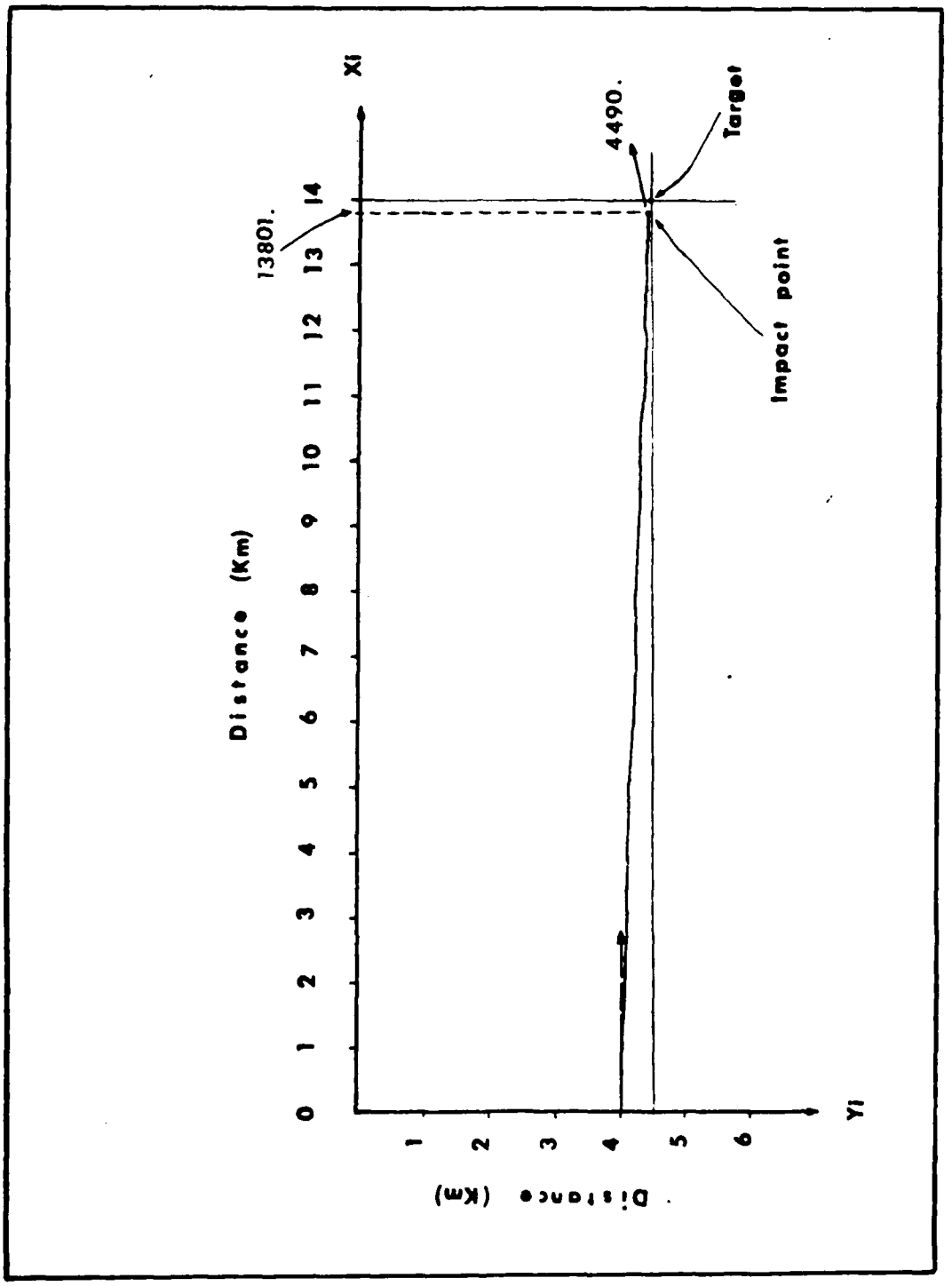

Figure D.3. Lateral trajectory for Inputs in File 1.

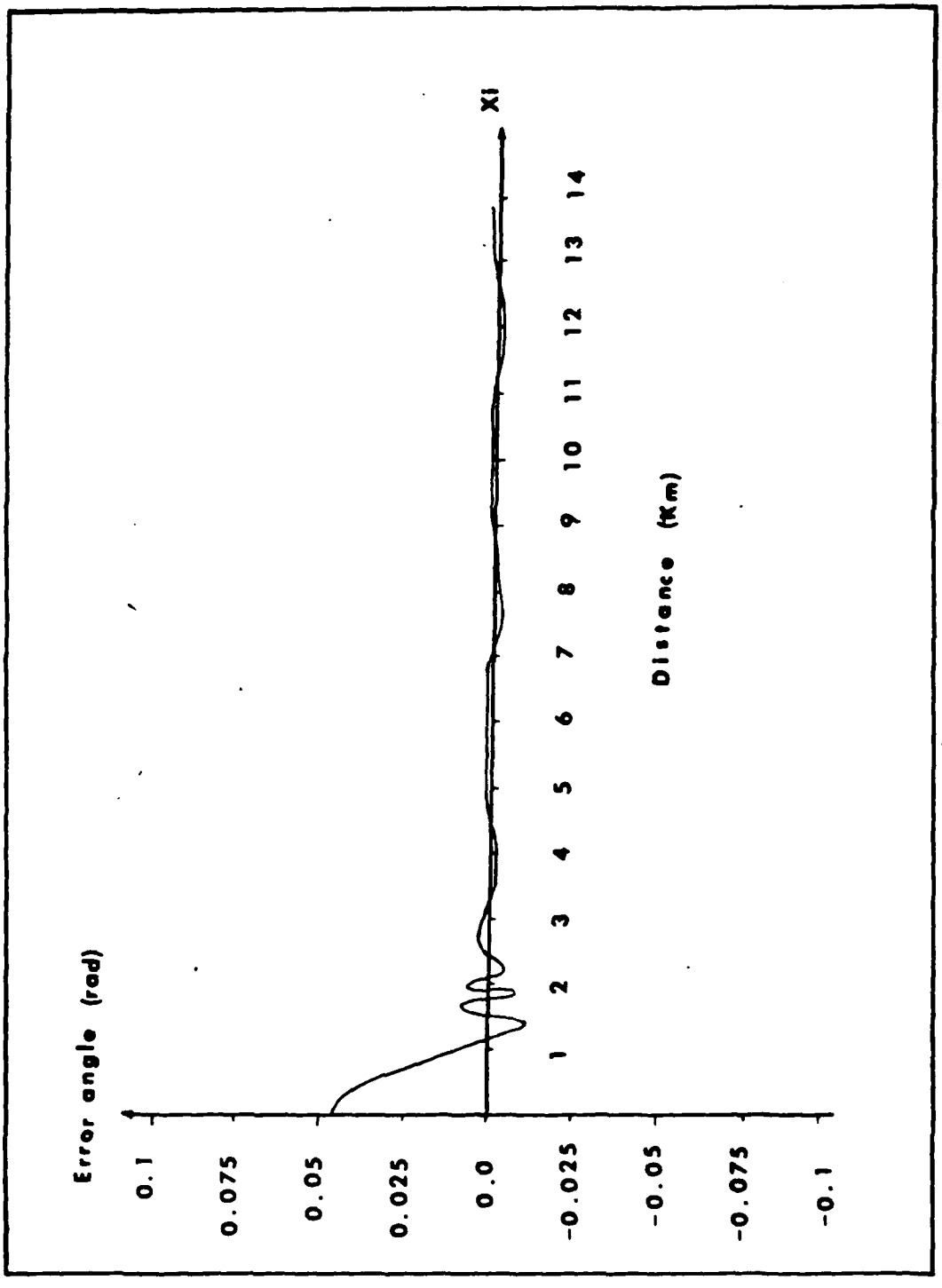

Figure D.4. Azimuth Error angle for Inputs in File 1.

Input File2

XT : 14000.0

YT : 4500.0

XB : 0.0

YB : 4000.0

ZB : 10000.0

θ_i : -.7853982

ψ_i : 0.0

u : 260

Vt : 0.0

a : 0.0

JMEX : 0.0

JMEY : 0.0

JVAX : 1.5

JVAY : 1.5

LEAZ : 0.0017453

LEEL : 0.0017453

DEME : 1/50

DEVA : 1/100

SPME : 1/40

SPVA : 1/160

DSEED: 873837365

GAINT: 1.8

GAINP: 0.8

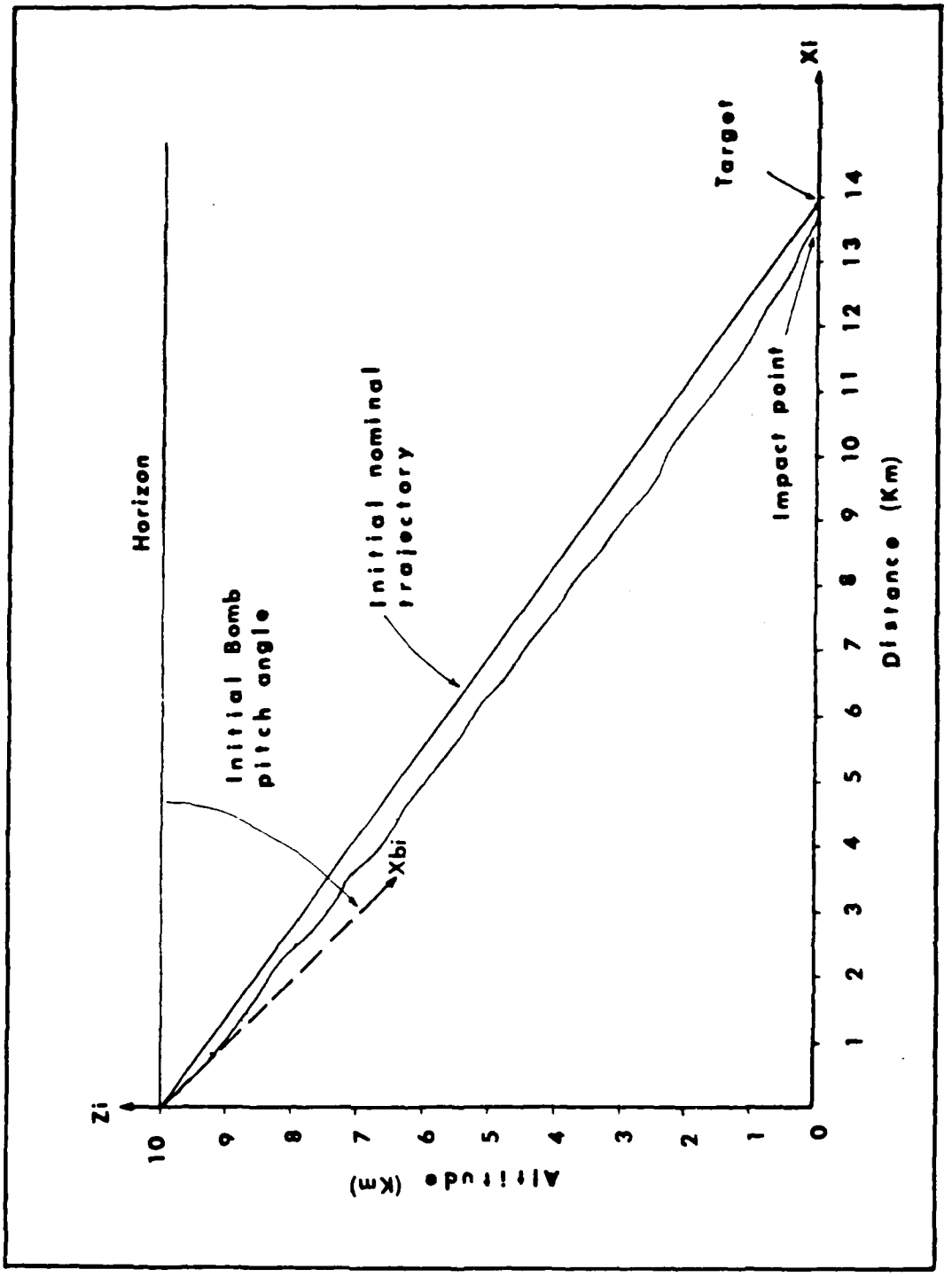

Figure D.5. Longitudinal Trajectory for Inputs in File 2.

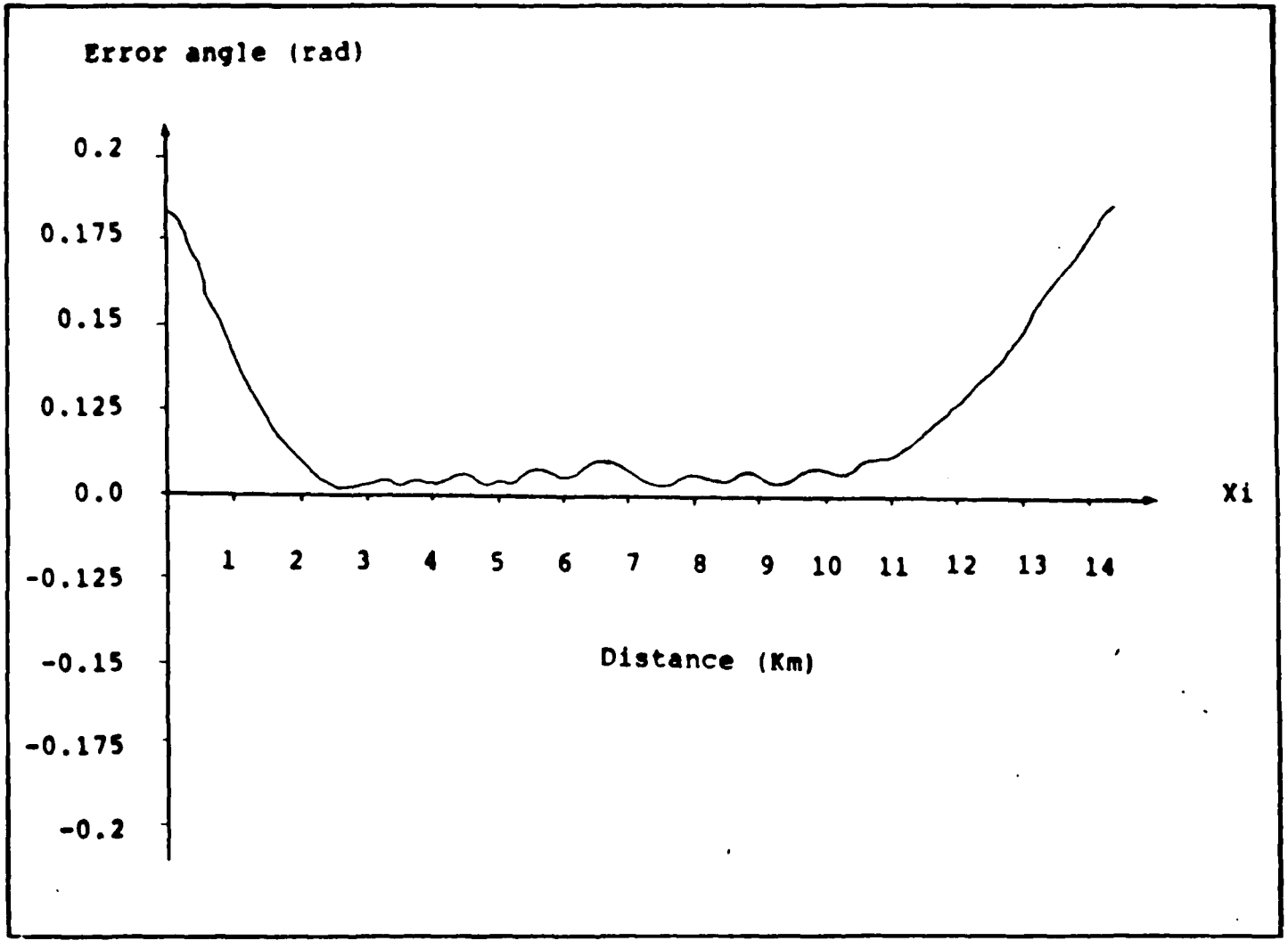

Figure D.6. Elevation Error Angle for Inputs in File 2.

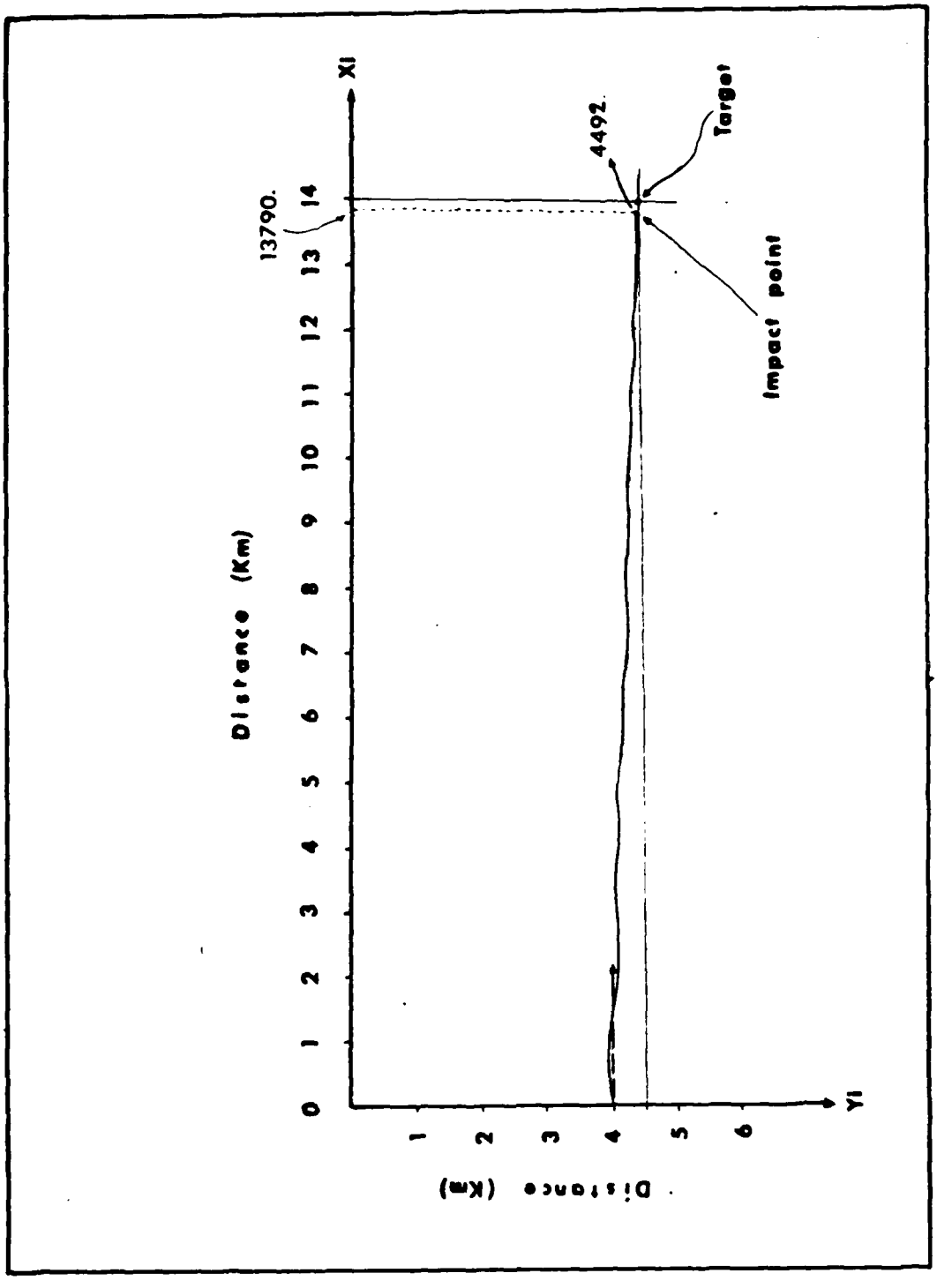

Figure D.7. Lateral trajectory for Inputs in File 2.

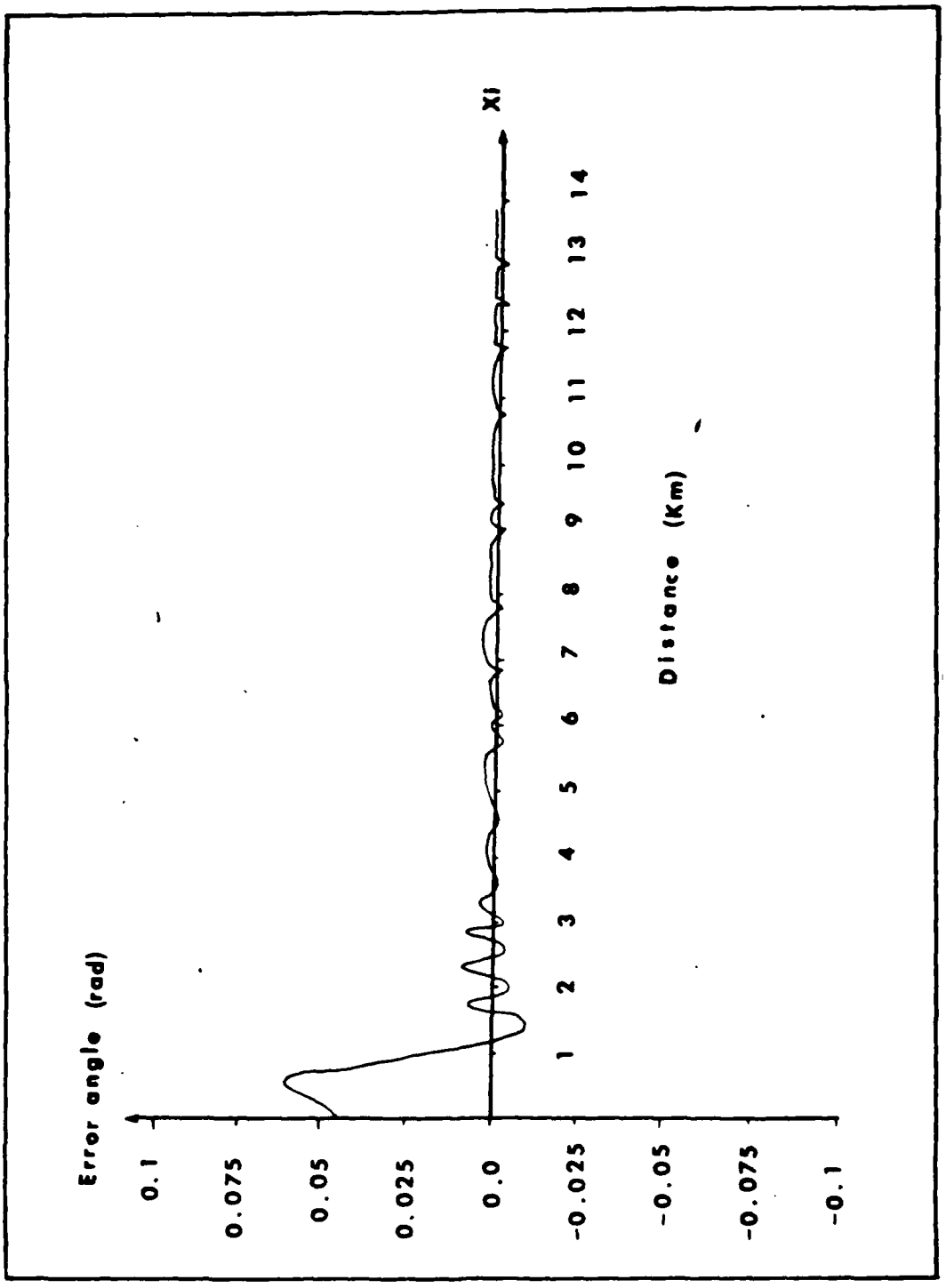

Figure D.8. Azimuth Error angle for Inputs in File 2.

Input File3

XT : 14000.0

YT : 4500.0

XB : 0.0

YB : 4000.0

ZB : 10000.0

θ_i : -.7853982

ψ_i : 0.0

u : 260

Vt : 0.0

a : 0.0

JMEX : 0.0

JMEY : 0.0

JVAX : 3.0

JVAY : 3.0

LEAZ : 0.0034907

LEEL : 0.0034907

DEME : 1/25

DEVA : 1/33.3

SPME : 1/8

SPVA : 1/50

DSEED: 453436363

GAINT: 1.8

GAINP: 0.8

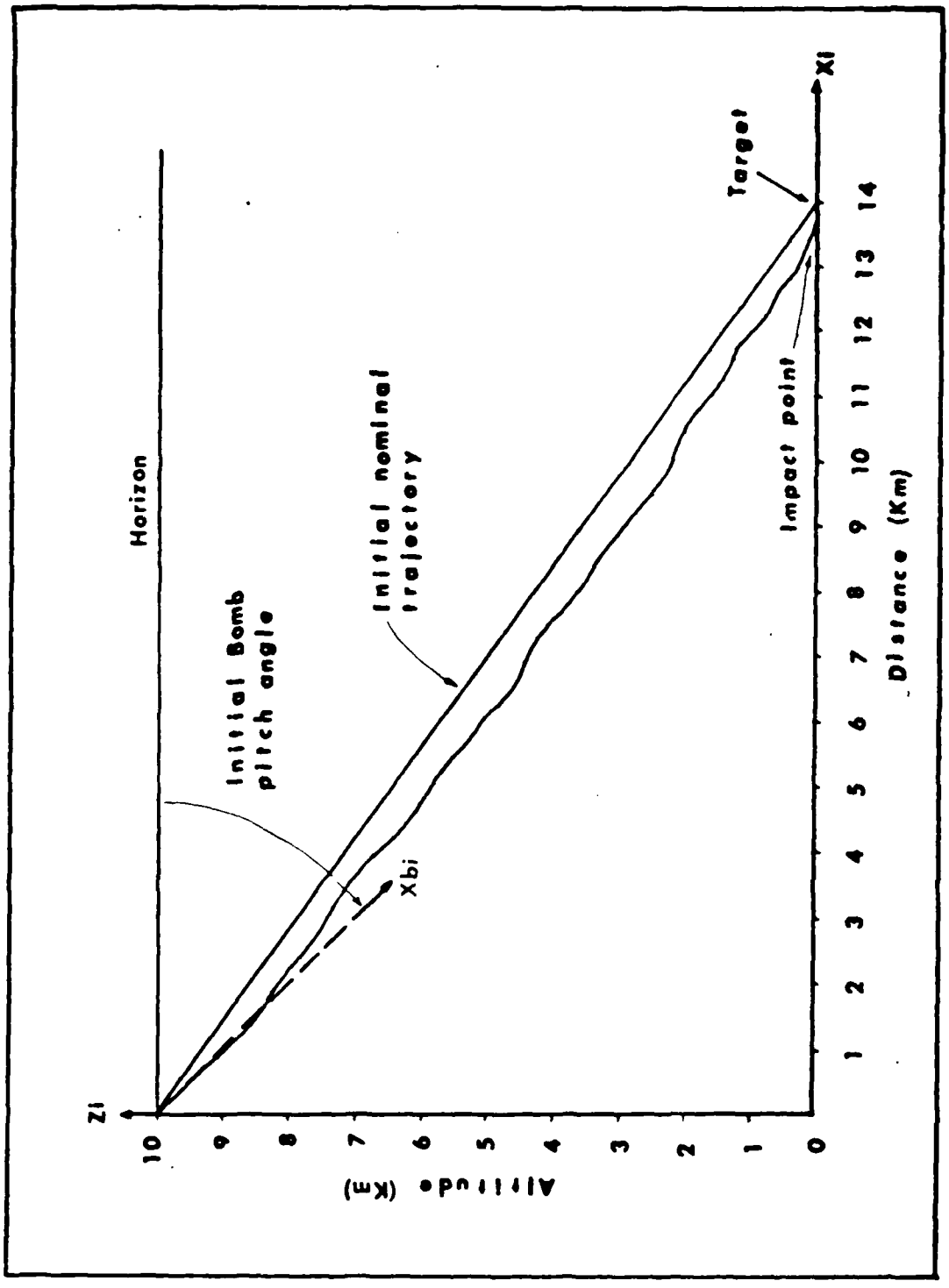

Figure D.9. Longitudinal Trajectory for Inputs in File 3.

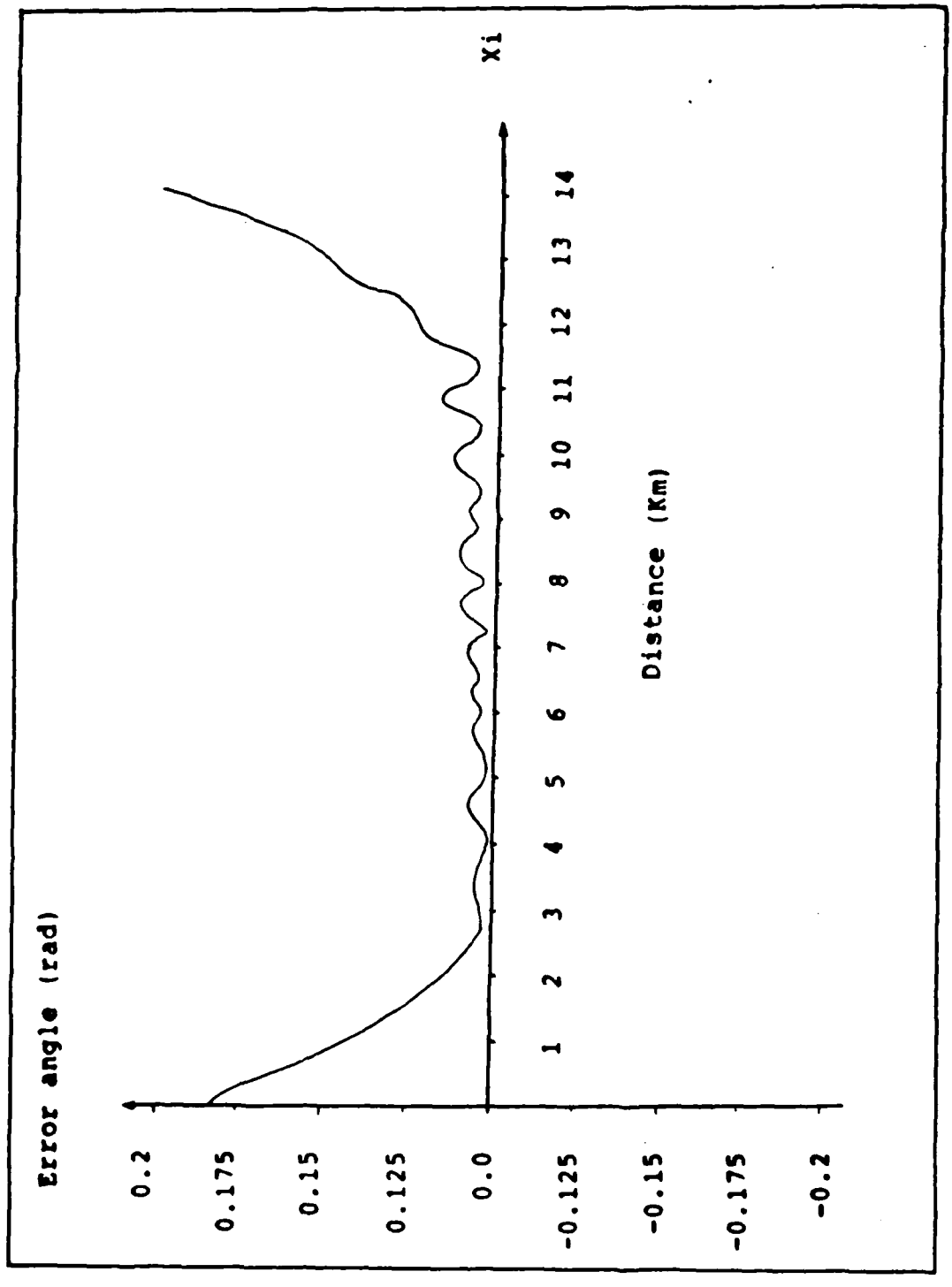

Figure D.10. Elevation Error Angle for Inputs in File 3.

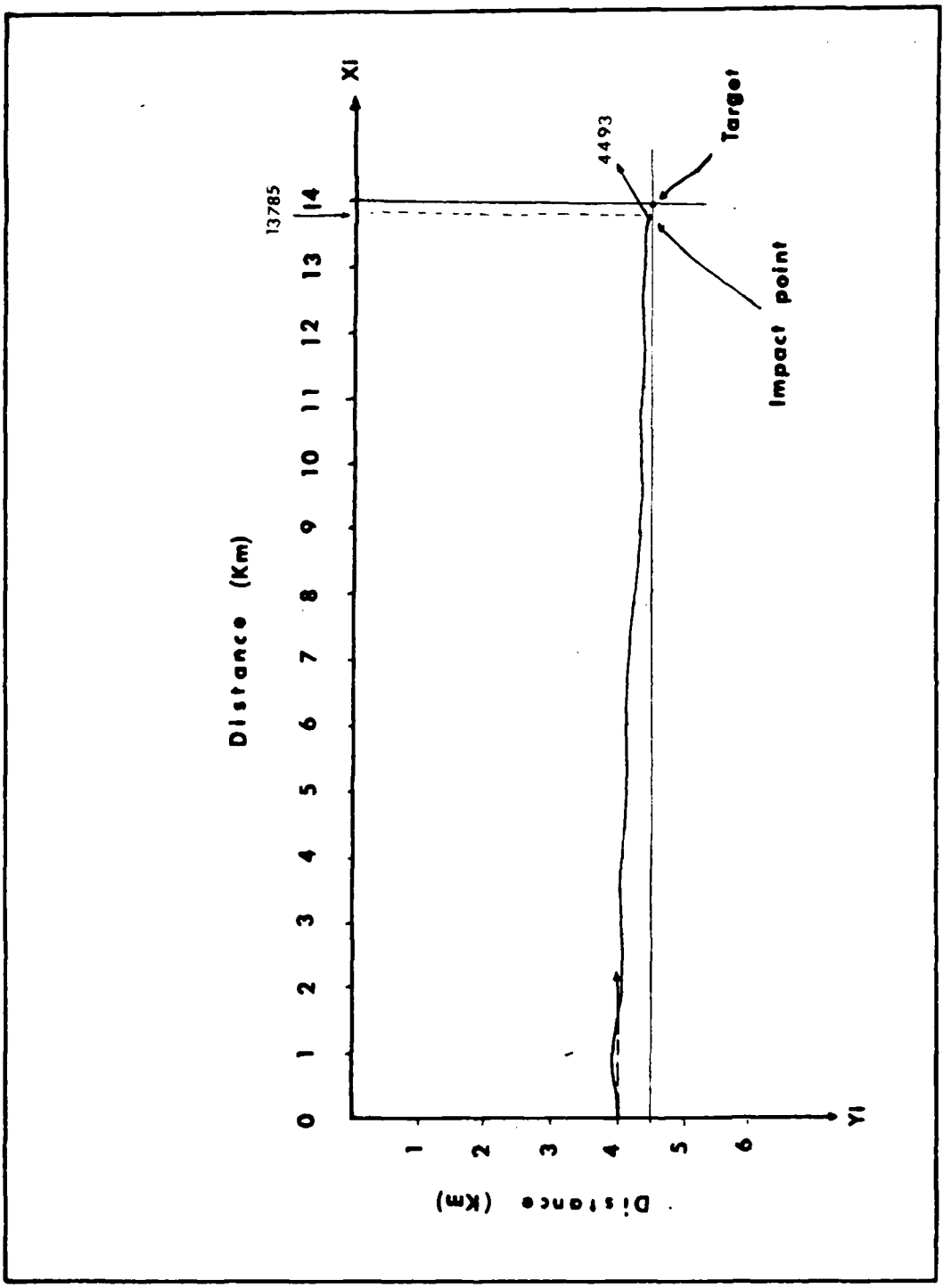

Figure D.11. Lateral Trajectory for Inputs in File 3.

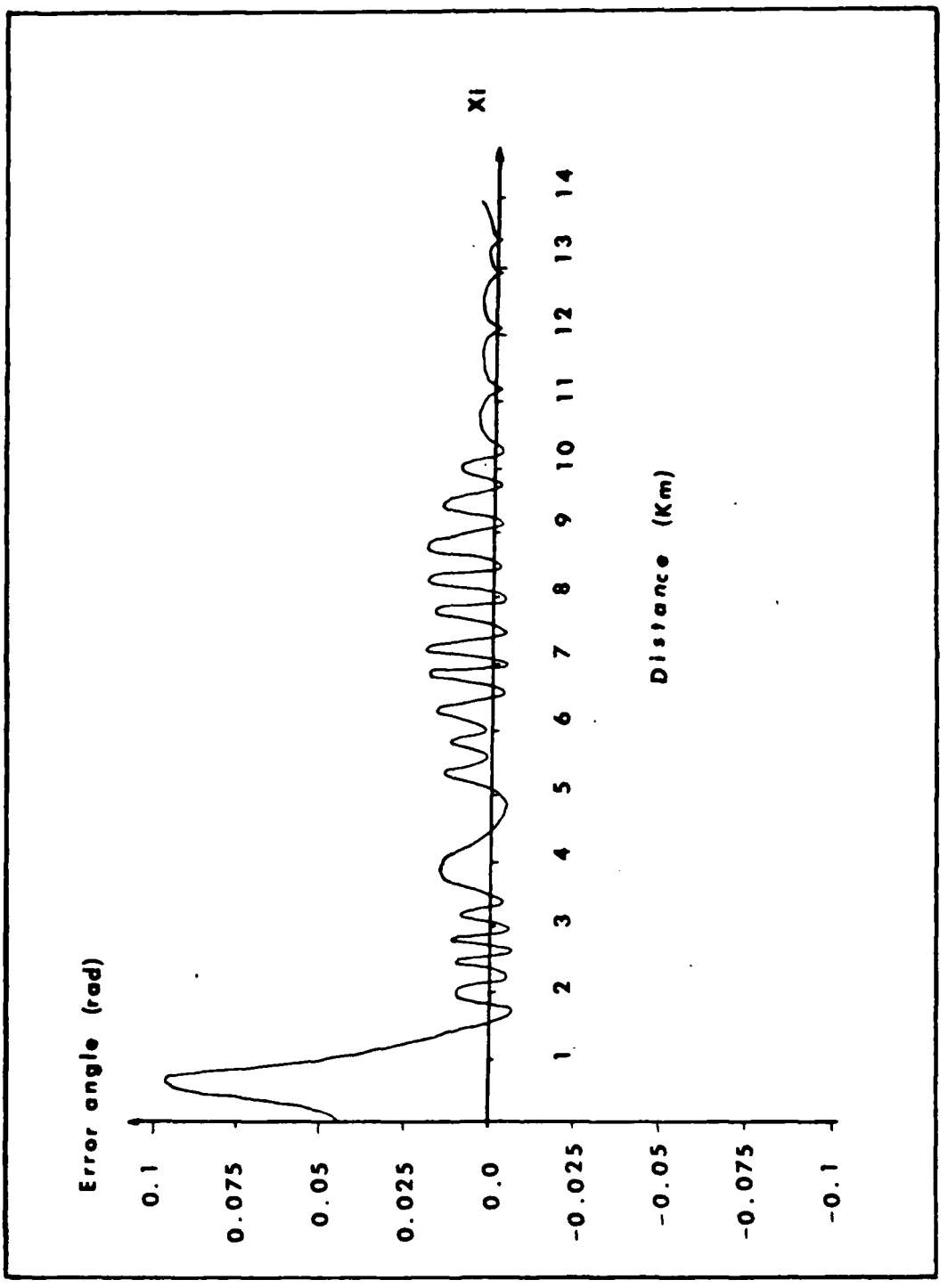

Figure D.12 Azimuth Error angle for Inputs in File 3.

APPENDIX E

Bomb trajectory and error angle plots for

Bomb Dynamics 2

Input File4

XT : 14000.0

YT : 4500.0

XB : 0.0

YB : 4000.0

ZB : 10000.0

θ_i : -.7853982

ψ_i : 0.0

u : 260

Vt : 0.0

a : 0.0

JMEX : 0.0

JMEY : 0.0

JVAX : 0.0

JVAY : 0.0

LEAZ : 0.0

LEEL : 0.0

DEME : 0.0

DEVA : 0.0

SPME : 0.0

SPVA : 0.0

DSEED: 234324332

GAINT: 0.02

GAINP: 0.08

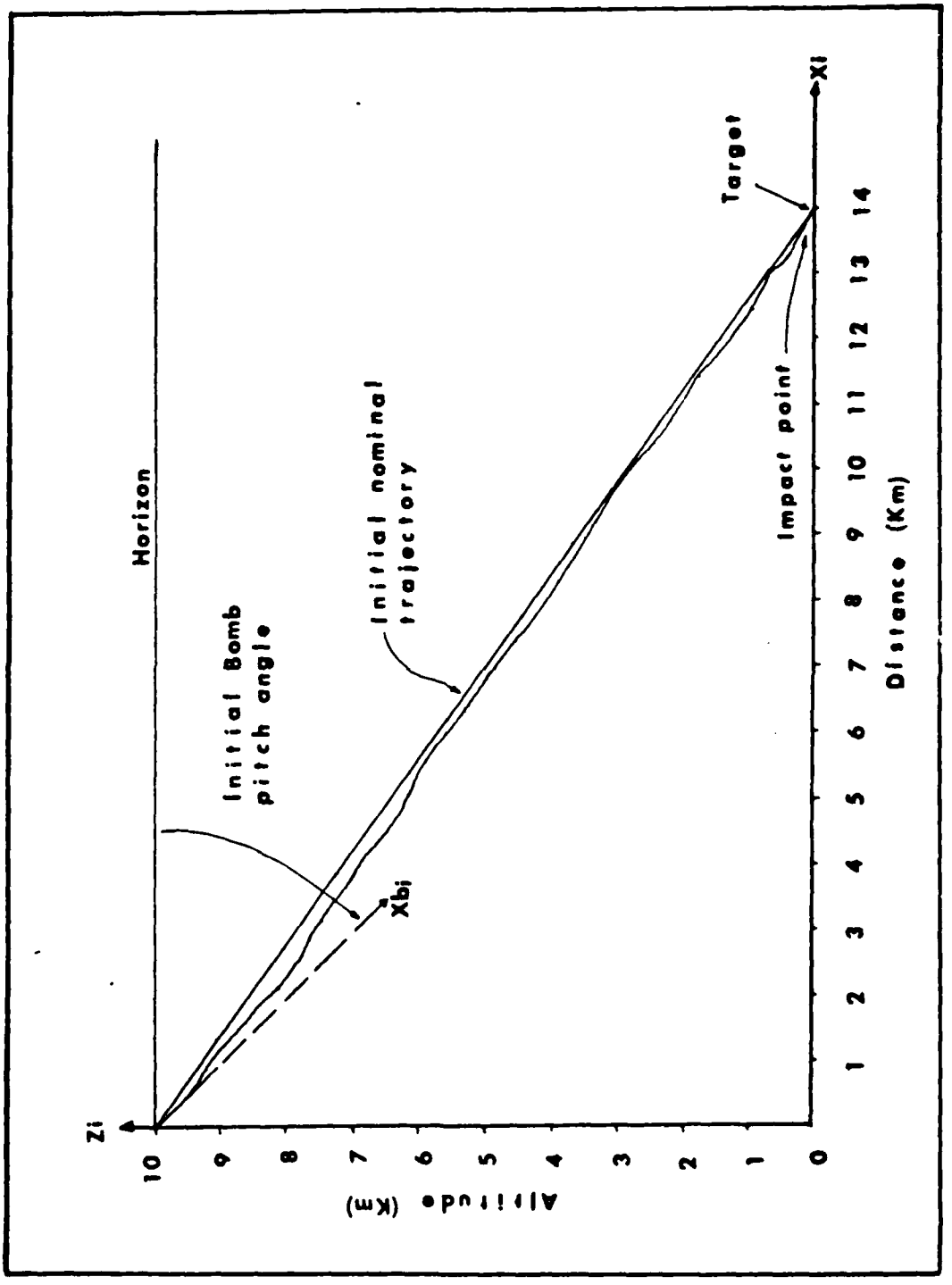

Figure E.1. Longitudinal Trajectory for Inputs in File 4.

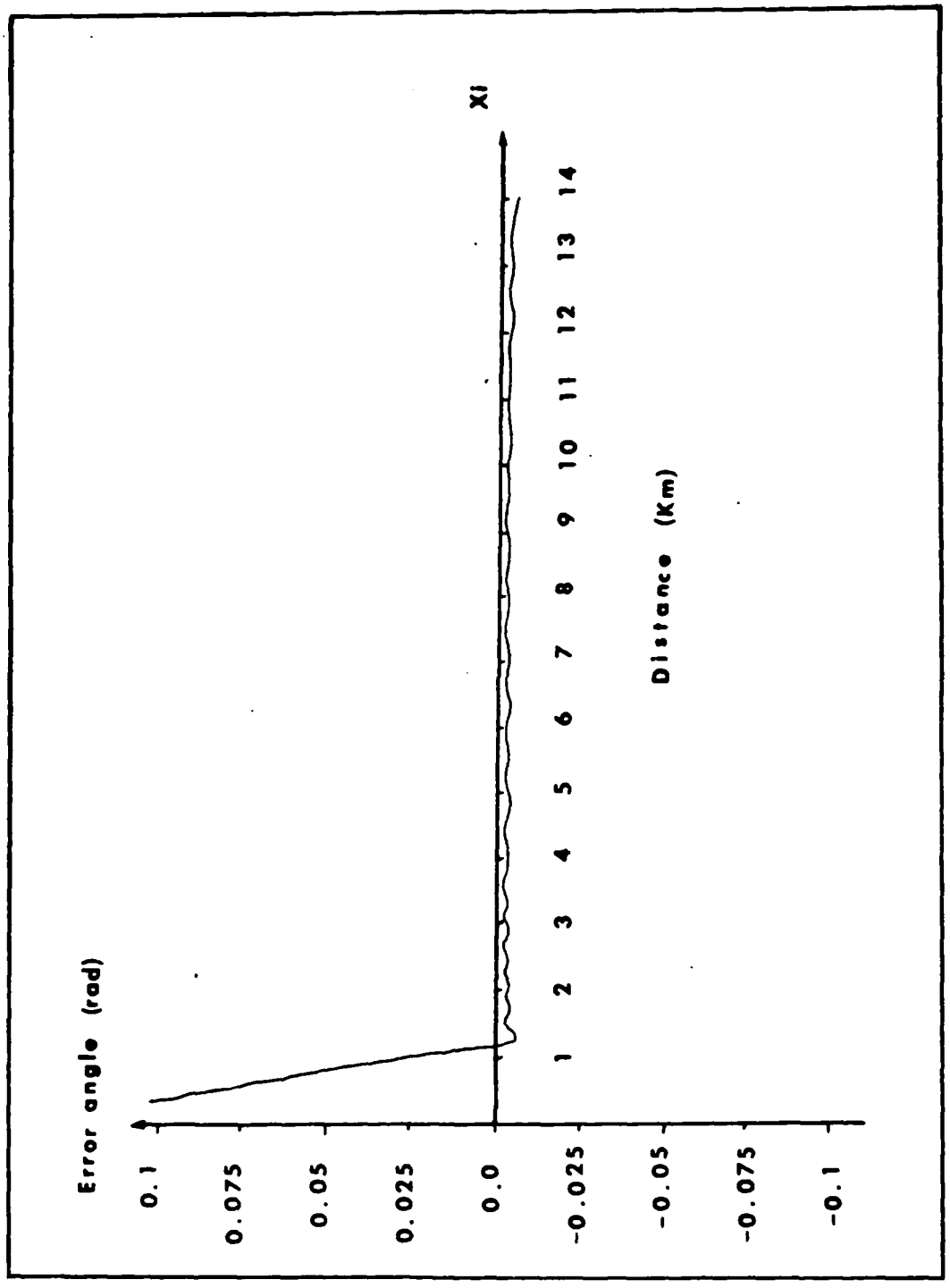

Figure E.2. Elevation Error Angle for Inputs in File 4.

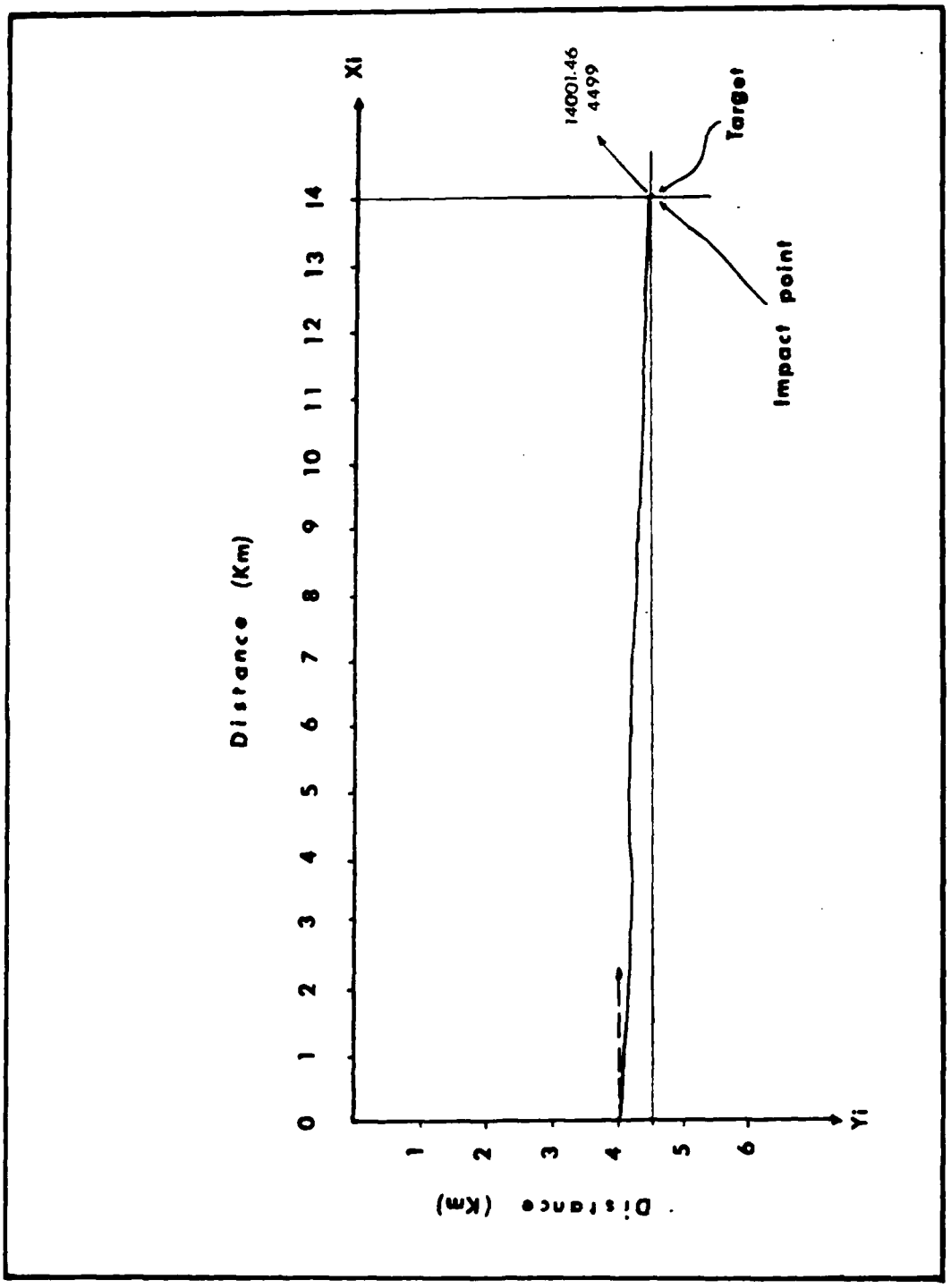

Figure E.3. Lateral Trajectory for Inputs in File 4.

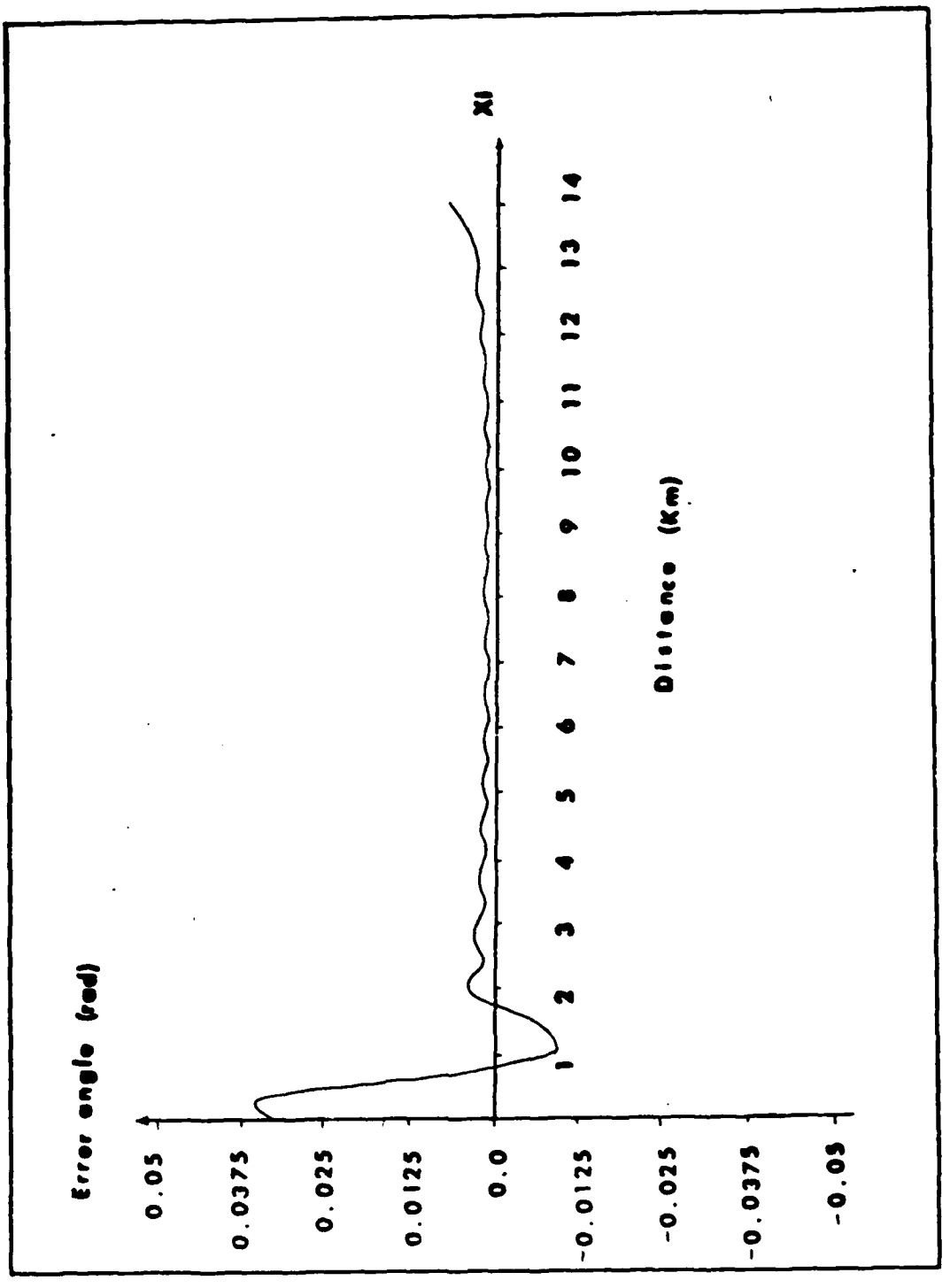

Figure E.4. Azimuth Error angle for Inputs in File 4.

Input File5

XT : 14000.0

YT : 4500.0

XB : 0.0

YB : 4000.0

ZB : 10000.0

θ_i : -.7853982

ψ_i : 0.0

u : 260

Vt : 0.0

a : 0.0

JMEX : 0.0

JMEY : 0.0

JVAX : 1.5

JVAY : 1.5

LEAZ : 0.0017453

LEEL : 0.0017453

DEME : 1/50

DEVA : 1/100

SPME : 1/40

SPVA : 1/160

DSEED: 234324332

GAINT: 0.02

GAINP: 0.08

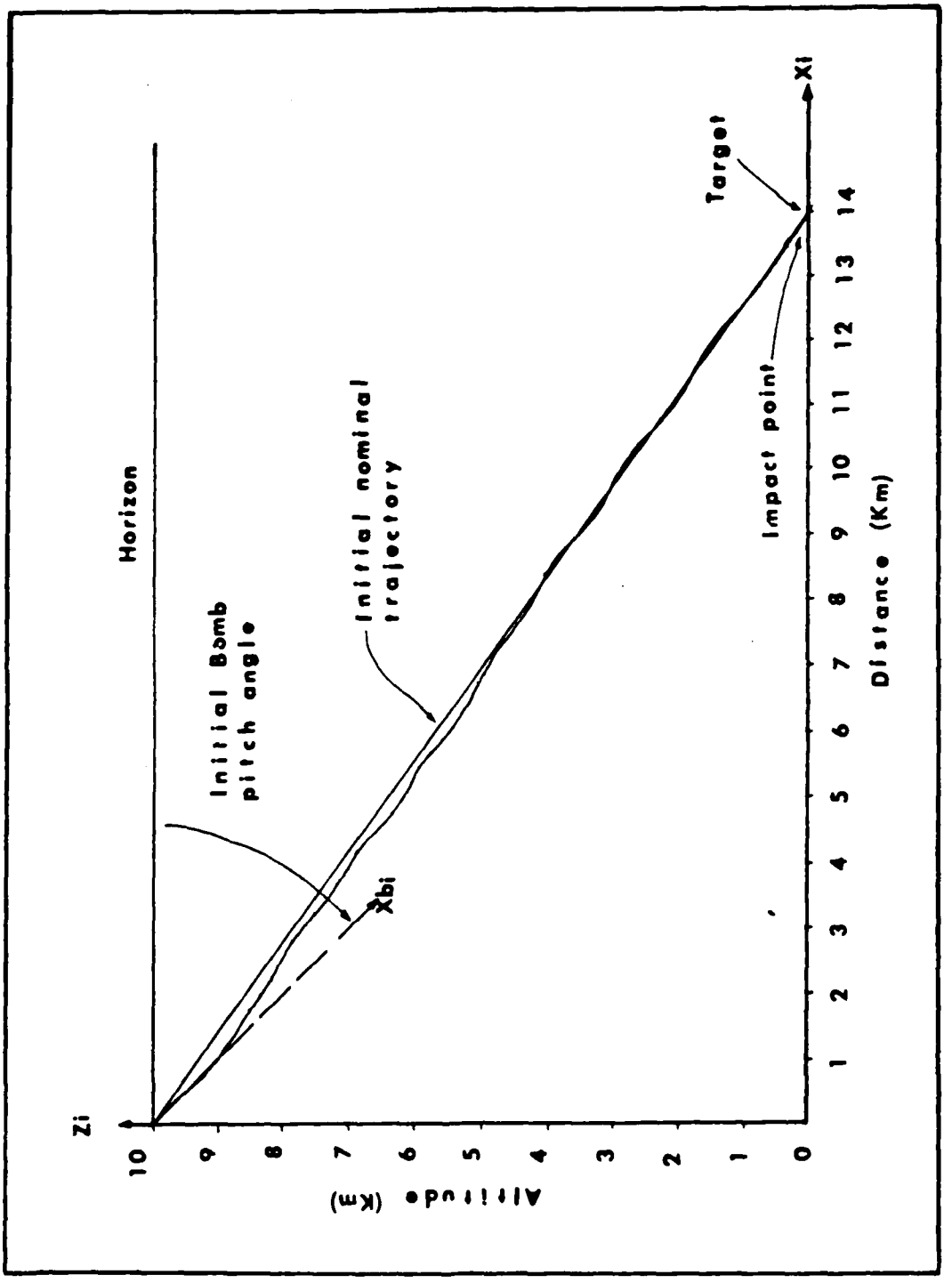

Figure E.5. Longitudinal Trajectory for Inputs in File 5.

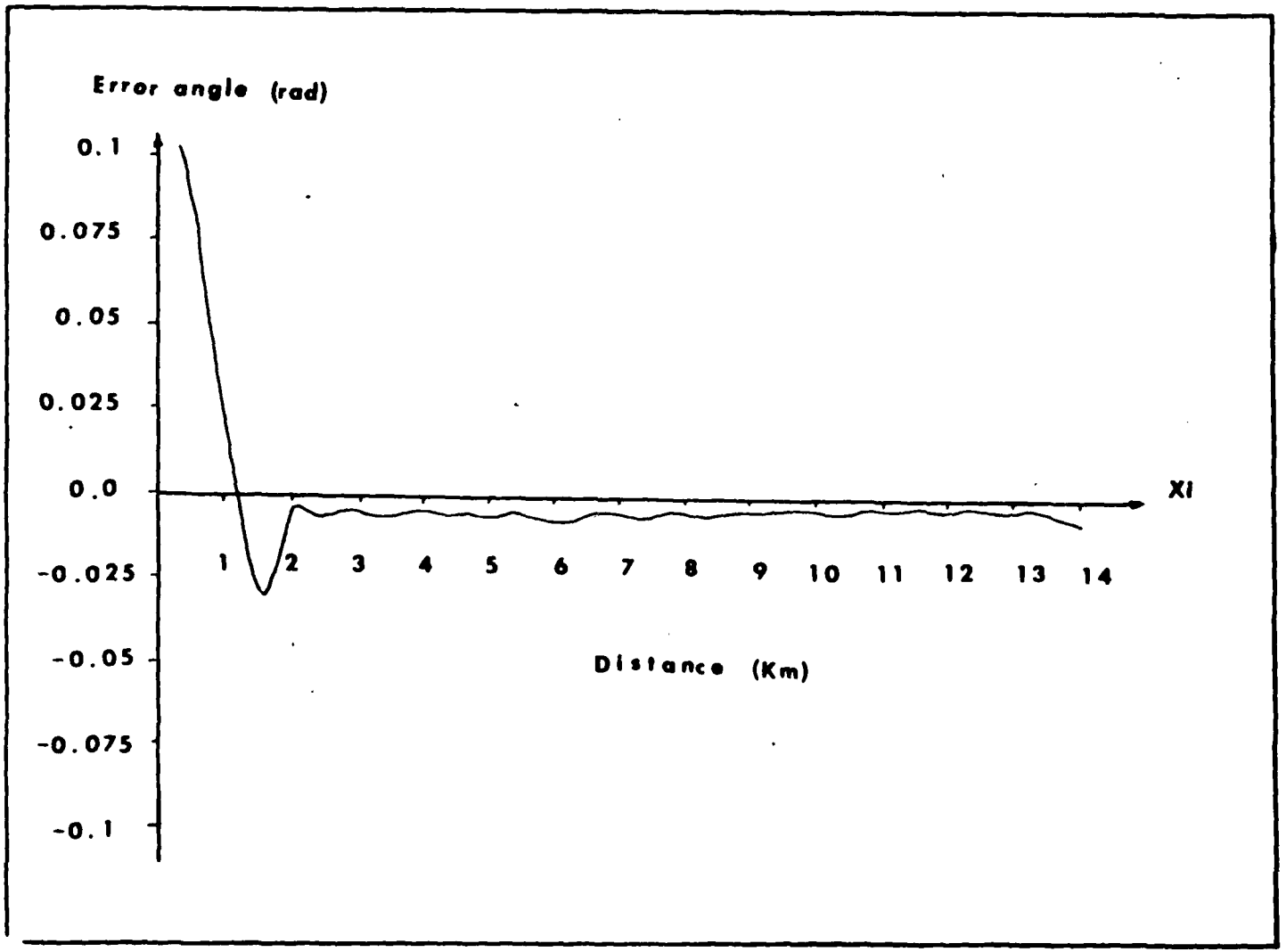

Figure E.6. Elevation Error Angle for Inputs in File 5.

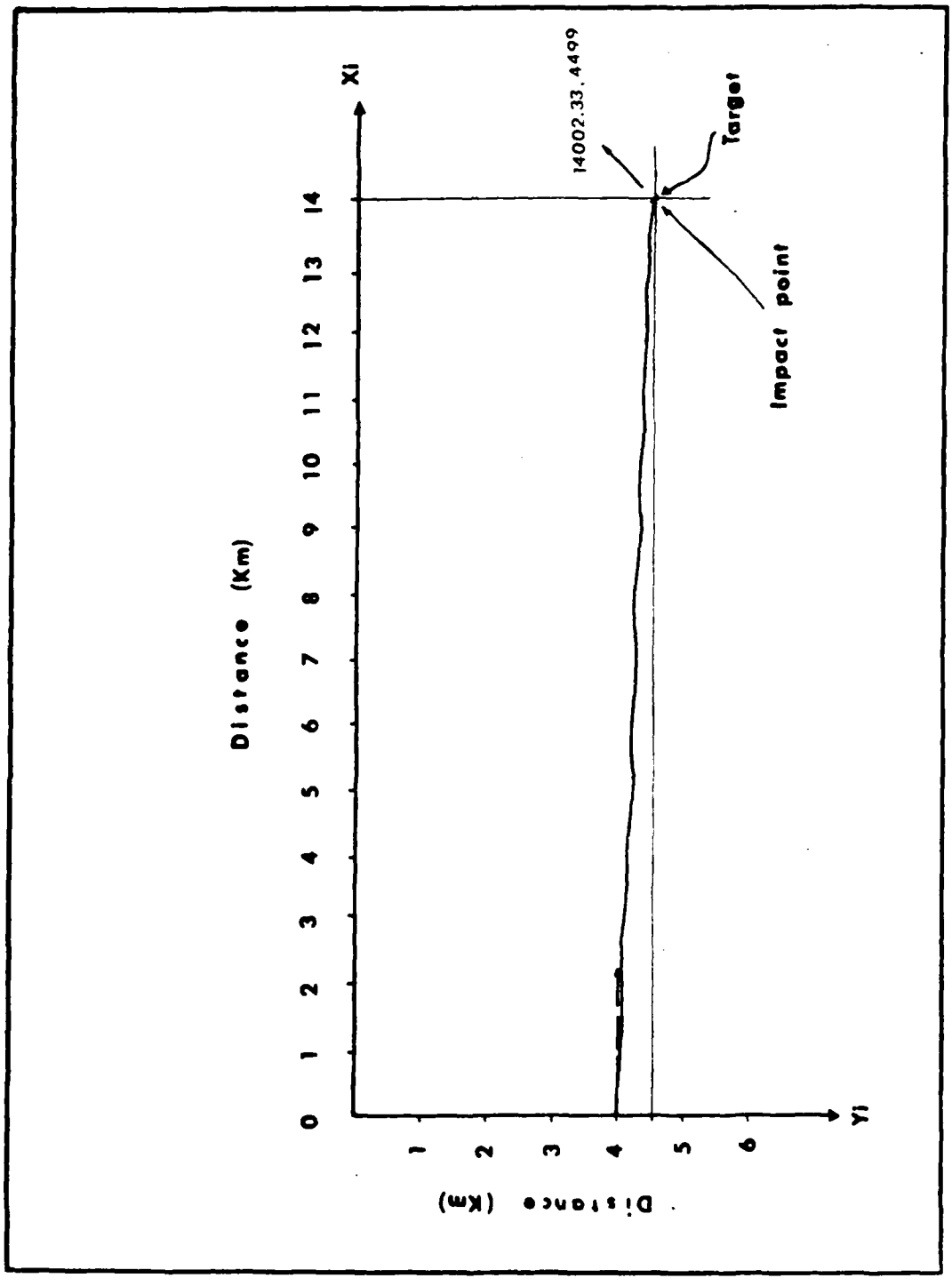

Figure E.7. Lateral Trajectory for Inputs in File 5.

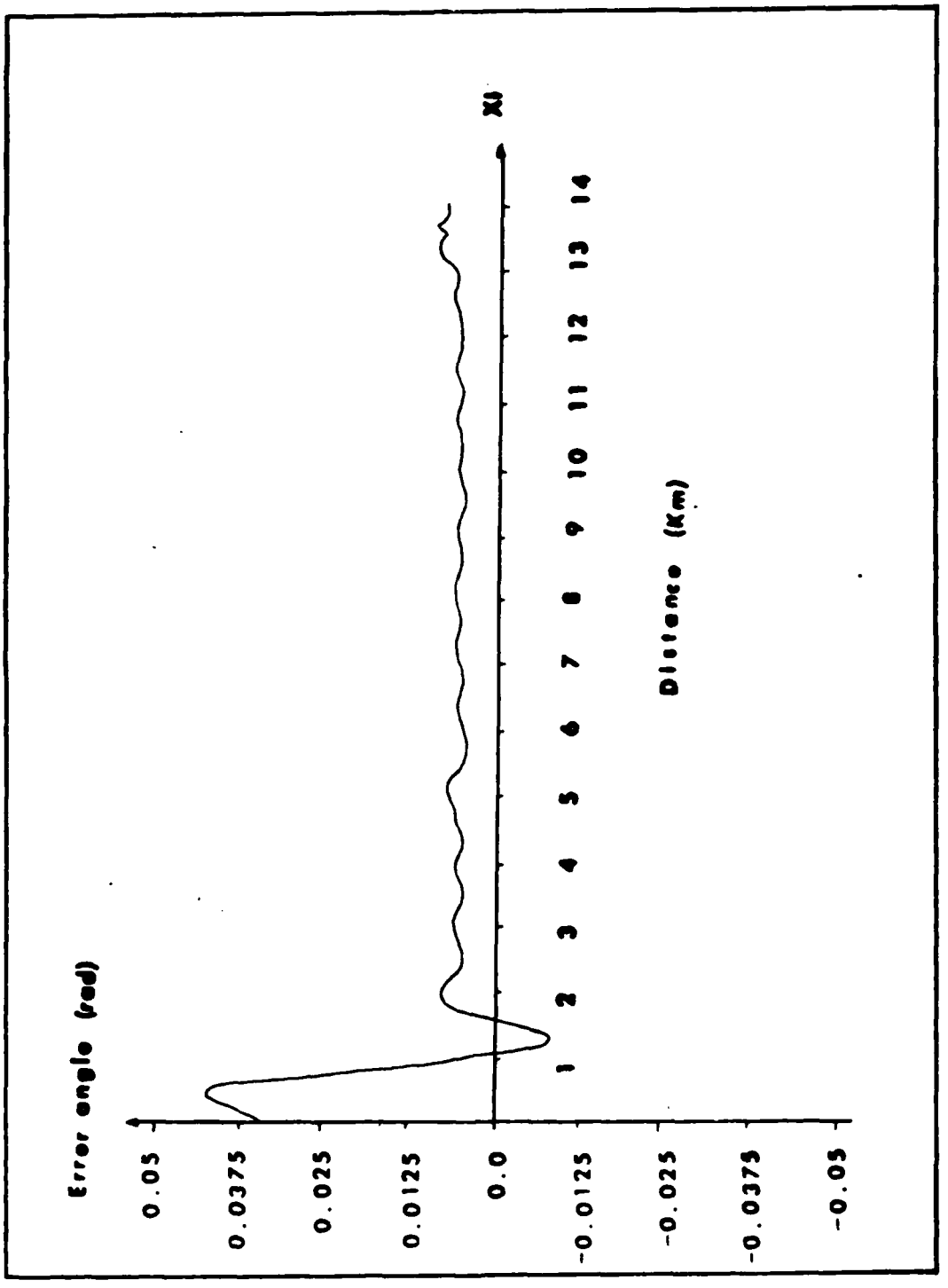

Figure E.8. Azimuth Error angle for Inputs in File 5.

Input File6

XT : 14000.0

YT : 4500.0

XB : 0.0

YB : 4000.0

ZB : 10000.0

θ_i : -.7853982

ψ_i : 0.0

u : 260

Vt : 0.0

a : 0.0

JMEX : 0.0

JMEY : 0.0

JVAX : 3.0

JVAY : 3.0

LEAZ : 0.0034907

LEEL : 0.0034907

DEME : 1/25

DEVA : 1/33.3

SPME : 1/8

SPVA : 1/50

DSEED: 45383936

GAINT: 0.02

GAINP: 0.08

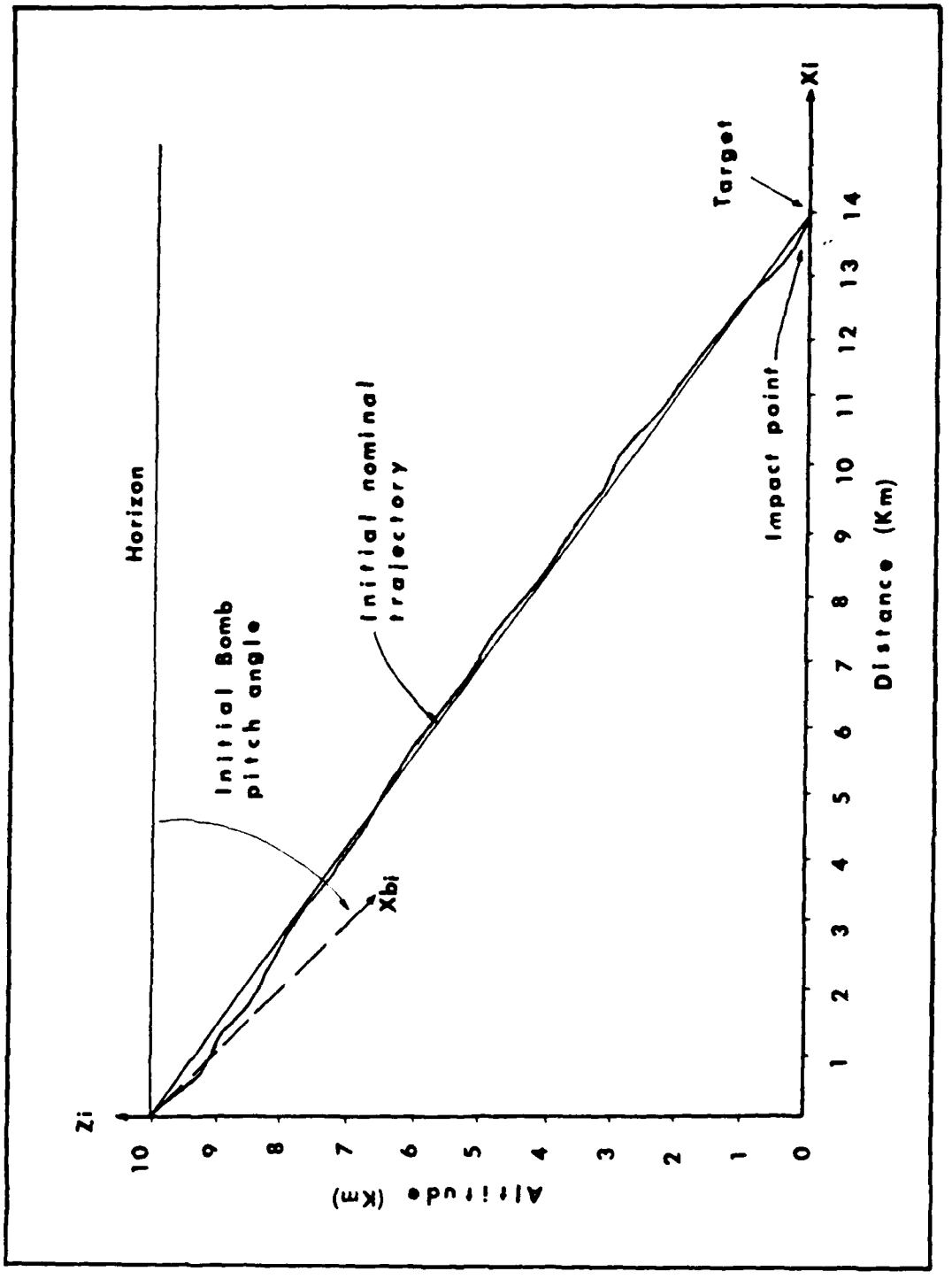

Figure E.9. Longitudinal Trajectory for Inputs in File 6.

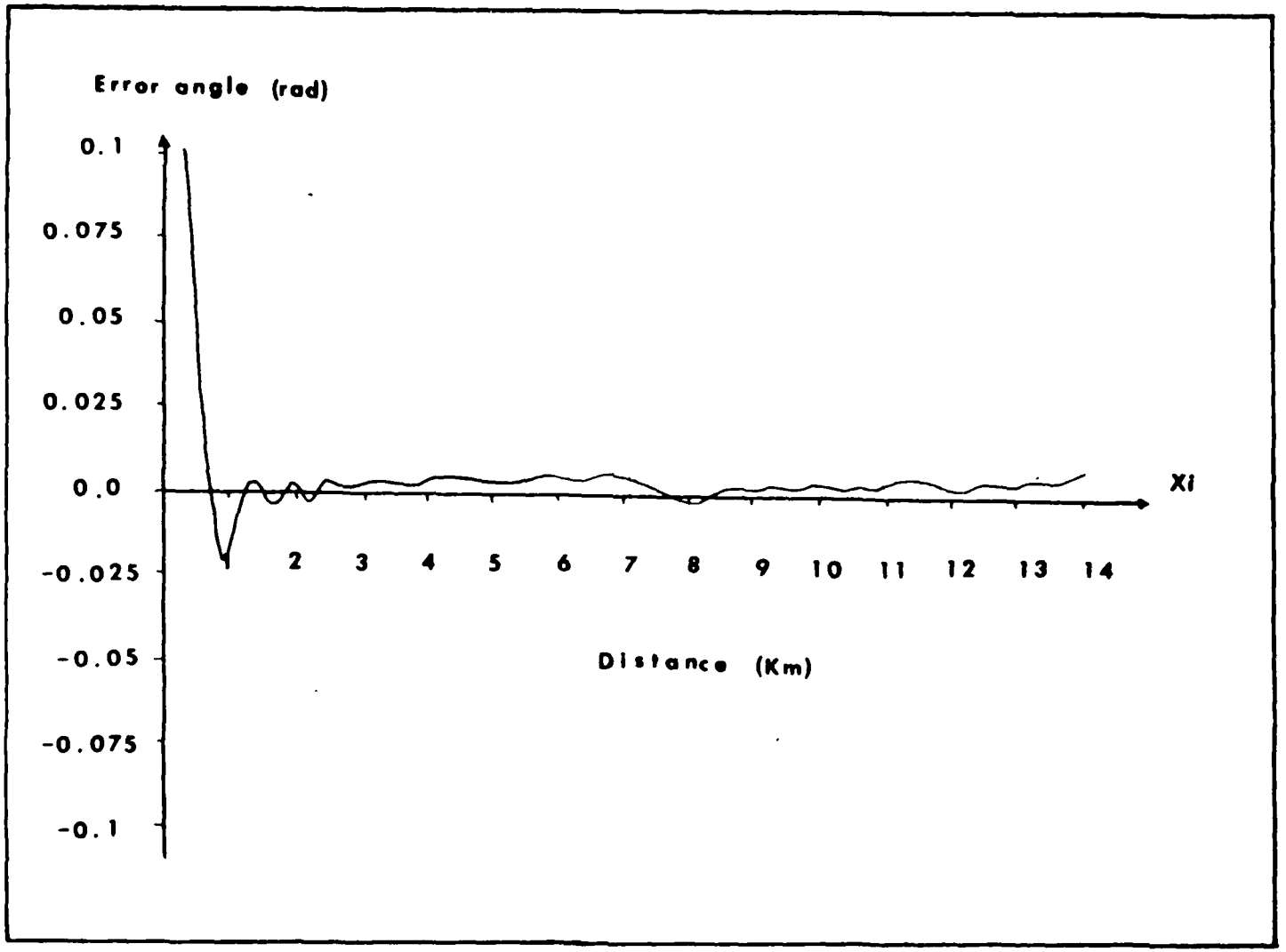

Figure E.10. Elevation Error Angle for Inputs in File 6.

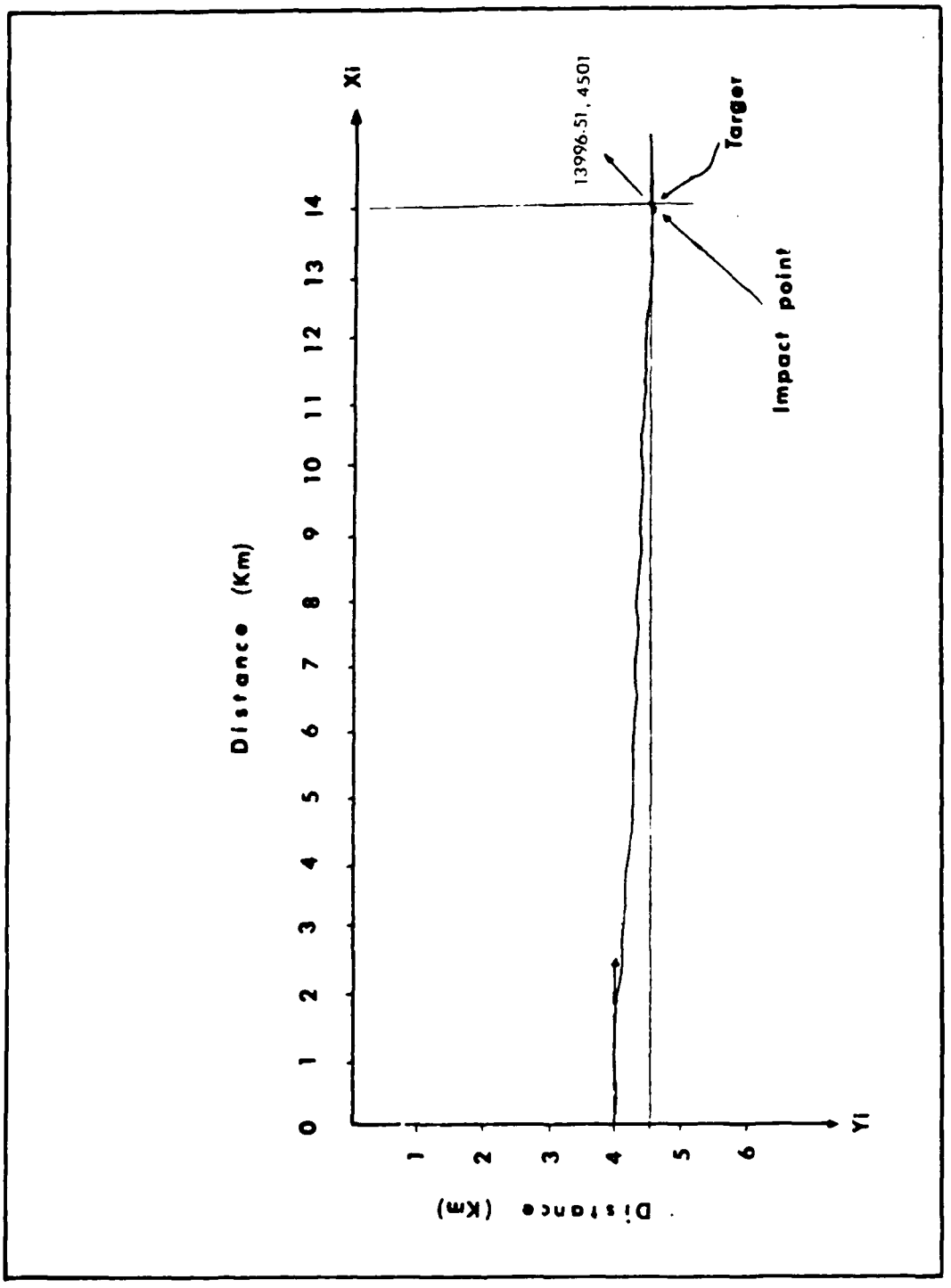

Figure E.11. Lateral Trajectory for Inputs in File 6.

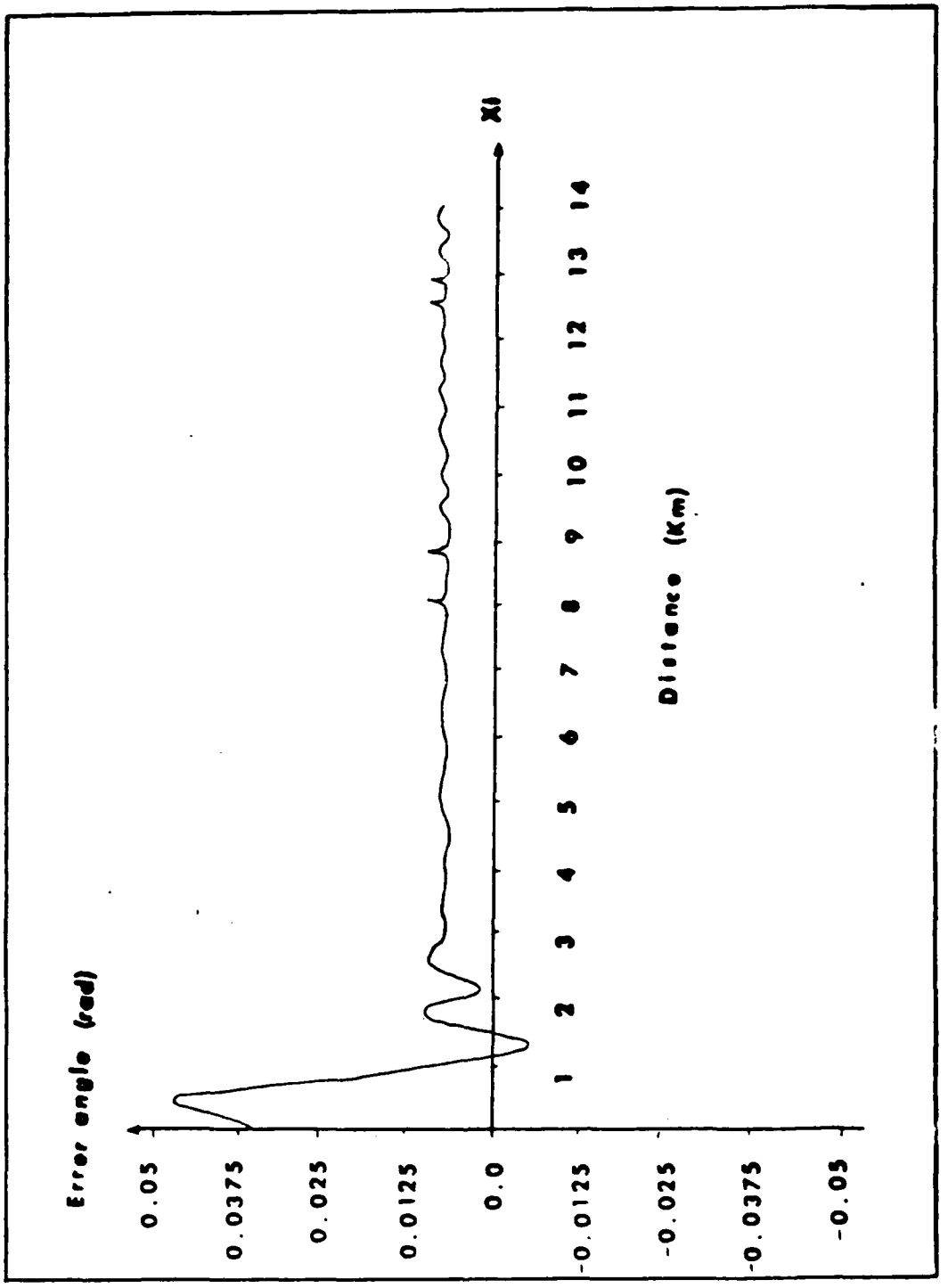

Figure E.12. Azimuth Error angle for Inputs in File 6.

APPENDIX F

Bomb trajectory and error angle plots for

Moving Targets and Bomb Dynamics 2

Input File7

XT : 14000.0

YT : 4500.0

XB : 0.0

YB : 4000.0

ZB : 10000.0

θ_i : -.7853982

ψ_i : 0.0

u : 260

Vt : 14.0

a : 0.7853982

JMEX : 0.0

JMEY : 0.0

JVAX : 0.0

JVAY : 0.0

LEAZ : 0.0

LEEL : 0.0

DEME : 0.0

DEVA : 0.0

SPME : 0.0

SPVA : 0.0

DSEED: 21217679

GAINT: 0.02

GAINP: 0.08

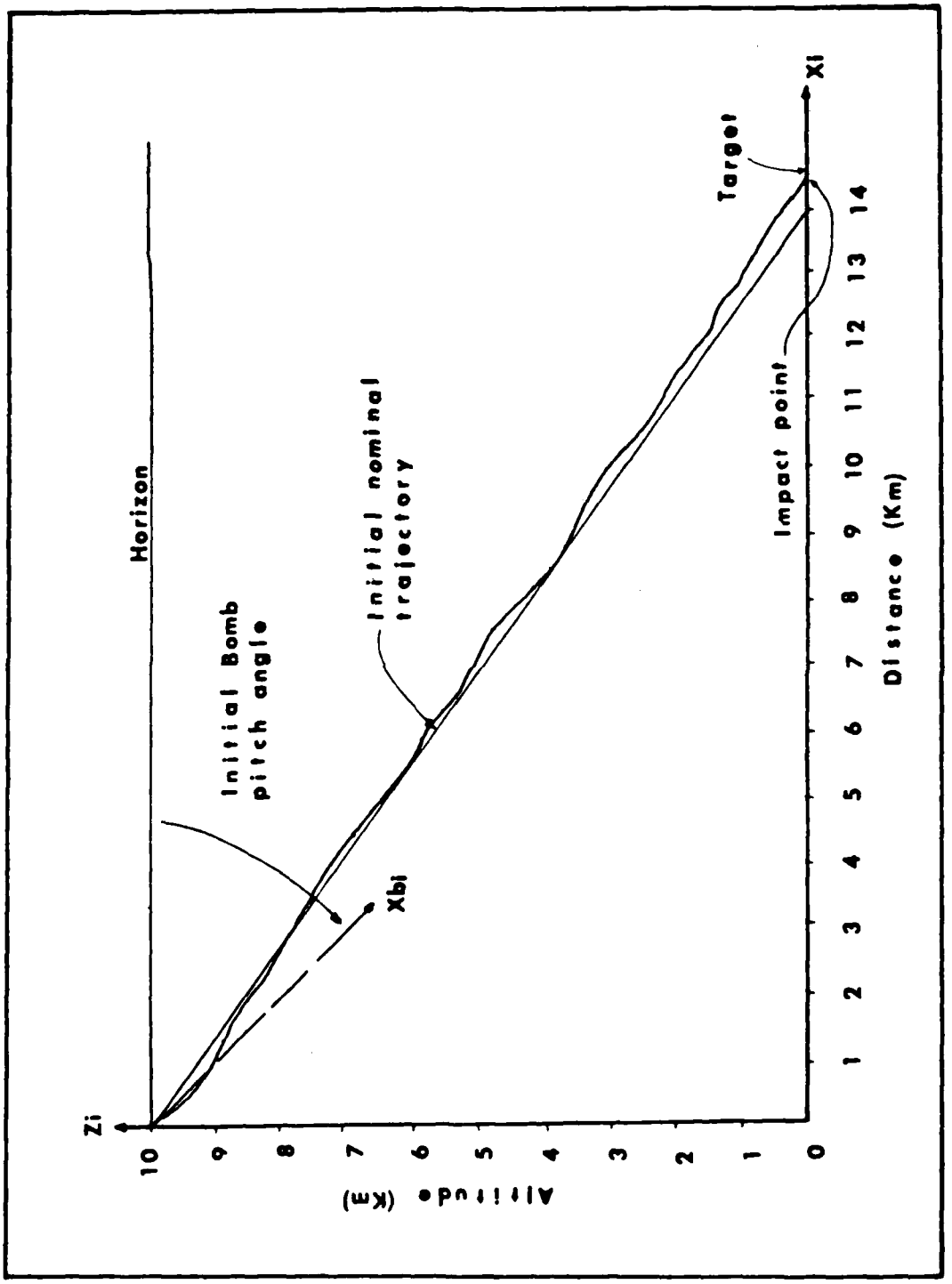

Figure F.1. Longitudinal Trajectory for Inputs in File 7.

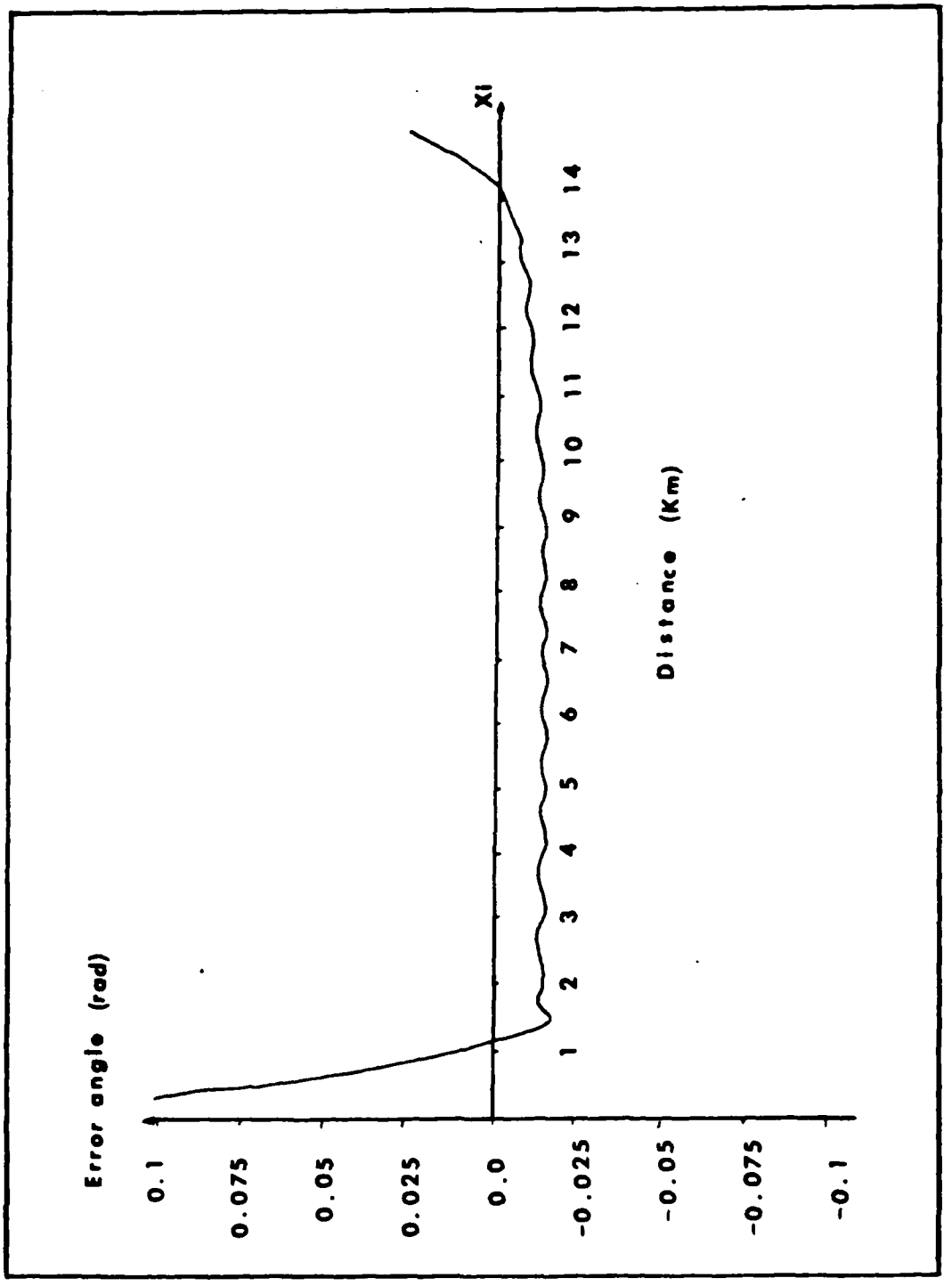

Figure F.2. Elevation Error Angle for Inputs in File 7.

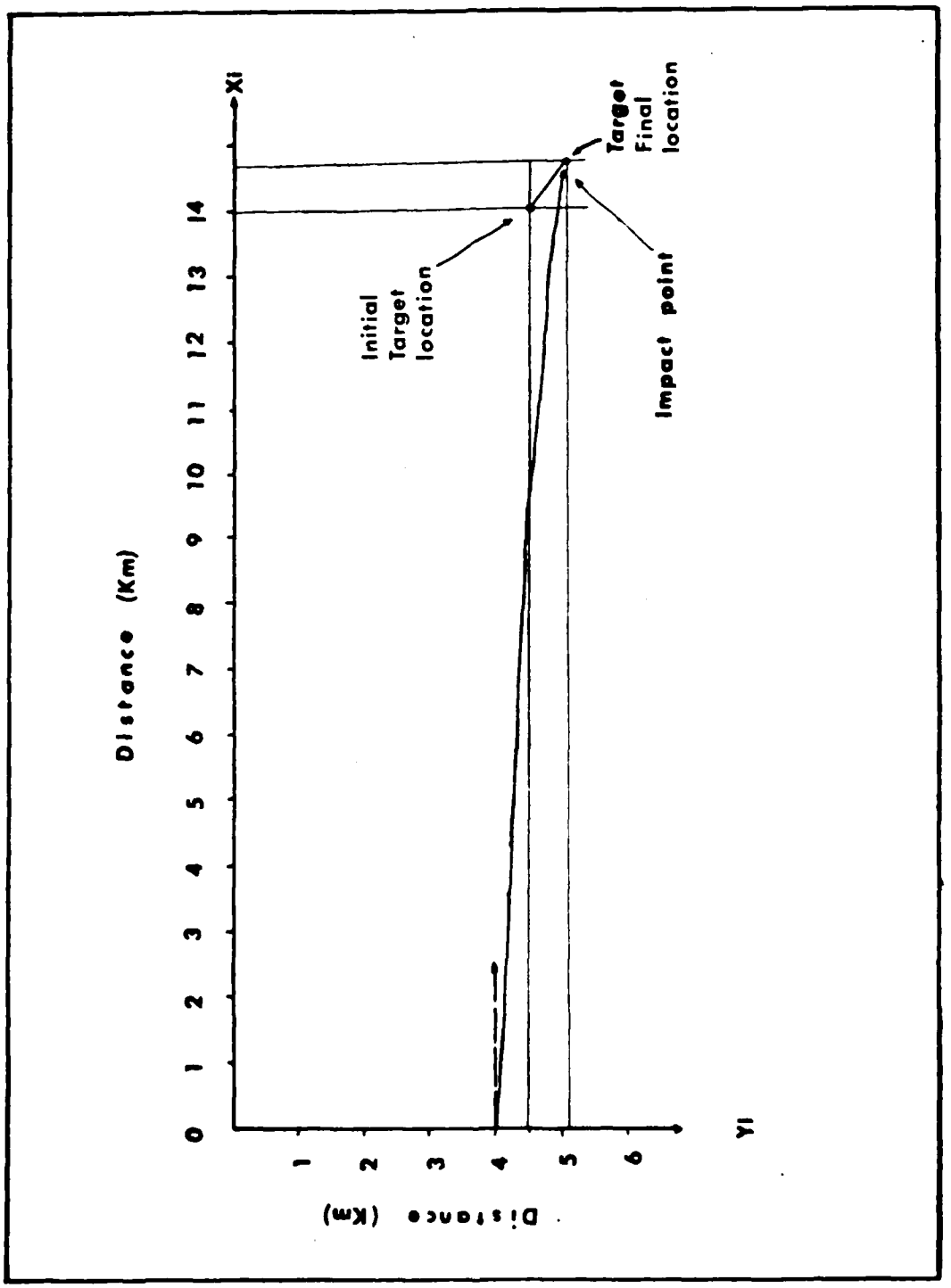

Figure F.3. Lateral Trajectory for Inputs in File 7.

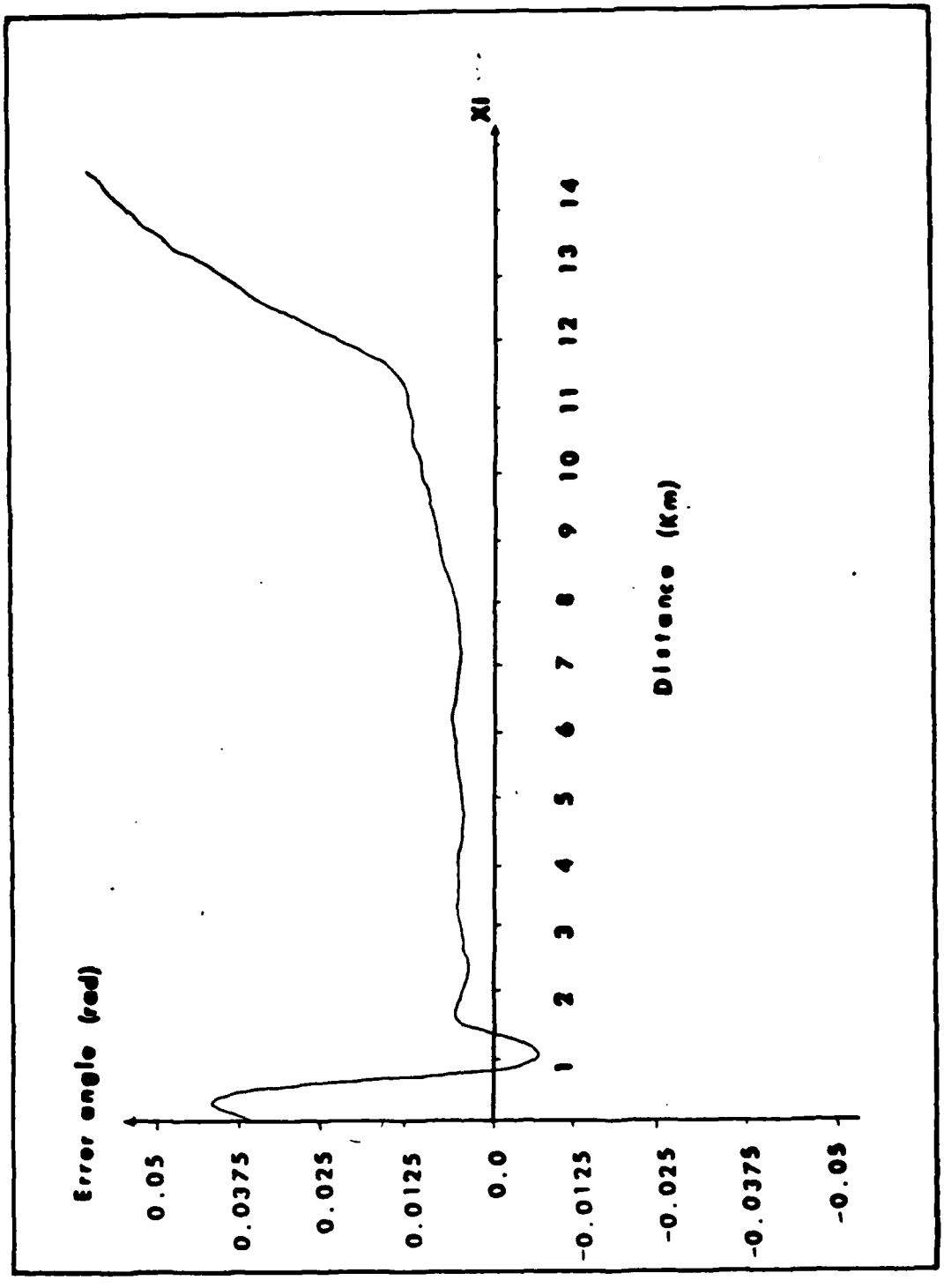

Figure F.4. Azimuth Error Angle for Inputs in File 7.

Input File8

XT : 14000.0

YT : 4500.0

XB : 0.0

YB : 4000.0

ZB : 10000.0

θ_i : -.7853982

ψ_i : 0.0

u : 260

Vt : -12.0

a : 0.7853982

JMEX : 0.0

JMEY : 0.0

JVAX : 0.0

JVAY : 0.0

LEAZ : 0.0

LEEL : 0.0

DEME : 0.0

DEVA : 0.0

SPME : 0.0

SPVA : 0.0

DSEED: 24237879

GAINT: 0.02

GAINP: 0.08

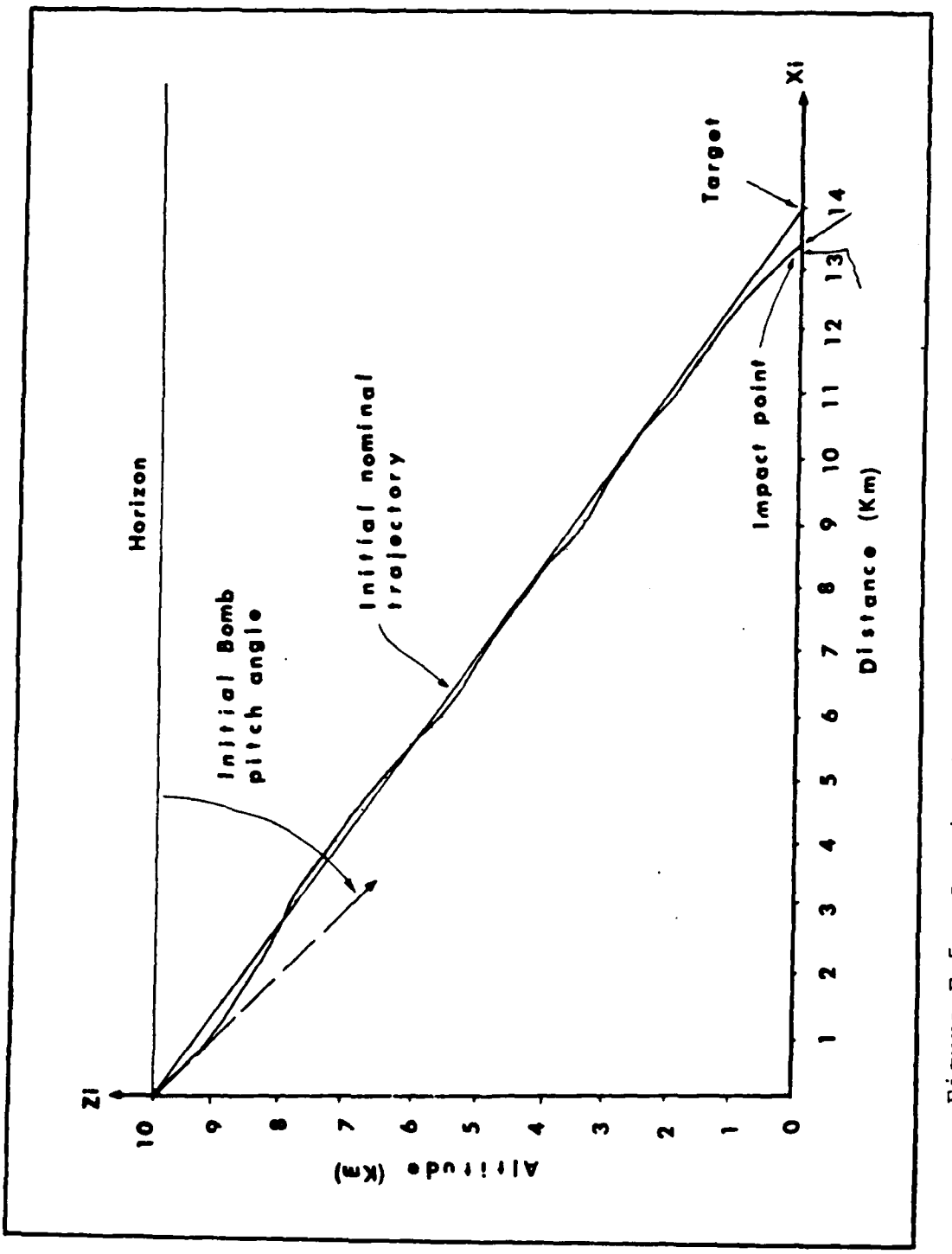

Figure F.5. Longitudinal Trajectory for Inputs in File 8.

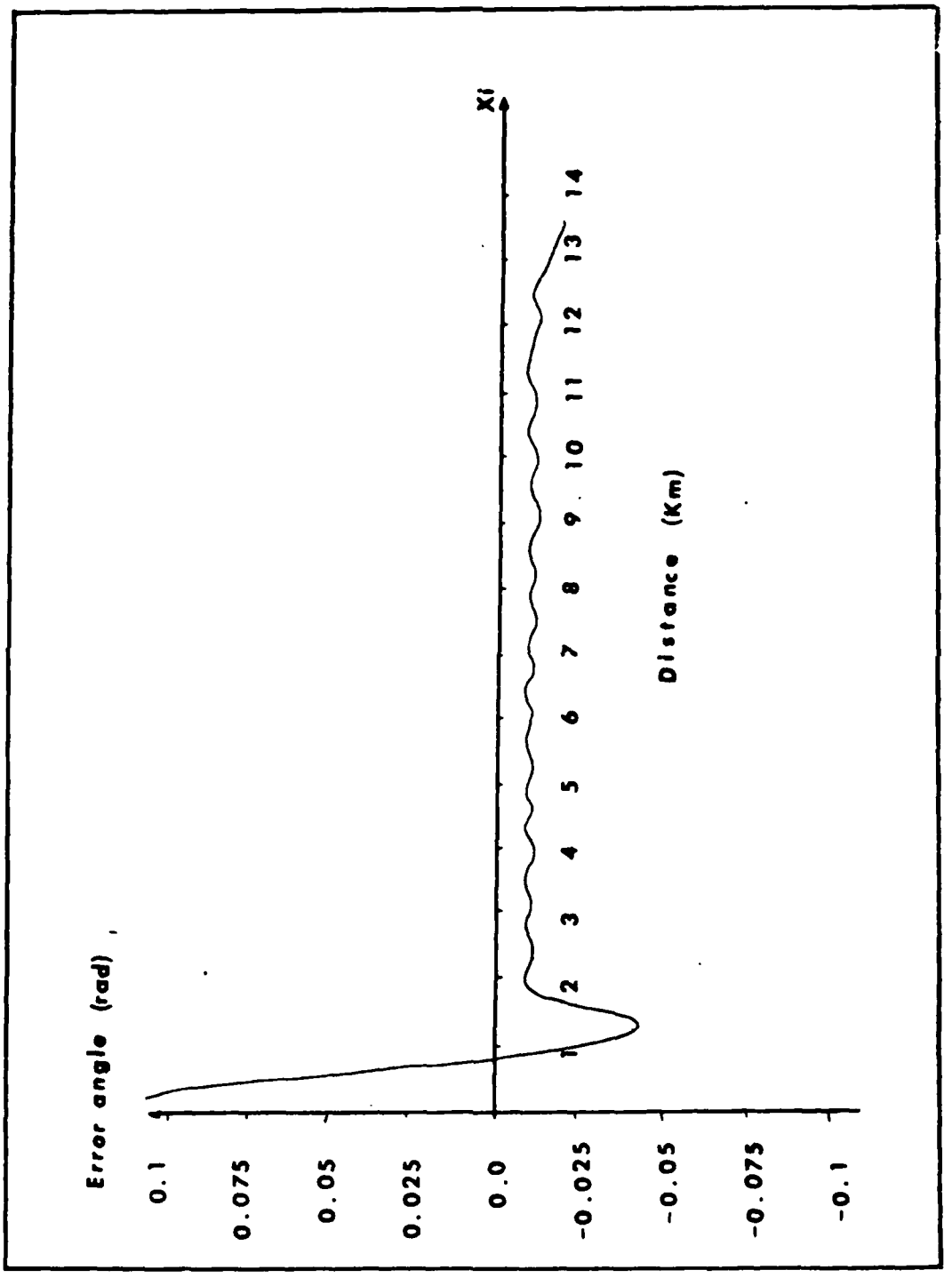

Figure F.6. Elevation Error Angle for Inputs in File 8.

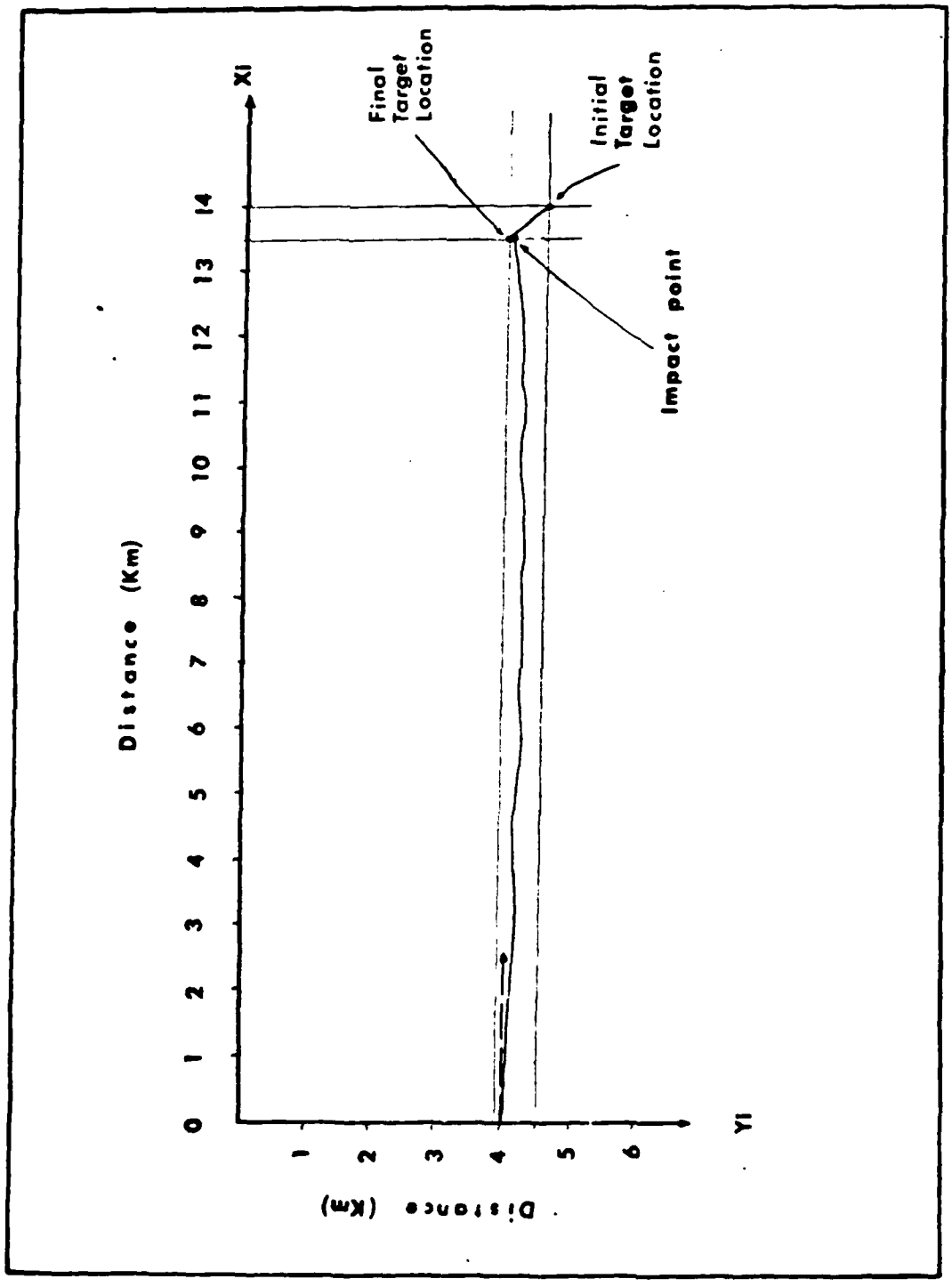

Figure F.7. Lateral Trajectory for Inputs in File 8.

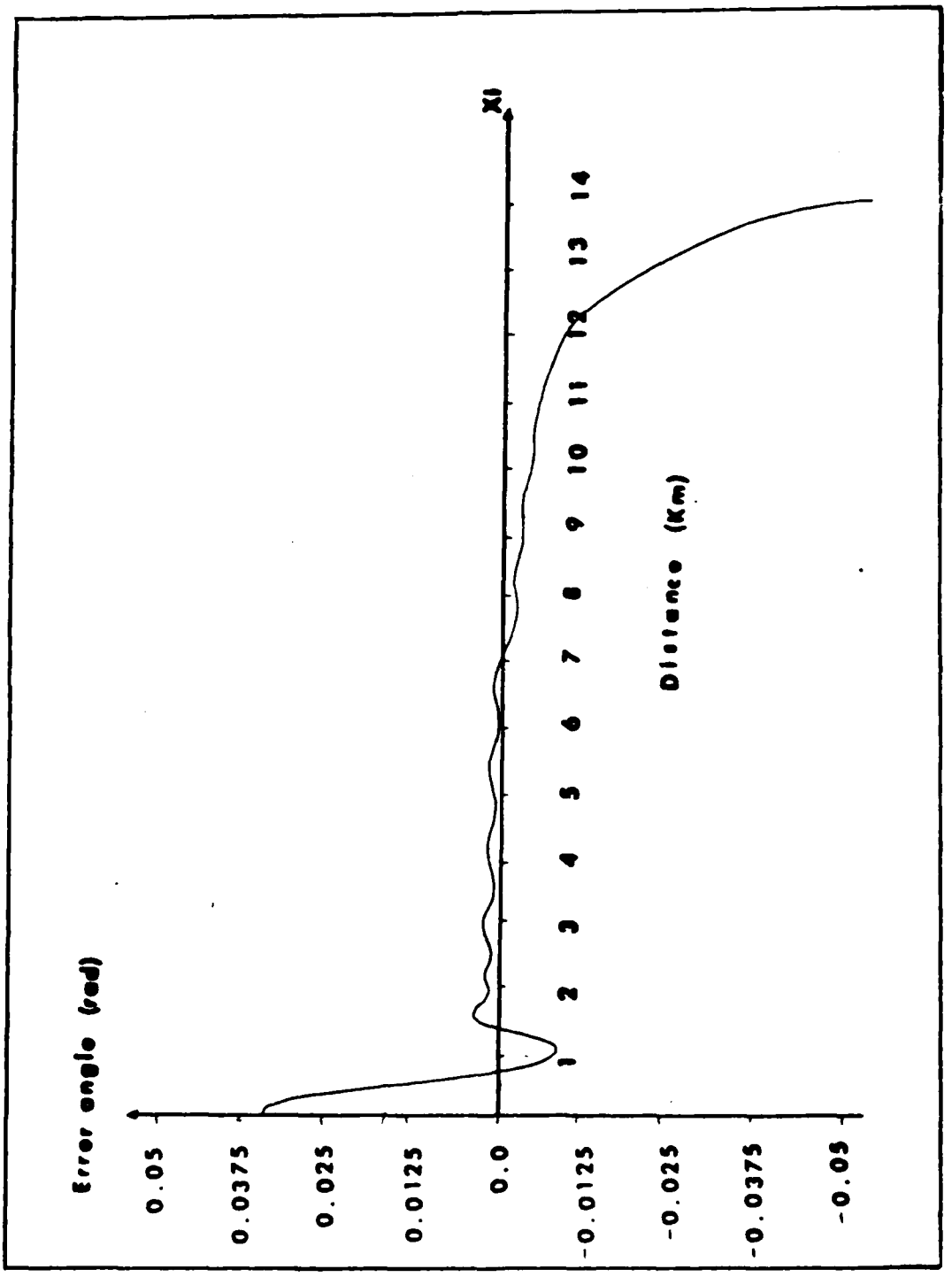

Figure F.8. Azimuth Error Angle for Inputs in File 8.

VITA

Nafi Kasikcioglu was born on 16 December 1960 in Bursa, Turkey. He graduated from high school in Konya, Turkey. Then, he entered the Turkish Air Force as a student in the Air Force Accedemy in Istanbul, Turkey. He graduated from the Accedemy in 1981 as a second Lieutenant. He was assigned as a communication officer and sent to the Air Force Technical Institute in 1982. Upon graduation he attended to the Air Force Language Institute for 6 months. After language training in English, he took GRE and TOEFL exams. The results of these tests entitled him to be a Masters student in Electrical Engineering at the Air Force Institute of Technology in the United States of America. He entered the school in June 1983. His next assignment is with the Avionics and Fire Control Systems Division of the Turkish Air Force.

UNCLASSIFIED

SECURITY CLASSIFICATION OF THIS PAGE

REPORT DOCUMENTATION PAGE

1a. REPORT SECURITY CLASSIFICATION UNCLASSIFIED	1b. RESTRICTIVE MARKINGS
2a. SECURITY CLASSIFICATION AUTHORITY	3. DISTRIBUTION/AVAILABILITY OF REPORT Approved for public release, Distribution unlimited
2b. DECLASSIFICATION/DOWNGRADING SCHEDULE	
4. PERFORMING ORGANIZATION REPORT NUMBER(S) AFIT/GE/ENG/85J-3	5. MONITORING ORGANIZATION REPORT NUMBER(S)
6a. NAME OF PERFORMING ORGANIZATION School of Engineering 6b. OFFICE SYMBOL (If applicable) AFIT/EN	7a. NAME OF MONITORING ORGANIZATION
6c. ADDRESS (City, State and ZIP Code) Air Force Insitute of Technology Wright-Patterson AFB, Ohio 45433	7b. ADDRESS (City, State and ZIP Code)
8a. NAME OF FUNDING/SPONSORING ORGANIZATION 8b. OFFICE SYMBOL (If applicable)	9. PROCUREMENT INSTRUMENT IDENTIFICATION NUMBER
8c. ADDRESS (City, State and ZIP Code)	10. SOURCE OF FUNDING NOS. PROGRAM ELEMENT NO. / PROJECT NO. / TASK NO. / WORK UNIT NO.
11. TITLE (Include Security Classification) See Box 19	
12. PERSONAL AUTHOR(S) Nafi Kasikcioglu 1 Lt TUAF	
13a. TYPE OF REPORT MS Thesis 13b. TIME COVERED FROM _____ TO _____	14. DATE OF REPORT (Yr., Mo., Day) June 1985 15. PAGE COUNT 149
16. SUPPLEMENTARY NOTATION	
17. COSATI CODES FIELD / GROUP / SUB. GR.	18. SUBJECT TERMS (Continue on reverse if necessary and identify by block number) Laser Guidance, Laser Seekers, Strapdown seeker, Semi-Active Guidance, Pursuit Guidance

19. ABSTRACT (Continue on reverse if necessary and identify by block number)

TITLE : LASER GUIDANCE WITH TRIAD DETECTOR ARRAY STRAPDOWN SEEKER

Approved for public release: IAW AFR 190-17.

19 AUG 85

LYNN E. WOLAVER
Dean for Research and Professional Development
Air Force Institute of Technology
Wright-Patterson AFB OH 45433

20. DISTRIBUTION/AVAILABILITY OF ABSTRACT UNCLASSIFIED/UNLIMITED ☒ SAME AS RPT. ☐ DTIC USERS ☐	21. ABSTRACT SECURITY CLASSIFICATION UNCLASSIFIED
22a. NAME OF RESPONSIBLE INDIVIDUAL	22b. TELEPHONE NUMBER (Include Area Code) 22c. OFFICE SYMBOL

DD FORM 1473, 83 APR EDITION OF 1 JAN 73 IS OBSOLETE.

UNCLASSIFIED

SECURITY CLASSIFICATION OF THIS PAGE

The triad detector array strapdown seeker is designed to guide a bomb toward the target designated by a laser. The signal processor determines the error signals related to the error angles of the bomb body fixed X-axis from the target LOS. Error signals are employed as correction commands to the bomb control surfaces in order to keep the bomb in the target LOS. The complete system is simulated as a computer algorithm to evaluate the performance of the triad detector array strapdown seeker. The trajectory of the bomb is determined by the computer algorithm from the release point to the impact point.

The results revealed that the triad detector array strapdown seeker provided pursuit guidance for nonmoving targets and achieved destruction.

END

FILMED

11-85

DTIC